



**University of
Zurich**^{UZH}

Tree-ring analyses to understand the impact of increasing drought frequency and severity on cacao trees in Ivory Coast (West Africa).

GEO 511 Master's Thesis

Author

Alice Gargano

14-923-668

Supervised by

Prof. Dr. Paolo Cherubini (paolo.cherubini@wsl.ch)

Faculty representative

Prof. Dr. Markus Egli

28.06.2020

Department of Geography, University of Zurich

Tree-ring analyses to understand the impact of increasing drought frequency and severity on cacao trees in Ivory Coast (West Africa)

By Alice Gargano
14-923-668



Supervisor: Prof. Dr. Paolo Cherubini
Faculty representative: Prof. Dr. Markus Egli

A Master thesis submitted to the Department of Geography of the University of Zurich
June 2020

Table of Contents

Abstract.....	3
Acknowledgements	4
1 Introduction	5
1.1 Cacao trees and cocoa production	6
1.1.1 Origin and distribution	6
1.1.2 Characteristics and complications	7
1.1.3 Cacao trees in Ivory Coast	8
1.1.4 Climate change	9
1.2 Dendrosciences	12
1.2.1 Dendroclimatology and dendroecology.....	12
1.2.2 Dendroecology in the tropics	15
1.2.3 Dendroecology in Africa.....	20
1.3 Dendroecology in Ivory Coast and cacao trees.....	22
1.3.1 Dendroecology in Ivory Coast	22
1.3.2 Wood anatomy of cacao trees	23
1.4 Research objectives.....	26
2 Material and methods	27
2.1 Sampling trips.....	27
2.1.1 First sampling trip.....	27
2.1.2 Second sampling trip.....	29
2.2 Sampling methods.....	31
2.2.1 Sampling sites.....	32
2.2.2 Samples descriptions	33
2.3 Samples' preparation	35
2.3.1 Preparation for ring width measurements.....	36
2.3.2 Preparation for wood anatomical analyses.....	38
2.3.3 Samples preparation for radiocarbon analyses	39
2.3.4 Samples preparation for stable isotope analyses.....	40
2.4 Samples' measurements and analyses	40
2.5 Climatic data	42
3 Analyses and results.....	45
3.1 Qualitative analyses	45

3.1.1	Feature identification.....	45
3.1.2	Growth rings description.....	49
3.1.3	Spatial comparison.....	51
3.2	Quantitative analyses.....	53
3.2.1	Ring width measurements.....	53
3.2.2	Ring-width permutations	55
3.2.3	Chemical analyses results: radiocarbon dating and stable isotopes	61
4	Synthesis.....	69
5	Conclusion	74
6	References	76
7	List of Tables	82
8	List of Graphs	82
9	List of Figures	83
10	Appendix.....	87
10.1	Samples tables	87
10.2	Samples ring width measurements.....	93
10.3	Climatic and production data	98
10.4	Tree Ring R-Script.....	102
10.5	Maximized correlation outputs after permutations	118
10.6	Sampling trips picture gallery	122
10.6.1	First sampling trip.....	122
10.6.2	Second sampling trip.....	125

Abstract

Tree rings of cacao trees from Ivory Coast were investigated and compared with climatic data. Different trees were sampled from the cocoa belt in Ivory Coast and analysed for dendroecological purposes. Ivorian cacao trees do form tree rings clearer in some regions than others, yet these are extremely difficult to interpret, because the growth rings are likely to be more than one per year. Conventional wood anatomical analyses are not enough for the dating of such rings. A combination between wood anatomy and ring width measurements but also radiocarbon dating and stable isotopes is essential. A permutation script was also used to identify which series of tree rings best correlates with annual precipitation. To further validate and confirm the identified seasonal rings per year, a suggestion for future studies is to use a dendrometer to measure the intra-annual tree growth each year. This master thesis gives a first insight on cacao tree rings, their structure and spatial differentiations in Ivory Coast, paving the way for further future studies in this field.

Acknowledgements

I would like to thank my supervisor Prof. Dr. Paolo Cherubini for his continuous guidance, enthusiastic motivation and constructive feedbacks. I would also express my gratitude to Prof. Dr. Markus Egli, the faculty representative for his support and suggestions.

I wish to also thank Barry Callbaut and also various people from Barry Callebaut who supported this master thesis project; Dr. Martin Gilmour, Matthieu Guemas, Timothy Lucas, John van Haastert, Jacqueline Rosch, Nicko Debenham and Martin Bischof. A special thanks to Franck Bernard Lago for accompanying, helping with communication and sampling in Ivory Coast.

I would also like to extend my thanks to WSL, especially to Loïc Schneider, Anne Verstege and Dr. Holger Gärtner for their suggestions and support in the laboratory. Thanks to Dr. Laurens Valentin Michiels van Kessenich from EMPA for writing the script and to Dr. Lukas Wacker from ETH for the radiocarbon analyses and help with the interpretation.

Finally I wish to thank all of the farmers, coaches and helpers encountered during the sampling trip, researchers who shared knowledge and data, and my family and friends.

1 Introduction

Tree biological features such as height, cambial age and physiological activity influence the growth of trees and interact with environmental variables. Climatic factors can therefore influence tree growth (Fritts, 1971). In a changing climate, using tree growth information to understand reactions to climatic factors is paramount, especially for forest management and crop cultivation. Particularly for crops that need a specific location and related site conditions for ideal growth. This is the case for cacao trees (*Theobroma cacao* L.), which are only grown in tropical regions, currently threatened by longer periods of drought (Schroth et al., 2016). Cacao cultivations are of great economic importance and might be severely affected by climate change leading to serious consequences in many countries where they are grown as well as in the confectionery industry. Therefore, understanding how cacao trees react to climatic variables is essential. Physiological processes in cacao trees are not fully understood yet, making it hard to interpret cacao's resilience towards climate change and differences between varieties (Lahive et al., 2019). When the cambial activity of trees stops in a colder or drier season, tree rings are formed. These growth features can be used not only for reconstructing past climatic conditions but also as indicators of the environmental conditions, tree growth, expression of tree productivity and tree photosynthetic rates. For example, Cherubini et al. (2002) used tree rings as indicators of tree health and photosynthesis rates of declining trees prior to death.

Approximately 70% of the global cocoa is produced in West Africa (Gray, 2000). Ivory Coast provides 39% of the world supply of commercial cocoa through mainly smallholder farmers (Bhattacharjee and Kumar, 2007). Future climatic projections show that longer dry seasons will strongly affect cocoa yields in northern Ivory Coast and neighbouring countries. It is expected, that the increase of dry season temperatures will limit the growth of cacao trees due to decreasing water availability (Schroth et al., 2016). Adaptation strategies must be implemented and the most vulnerable sites must be detected. The most resistant cacao varieties should be identified, to ensure future cocoa beans production. A deeper look into cacao trees' wood anatomy can be beneficial to understand their physiological processes. Investigating cacao tree rings can contribute to the understanding of their reaction to severe

drought events. The aim of this master thesis is an assessment of the potential of dendroecological studies to get a better understanding of physiological processes in cacao trees based on a case study in Ivory Coast.

1.1 Cacao trees and cocoa production

1.1.1 Origin and distribution

Cacao is a tropical tree and belongs to the Sterculiaceae family, *Malvaceae sensu lato*. It grows ideally 20°N and 20°S of the equator but originally comes from the central and northern parts of South America (Bhattacharjee and Akoroda, 2018). The Maya and Aztecs cultivated cacao for its beans, which they used to make a drink similar to the modern chocolate drink. In the sixteenth century during the post-Colombian era, Hernando Cortez discovered the drink and sent it to Europe. Cacao cultivation in other continents started during the colonial era. Thanks to the West African peasant farmers, the cacao industry developed enormously, transforming the West African cocoa belt into a hub for cocoa production. Most of the cacao comes from Ivory Coast, Ghana, Indonesia, Nigeria, Cameroon, Brazil, Ecuador and Malaysia. However, it is also cultivated for export in other countries (Bhattacharjee and Kumar, 2007).



Figure 1 World cocoa production. Source: icco.org

1.1.2 Characteristics and complications

The following descriptions about the characteristics of cacao trees originate from the International Cocoa Organization (ICCO), which is a global organization, composed of both cocoa producing and cocoa consuming member countries.

Cocoa plants are resistant to relatively high temperatures up to an average of 30 – 32°C and a minimum of 18 – 21°C. The variation of cocoa yields seems to be more affected by rainfall, whereby cacao trees appear to be extremely sensitive towards soil water deficiency. Ideal climatic conditions are where the annual rainfall ranges between 1'500 mm and 2'000 mm and is well distributed throughout the year. Dry periods with less than 100 mm per month for more than three months become problematic for cacao trees. For the optimal development hot and humid atmospheric conditions are paramount with a high relative humidity optimally between 80-100%. However, especially at the early growth stage, it is important for cacao trees to have shading.

Soil conditions also play an important role for cocoa plants. The ideal soil composition must contain coarse particles with enough nutrients and abundant depth in order for the root system to properly develop. Cacao trees can grow on slightly acid and alkaline soils, but start suffering at pH values below 4.0 and above 8.0.

There are different types of cacao trees. Forastero is the largest cultivated group type. It includes cultivated and wild populations, whereby the Amelonado type is the most planted of them. The majority of the cocoa plantations in Brazil and West Africa are cultivated with Amelonado. Upper Amazon hybrids have recently been spread around the world as well.

Cacao trees suffer from different diseases that can impact the yield and tree's performance. Different kinds of fungus are known to attack cacao trees, such as the witches' broom which invades growing tissues causing trees to produce branches without fruits. Frosty pod rot shows symptoms of white fungal mats on the pod surface and pod rot is the most important pathogen in West Africa, resulting in the rotting of pods.

Insects also affect cacao trees. The most threatening ones are mirids. They dig a hole into the stems, branches and pods resulting in necrotic lesions. These insects are a huge threat to West African countries because they can cause the death of branches and leaves.

The cacao swollen shoot virus (CSSV), often identifiable via swollen stems and roots, is another threat to cacao trees. This virus can spread easily because it takes a long time for the symptoms to show (ICCO, 2013).

1.1.3 Cacao trees in Ivory Coast

Ivory Coast is located on the south coast of West Africa. Its political capital is Yamoussoukro in the middle of the country and its economic capital is Abidjan located by the coast. Before the colonization period, the area of what is now known as Ivory Coast consisted of different states such as Gyaam, the Kong Empire and Baoule. After the arrival of the French, Ivory Coast gained its independence as most other West African countries in 1960. During this period, thanks to the production of coffee and cocoa, the country was among the most economically successful countries in West Africa. Due to the stagnant commodity prices and monetary adjustments, Ivory Coast went through a social and economic crisis in 1980 (The World Factbook, 2008). Stagnant economy led to declining living standards resulting in ethnic tensions especially on foreign workers and between Muslims in the north and Christians in the south. When the military took over power, the country was driven to a series of crises and tensions towards the northern part of the country. In 2002 with the death of the military ruler, a civil war broke out (Woods, 2003). "The Ivorian property rights regime encouraged a rent-seeking process that shifted social and political interactions from a relatively peaceful dynamic to a more conflictual one, as the rent derived from the exploitation of tropical forest land declined" is Woods (2003) main argument explaining how Ivory Coast ended up in ethnic conflicts and civil war. According to him, conflict is triggered by the way access to land is given. In this case, the government was the mediator. Since tropical forests were treated as free resources, their exploitation consequences led to higher rental costs causing social conflicts. The possibility to rent the forest was one of the

factors shaping the exploitation, yet not the only one. Developing unexploited tropical lands to plant cocoa trees also had a major contribution (Woods, 2003). After several cycles, replanting cacao trees becomes harder, since the soil does not recover fast enough and the amount of nutrients decreases. Without the forest, younger plants and trees also suffer from the lack of protection against, for instance, winds. Therefore, the costs of production rise as well as the need for external inputs such as fertilizers (Woods, 2003). Being one of the biggest cocoa producing countries and having a complex background, the cocoa production in Ivory Coast faces a challenging future especially given the climatic uncertainties.

1.1.4 Climate change

There have been drastic ecological changes in West Africa in the past decades. Climatic zones have been shifted, resulting in the expansion of the Saharan desert. Increasing anthropogenic activity has also contributed to landscape changes (Wittig et al., 2007). Especially the sub-Saharan regions are often described as vulnerable due to the lack of understanding of the impact of climate change on crop yields (Sultan et al., 2013; Schroth et al., 2016). Future climatic projection scenarios show a negative impact on yields, especially in Sudanian and Sahelian regions (Sultan et al., 2013). Nearer to the coast in southern Ivory Coast and Ghana, where most of the cacao is grown, dry season temperatures are expected to be more limiting for cocoa than dry season water availability. Climate change will affect spatial differentiation, probably resulting in a shift of the cocoa belt, whereby most vulnerable areas are near the savannah area in northern and eastern Ivory Coast. The least vulnerable zones are towards the southern coastal zones (Schroth et al., 2016).

The way in which the cacao trees are planted plays an important role, especially given the projected future climatic changes. A lot of research on cacao agroforestry, shade tree management and their effects on diseases and reactions to climatic changes has been done. According to a study conducted in Indonesia, cacao trees seem to be highly sensitive towards drought but can acclimatise and become more tolerant thanks to agroforestry systems (Schwendenmann et al., 2010). Most of the current cocoa farming in Ivory Coast is full-sun, leading to higher yields but severe consequences in the long-term. Such

consequences include biodiversity loss, soil fertility depletion and degradation (Tondoh et al., 2015). Furthermore, shade trees have proven to reduce stress for cocoa and coffee plantations, yet at the same time compete for resources. Also regarding diseases and pests some shade trees can contribute to the increase and others to the decrease (Beer et al., 1998). The importance and effect of interactions between cocoa trees and shade trees remain dependent on many different factors such as site conditions, species and varieties and management practices (Beer et al., 1998). More recent research showed that pod production, cacao tree density and the spatial distribution of shade trees has independent influences in the intensity of diseases. Disease intensity seemed higher in relation to cacao tree density and self-shading. Only forest trees that were regularly distributed reduced the intensity of diseases as opposed to randomly or aggregated distribution (Gidoïn et al., 2014).

Cocoa's vulnerability towards climate change based on climate projections for the 2050s under the Intergovernmental Panel on Climate Change (IPCC) intermediate emissions scenario RCP 6.0, was thoroughly analysed for the West African cocoa belt by Schroth et al. (2016). They found that temperature as the limiting factor for cocoa shade trees has an essential influence on cacao trees' survival. They modelled the climatic suitability areas for cocoa and projected it in the year 2050 using variables like maximum temperature, total rainfall and intensity of dry season.

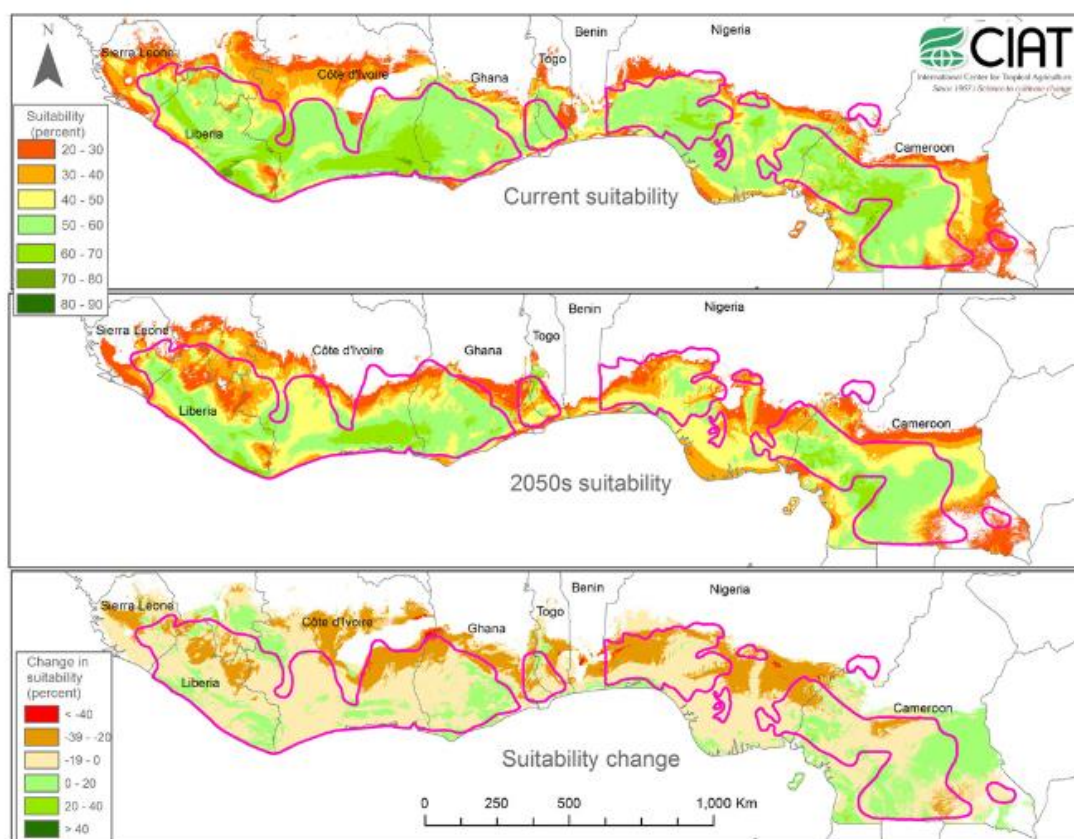


Figure 2 Relative climatic suitability (in percent) for cocoa of the West Africa cocoa belt under current and projected 2050s climate conditions, as well as suitability change, according to a Maxent model based on 24 climate variables. The red lines show areas of cocoa production (Schroth et al., 2016).

In the current climate, drought seems to be more threatening for cocoa than high temperatures in West Africa. In fact, cocoa is also considered to be rather drought sensitive, especially in areas like West Africa with longer dry seasons (Carr and Lockwood, 2011; Wood and Lass, 2008). Drought years have severely affected cocoa yields in the past especially during El Niño (Ruf et al., 2015, Gro Intelligence, 2019). Maximum temperatures during the dry season will be similar to the temperatures now only found in the savannah and will also pose a threat to cocoa's tolerance. Furthermore, the projected impacts will differ spatially and among countries (Schroth et al., 2016). In Ivory Coast as seen in figure 2, a noticeable part of the central-western region, the western coast and some northern areas in the eastern region will decrease in suitability by 2050. Nevertheless, how cacao trees really react to limiting factors like water availability and temperature remains unclear and debated (Lahive et al., 2019). Any contribution to understanding the reaction of cacao trees towards climate change can be of immense value.

This is especially true, since cocoa production might be strongly affected and in return influence many farmers, companies and the whole cocoa and chocolate market (Gro Intelligence, 2019).

1.2 Dendrosciences

1.2.1 Dendroclimatology and dendroecology

Due to seasonal changes, trees usually form annual growth rings that can be used to study variability in climate. This discipline is called dendrochronology. Dendrochronological methods are used to reconstruct past climate in dendroclimatology, whereas in dendroecology to study the impact of disturbances such as insects, pests or avalanches (Fritts, 1971). Growth rings are formed by early wood and latewood. The early wood is made up of cells with thin walls and large diameter and appears in lighter colour. At the beginning of the growth period early wood is formed. Towards the end of the growing period, late wood cells are formed. These have thicker cell walls, smaller diameter and the wood appears darker and denser (Laboratory of Tree-Ring Research Arizona, 1999).

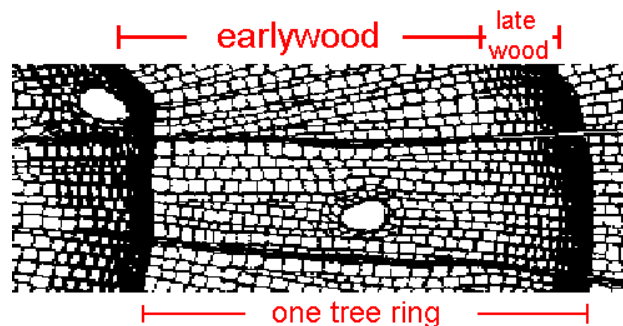


Figure 3 Conifer tree ring visualisation (Laboratory of Tree-Ring Research Arizona, 1999).

Ring formation depends on the growing periods, which are limited by factors like precipitation and temperature. Therefore, the growth pattern of tree rings reflects climatic variations. By analysing and assessing these growth patterns, correlations between radial growth and climatic variables can be detected (Nishimura, 2009; Hughes et al., 2010). Such analyses are useful to reconstruct past climatic conditions. However, when past climatic conditions are known, analysing growth patterns can provide a better understanding about how a tree reacts to certain climatic variables (Fritts, 1971). Moreover, with a significant

spatial sample distribution, geographical analyses can provide information about the spatial organization and correlations between sites with corresponding regional climate and tree growth. For instance, in the Duck Mountains of west-central Manitoba a multidisciplinary approach was used to document natural disturbance regimes (Sauchyn, 2000). The SFM Network Project combined Geographic Information Systems (GIS), remote sensing data and analyses with tree ring data to successfully extend the temporal perspective. Thanks to the appropriate spatial and temporal scale enhancements, the results strongly supported forest management planning (Sauchyn, 2000).

“Dendroecology refers to applications of dendrochronological techniques to problems in ecology” (Fritts and Swetnam, 1989). Ecological problems that can be tackled with dendroecological techniques are, for example, the spread of insects in forests, the decline of trees in Europe and North America and potential environmental changes due to the increase of atmospheric CO₂ and other gases. These techniques are based on the measurement of the structural characteristics of tree rings or wood anatomy. For instance, ring width, wood density and vessel size reflect differences from one ring to another. Despite not being rules of nature but best inferences based upon facts at a particular time, dendroecological principles and practices are essential. Part of these principles include limiting factors, sample replication, crossdating, modelling and many more (Fritts and Swetnam, 1989). In temperate climates, the cambial activity of trees and shrubs stops during the cold season and annual tree rings are formed. Tree rings have been widely used for reconstructing past climatic conditions and events, and tree ring records can provide information about the reaction of trees to past environmental stress and disturbances. For example, in Europe dendroecological principles and analyses have been used to identify drought tolerance and reactions to climate change of different alpine mountainous trees (Hartl-Meier et al., 2014).

More broadly, tree rings can be used as indicators of not only climatic, but also environmental conditions in which trees have been growing. Depending on the geographic location and the corresponding climatic conditions trees grow differently.

There are also trees that form intra-annual density fluctuations (IADFs) due to changes in the environmental conditions in Mediterranean ecosystems. A combination of dendrochronology, quantitative wood anatomy and high-resolution isotopic analysis using the laser ablation technique can be applied to detect and identify such IADFs, which may in some cases almost look like normal tree rings (Battipaglia et al., 2010). Battipaglia et al. (2010) results showed that IADFs characterization can reveal seasonal information about how environmental factors and tree growth are related. Additionally, in olive trees, the identified IADFs enabled the determination of the number of tree rings through dendrochronological analyses (Cherubini et al., 2013). The measurement of growth-rings of olive trees is not a trivial task. Identifying the difference between IADFs and true, maybe even annual, tree rings is very difficult. To improve the definition of wood-density variability, Cherubini et al. (2013) used Neutron-Imaging Radiography, which showed similar results to the analyses done with dendrochronological approaches. To detect elemental boundaries, Scanning X-Ray Fluorescence Microscopy (SXF) was used.

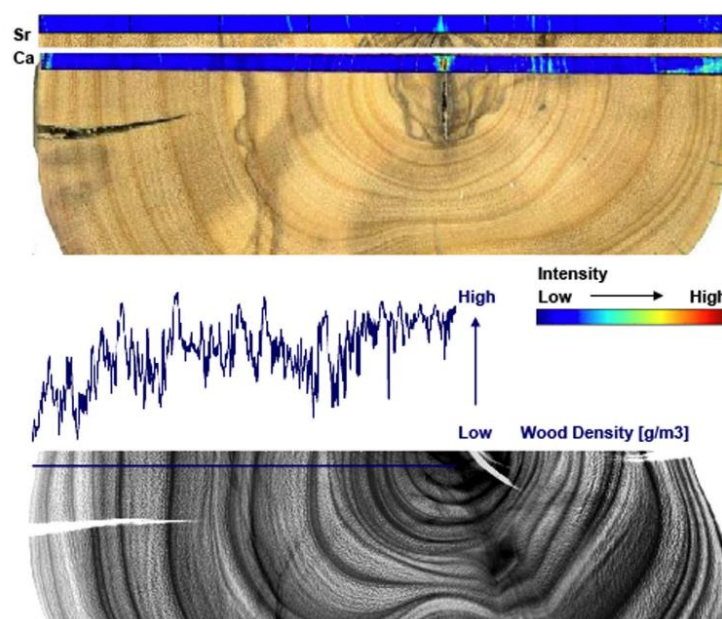


Figure 4 Above: Stem disc from sample E3 overlaid by a SXFM-profile. Content of calcium and strontium increases at the tree-ring borders. Below: Neutron Image of a section of the same sample (E3). Higher density peaks should reflect tree-ring borders but can also be induced by Intra-Annual-Density-Fluctuations, making tree-ring dating impossible (Cherubini et al., 2013).

Evergreen shrubs and trees are often found in dry environments, such as the Mediterranean region or in sub-tropical areas. They cope with drought by either shedding leaves or

continuing growth during drier periods. The growth starts in the roots as the first rain comes. During drought events some trees may close the stomata to retain water, however the physiological adaptations at the tree level may be responsible for the changes in cambial responses to climate. Double or false rings were detected in trees where cambial activity was stopped not only by limiting temperatures but also by the lack of water. Double rings occur when the normal growth pattern of a tree is interrupted during a seasonal change (Cherubini, et al., 2003).

1.2.2 Dendroecology in the tropics

Tropical dendroecology is a field that only started to develop in the past few decades, yet extremely rapidly and with important achievements. Due to the lack of seasonality in the tropics, the existence of annual growth rings in the tropics was long denied. However, when tropical trees experience cambial dormancy due to disadvantageous environmental conditions they can still form rings because of those difficult circumstances. The dormancy period might be due to a dry season, a flooding or fluctuations in salinity (Rozendaal and Zuidema, 2011; Jacoby, 1989; Vieira Aragao et al., 2019). The influence that climatic factors have on tree radial growth has been proven for numerous species in the tropics. The responses were often different depending on the tree species. Some responded to total annual rainfall, others to total rainfall in the rainy, dry season or even during the transition. Therefore, usually in tropical lowlands the formation of tree rings is caused by variation in precipitation. So far 230 tropical species around the world were proven to form annual rings (Brienen et al., 2016; Rozendaal and Zuidema, 2011). Giraldo et al. (2020) have recently classified the tree rings of 81 tree species from America's rainiest region. Such regions are under extreme humid conditions presenting no hydric seasonality. Nevertheless, more than 80% of the analysed species had growth rings and some even with dendrochronological potential. This kind of research suggests that there are still many open questions within the field of tropical dendroecology. The periodicity of tree rings in such an extremely humid environment with no seasonal variation needs further investigation (Giraldo et al., 2020). There are also many trees in the tropics with extremely unclear rings or with no rings at all. For such trees usual dendrochronological techniques are too limited. Tropical

dendrochemistry includes alternative techniques and methods to estimate age and growth from ringless trees. X-ray microprobe synchrotron records of calcium from a ringless tree from Thailand were used to estimate the tree's age and growth (Poussart et al., 2006). Furthermore, using the "wounding technique" the radial growth of five species in Brazil was determined. The growth was obtained for five periods of three months over a total of 15 months. It was related to various environmental indicators, yet only precipitation showed an association with growth. In most of the species the presence of growth rings was observed and described as distinct, only one species *A.heterophyllus* had indistinct growth rings (Bressan-Smith et al., 1997).

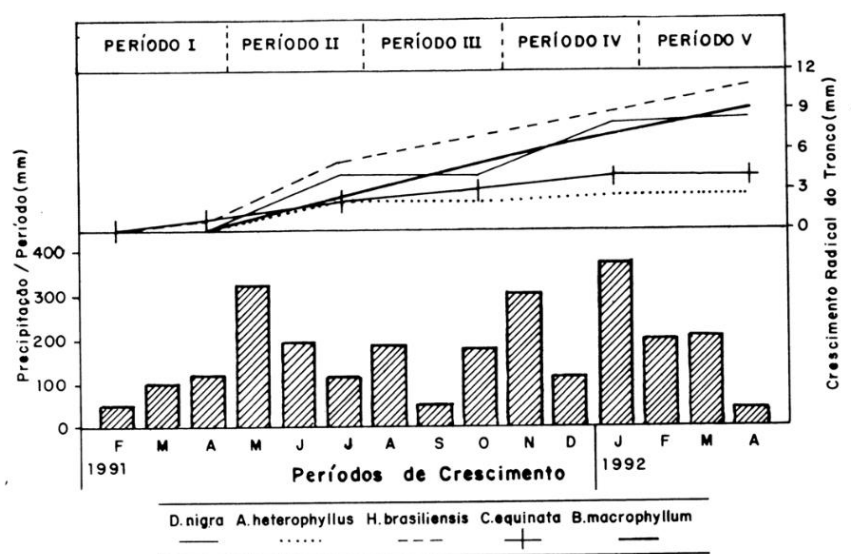


Figure 5 Radial growth of the trunks of five different tropical species from Brazil and the precipitation curve (Bressan-Smith et al., 1997).

Dalbergia nigra showed a decrease in radial growth during period 1, 3 and 5. These periods correspond to the periods of hydric deficiency. Other species show different patterns which might be explained by the cultivation conditions (Bressan-Smith et al., 1997).

1.2.2.1 Stable Isotopes

Environmental and physiological effects characterize the isotopic composition of wood in tropical trees (Van der Sleen et al., 2017). The basis of the method is that the isotope ratios are not exactly constant, but vary slightly in the organic matter of plants due to physical and biochemical isotope fractionation mechanisms. The carbon isotope ratio is affected by

the diffusion of CO₂ through the stomatal pores and by the C-fixation during photosynthesis (Farquhar et al., 1989). Changes in environmental conditions may thus also change the isotope discrimination and this signal will be recorded in the isotope ratio of the tree rings. Imposed stress on plants has been shown to result in increasing ¹³C/ ¹²C (δ¹³C) ratios in two ways: by stomatal closure, e.g., under drought, and by increasing the PEP-carboxylation activity, e.g., due to increased ozone levels. The first mechanism is useful for retrieving climatic information or the past water-use efficiency of trees. When plants close their stomata in order to save water, the intercellular CO₂-concentration is decreasing, the ratio of carbon gain to water-loss is improved and the ¹³C-discrimination reduced. The second mechanism is related to the differential discrimination of the CO₂-fixing enzymes Rubisco and PEP-carboxylase. Combining ¹³C with ¹⁸O may help to separate water-related from other environmental influences, as ¹⁸O is more influenced by isotope fraction and processes in the water-cycle than by biochemical changes. The ¹⁸O /¹⁶O (δ¹⁸O) ratio in plant matter is reflecting variations in the source water isotope ratio and evaporative enrichment of leaf water via transpiration. This latter effect is caused by slower evaporation of the heavier H₂¹⁸O-molecule compared to the lighter H₂¹⁶O-molecule (Saurer et al., 2003; Saurer et al., 1997).

The abundance of ¹³C depends on water, light and nutrient availability. The values of ¹⁸O can be determined through values of rainwater and water from under the soils at root depth. The nitrogen uptake is reflected in the ¹⁵N signature depending on complex paths nitrogen goes through in its cycle. However, for isotopic analyses it is recommended to have reliably dated rings and to consider that temporal changes could be confused with changes due to tree size. After reviewing several studies using stable isotopes in tropical trees, the results show that temporal variation in δ¹³C and δ¹⁸O is correlated with precipitation and also El Niño Southern Oscillations. Seasonality helped out with non-distinct annuals rings and the responses of tropical trees to the increase of atmospheric CO₂ was clearly quantified with the δ¹³C as a measure of water use efficiency (Van der Sleen et al., 2017).

1.2.2.2 Radiocarbon dating

To estimate the age of trees in an old tropical wet forest in Costa Rica, tree-ring analyses were combined with radiocarbon ^{14}C dating. ^{14}C dating demonstrated with wood anatomical studies, that some species formed annual growth rings. Despite the wet conditions tree growth may be rhythmic and with annual periodicity (Fichtler et al., 2003). Hua et al. (2013) present a compilation of tropospheric $^{14}\text{CO}_2$ for the period of 1950 to 2010. The compilation is based on tree ring series and published radiocarbon data from atmospheric CO_2 records. The application of bomb radiocarbon has also been used to validate tree ring ages and to date recent trees having no annual growth rings (Worbes and Junk 1989; Poussart and Schrag 2005; Lovelock et al., 2010). The tropospheric ^{14}C started to rise in 1955 due to nuclear activity aboveground. The levels of ^{14}C increased and reached a maximum in the 1960s and have been decreasing since then.

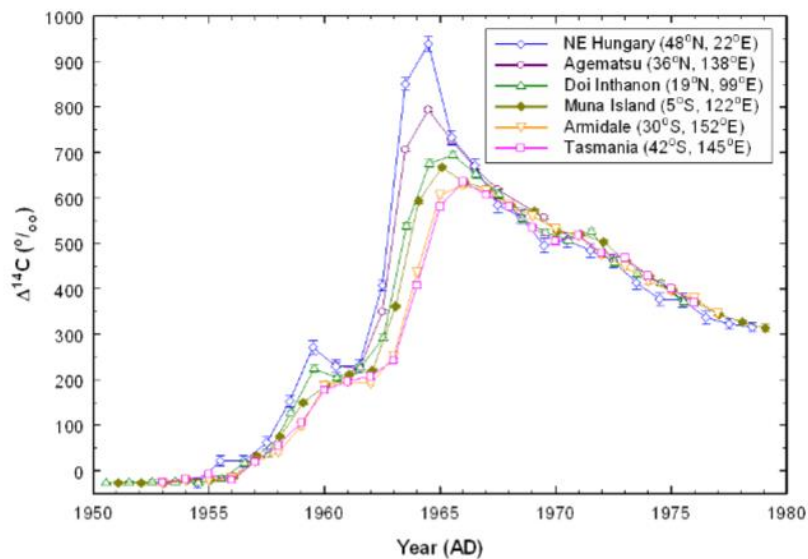


Figure 6 Radiocarbon in tree rings at different locations. Data representing the 4 different zones defined by Hua and Barbetti (2004) include NE Hungary (Hertelendi and Csongor 1982) in NH zone 1; Agematsu, Japan (Muraki et al., 1998) in NH zone 2; Doi Inthanon, Thailand (Hua et al., 2000, 2004) in NH zone 3; and Armidale (Hua et al., 2003) and Tasmania (Hua et al., 2000) from Australia in the SH zone. The new tree-ring data are from Muna Island, Indonesia (Hua et al., 2012b).

Error bars are 1σ (Hua et al., 2013).

Since most of the nuclear tests took place in the northern hemisphere, the distribution of tropospheric radiocarbon differs around the world. In fact, the graph above shows different ^{14}C levels between 1955 and 1960, depending on the location. The zonal atmospheric bomb ^{14}C is divided into three northern hemisphere zones and two southern hemisphere zones.

Tropospheric ^{14}C levels decrease from north to south (Hua et al., 2013). In tropical areas ^{14}C enriched CO_2 coming from the terrestrial atmosphere might have influenced higher ^{14}C levels in comparison to mid-northern hemispheric areas (Reimer et al., 2004). Therefore, Reimer et al. (2004) argue that ideally regional or local datasets are needed to calibrate post-bomb ^{14}C , for certain locations however, it is not feasible to develop such records yet.

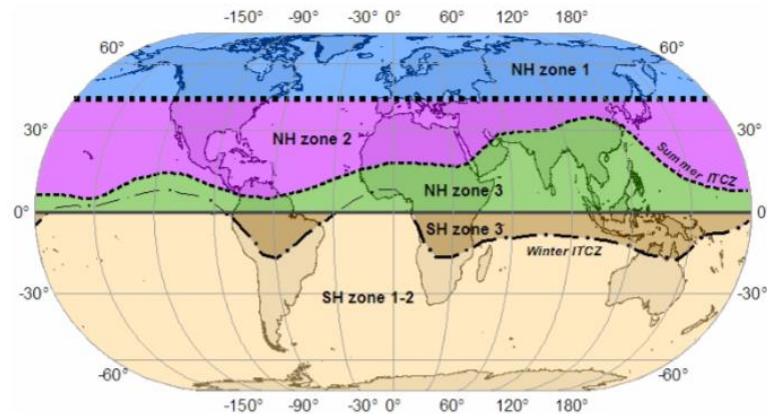


Figure 7 World map showing zonal atmospheric bomb ^{14}C . The mean positions of the summer and winter ITCZ are adapted from Linacre and Geerts (1997) (Hua et al., 2013).

Radiocarbon has proven to be extremely useful in annual tree ring identification and confirmation. The periodicity of ring formation in *Cedrela* from different sites in tropical South America was analysed. The results showed that *Cedrela* trees from Bolivia, Ecuador and Venezuela form one ring per year. However, *Cedrela* trees from Suriname form two rings per year. This finding proves that the same species may grow differently depending on the site and their tree rings periodicity may differ (Baker et al., 2017). Recently a ring width chronology of a *Cedrela odorata* tree was developed using dendrochronological techniques. To confirm the independent annual periodicity and validate the dendrochronological dates, high-precision radiocarbon bomb pulse dating of selected trees was performed. The dendrochronological dates and ^{14}C values were matching the southern hemisphere ^{14}C bomb curve and confirmed the validity of the study (Santos et al., 2020).

1.2.3 Dendroecology in Africa

In Africa climate driving factors, their interactions and impacts are poorly understood, partly due to the scarce instrumental data. Dendroecological and stable isotopes techniques can fill in gaps to reconstruct climate variability, trends and atmospheric circulation patterns in different regions in Africa (Gebrekirstos et al., 2014). In Western Kenya, after analysing 14 different tree species, *Acacia mearnsii*, *Cupressus lusitanica*, the *Eucalyptus* spp. and *Mangifera indica* showed the highest dendrochronological potential (David et al., 2014). In the Congo Basin, carbon and oxygen isotopes of *Pericopsis elata* trees were measured. The tree rings were anatomically distinct. Results showed that oxygen isotopes have common high signals and respond to multi-annual precipitation variation. With wetter conditions, $\delta^{18}\text{O}$ is lower. $\Delta^{13}\text{C}$ was mostly related to growth variation driven by competition for light (Colombaroli et al., 2016). *Pericopsis elata* had already been studied for dendrochronological potential by De Ridder et al. in 2014. Being a rare tropical timber of endangered species the need for accurate and reliable growth data is clear. Tree ring chronology measured with 24 stem disks showed a significant correlation with the second half of the rainy season. Higher tree-ring indices were linked to higher precipitation during El Niño years (De Ridder et al., 2014). In Keita Valley, Niger in Sahelian semiarid ecosystems, *Acacia* trees survive despite the extreme environmental conditions. *Acacia seyal* Delile trees were studied to analyse the relationship between tree growth, ring patterns and climatic conditions. Also, these trees have a precipitation dependant climate signal and tree rings formed during the rainy season (Nicolini et al., 2010). Individual African *Acacia* trees of known age had previously been examined in 1994 by Gourlay and Grime. Growth-ring borders were described as “narrow bands of marginal parenchyma filled with long crystal chains”. Using the scanning proton microprobe method, the crystals turned out to be calcium oxalates. The number of parenchyma bands was similar to the number of peaks in the annual rainfall distribution which together with the crystals define the growth phases (Gourlay and Grime, 1994). Crystals usually reflect tree reserves and were also found in commercial timbers (Richter and Dallwitz, 2000). Cailleau et al. (2011) found crystals in Iroko trees (*Milicia excelsa*) identified as oxalate crystals, which result from processes involving the upper part of the soil where the tree is located. When organic matter decays, whewellite crystals are released

in the soil. Moreover, there is a carbonate flux within the wood tissues, whereby the oxalate oxidation in the upper part of the soil results in calcite biomineralization inside the tree (Cailleau et al., 2011). After preparation in the laboratory, Cailleau et al. (2011) used SEM observations and X-ray diffraction to identify calcium oxalate crystals.

Dendroecological studies can also provide insight into the products provided by trees, such as crops and wood. In Cameroon tree-ring analysis delivered chronological growth data of different timber species. This data combined with logging inventory was used to forecast timber yields. The result was that under the current logging cycles and frequency, future timber volumes will decrease by more than 70%. With lower volume ingrowth of the trees, yields also resulted lower, suggesting that lengthening the logging cycle and so letting the trees grow longer depending on the species, can ensure a yield decrease lower than 30% (Groenendijk et al., 2017). The Brazilian native tree *Caryocar brasiliense*, is heavily exploited for food and industrial purposes by the rural population. In a study, the fruiting and growth rate of these trees were monitored during two whole growing seasons. The fruit production in 2006 was significantly higher than in 2007. The number of fruit per individual increased per diameter. Yet the increase per diameter was lower in 2007 than in 2006, meaning that the trees grew less and delivered less fruits in 2007. These observed differences strongly suggest that higher production dependeds on the precipitation, since it rained less in 2007 than in 2006. Similar studies also suggested the influence of precipitation on fruit production (Zardo and Henriques, 2011). Masting events of Mexican beech also showed direct dependency on precipitation. The influence of temperature and precipitation on changes in tree-ring width was analysed and resulted in vessel frequency and diameter modifications. The results suggested that masting events depend on minimum annual precipitation and take place on average every 5.5 years (Rodríguez-Ramírez et al., 2019). Climate change is highly likely to further influence the functions of tropical forest as well as trees production of commercial crops and dendroecological studies can potentially improve the understanding of their reactions (Groenendijk et al., 2017; Zardo and Henriques, 2011; Rodríguez-Ramírez et al., 2019).

1.3 Dendroecology in Ivory Coast and cacao trees

1.3.1 Dendroecology in Ivory Coast

Ivory Coast's terrain is similar to a plateau rising to almost 500 meters elevation above sea level in the northern part of the country. The south-eastern area has coastal inland lagoons stretching throughout the coast. In the south, especially in the southwest region, the landscape is mainly tropical moist forest. Further northwest near to the Guinean border the mountainous region is surrounded by montane forests. In the middle of the country towards the north, the savannah area increases with sandy soils and the vegetation decreases (World Atlas, 2019; Butler, 2006). The main forest disturbance is deforestation, which caused the primary forest coverage to decrease down to 3 % in 2005. For agricultural purposes, logging and uncontrolled fires are responsible for major forest loss. In 1990 the Ivorian government declared 15% of the country as protected area by taking measures against logging, poaching and encroachment in parks. The forest cover loss rate was reduced, nevertheless, the state of conservation efforts remains unclear and ecosystems in Ivory Coast are still threatened (Butler, 2006). Among others, cacao plantations now cover a significant part of Ivory Coast's landscape. Climate change also has an influence on remaining forests and cacao plantations. Physiological responses to climatic factors in cacao trees are mainly induced by water limitation or experiencing higher temperatures. There are contradictory results regarding shade trees and elevated environmental stress. Nevertheless, understanding cacao's resilience towards climate factors remains unclear and with significant gaps (Lahive, 2019).

Through the dating of annual tree rings, dendroecology aims to learn about past and present environments (Fritts, 1971). In certain cases, dendroecology can provide an improved understanding of physiological response to climate and fill in research gaps. Apart from the climatic influence, tree ring growth is also affected by abiotic and biotic interactions, which can provide information about reactions towards diseases or insects (Nishimura, 2009). In Ivory Coast, teak (*Tectona grandis*) tree rings showed a different response to climate when differentiating between managed and non-managed plantations (Dié et al., 2015).

Dendroecology involves the investigation of tree rings and wood anatomy, delivering

information about reactions towards disturbances like insect outbreaks and past climatic events, enabling improved understanding of causes, magnitude and regional differences (Nishimura, 2009).

1.3.2 Wood anatomy of cacao trees

As discussed in the previous chapters, dendroecological analyses provide an added value not only for past climate or age reconstruction but also for the understanding of how certain trees react to climate change. Understanding cacao's tree-ring formation and derived information of tree physiological processes, such as water uptake, stomatal activities and water use efficiency, could be useful to reconstruct past tree growth. Also its relationships with environmental conditions, for example its resistance and resilience to drought, and the impact of different management techniques could be better understood. Our current understanding of cacao tree's physiology is very poor (Lahive et al., 2019), and any improvement of the knowledge will have a terrific impact on the management of cacao plantations. Studying past tree growth may help to predict future response to climate change. A recent study about the phenology of cacao trees in tropical forests in Colombia found out that precipitation, photosynthetically active radiation and water balance showed a significant correlation with flowering (Gil Restrepo et al., 2017).

Some researchers have taken a look at the wood of cacao trees and even identified circular structures similar to growth rings, through a transversal cut through the trunk of a cacao tree in Costa Rica (Alvim, 1957). Humphries (1944) used a dendrograph to measure the growth of a cacao tree's trunk, studying at the same time the expansion of the branches. His conclusions were that the growth cycle of the trunk was similar to the one of the branches and more accelerated during the sprouting period (Häkkinen et al., 1998). In Alvim's (1957) experiment several cacao trees' growth activities were measured with dendrometers for a few years in Costa Rica. The average trunk increase in diameter was 3.81 mm per year, with the greatest growth in June and July. The growth resulted in being positively correlated with temperatures rather than rainfall and diminished during periods of intense leaf flushing (Alvim, 1957).

Williams León published in 2015 a comparative study between wood anatomy in trunk and branches of *Theobroma cacao*. He detected growth rings defined as distinct to slightly distinct. He confirmed the presence of tylosis and traumatic gum-ducts, which he found in almost all samples. Such gum-ducts seem to be the trees' response to disturbances.

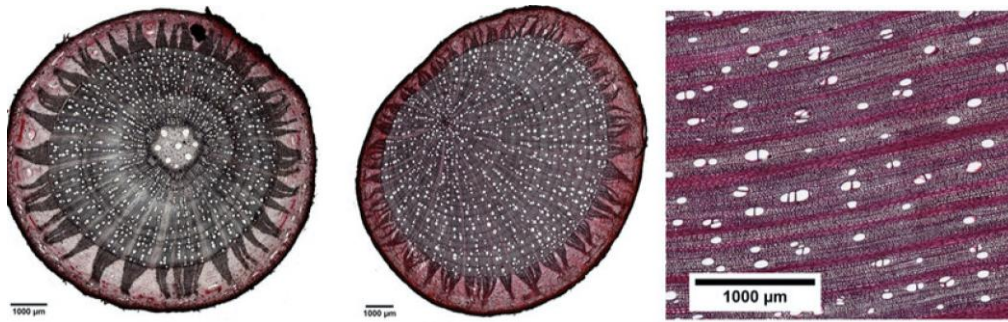


Figure 8 Microscopical images of cross-sections of different parts of cacao tree: branch (left), root (middle) and stem (right).
These pictures were taken in cacao tree grown in Sulawesi, Indonesia, by Kotowska et al. (2015).

León's descriptions state that qualitative features are similar between the branches and the trunk, yet differ quantitatively. The main differences are in vessel diameter, vessel frequency and fibre length. The diameter of vessels decreases in height towards the branches yet simultaneously the frequency of vessels increases (León, 2015; Kotowska et al., 2015).

A very recent study investigated the wood anatomy of five different *Theobroma cacao* biotypes from Ecuador: Criollos, Forastero, Trinitarios (Criollo + Forastero), Aromatico (National) and its clone CCN51 (Zhinin et al., 2019).

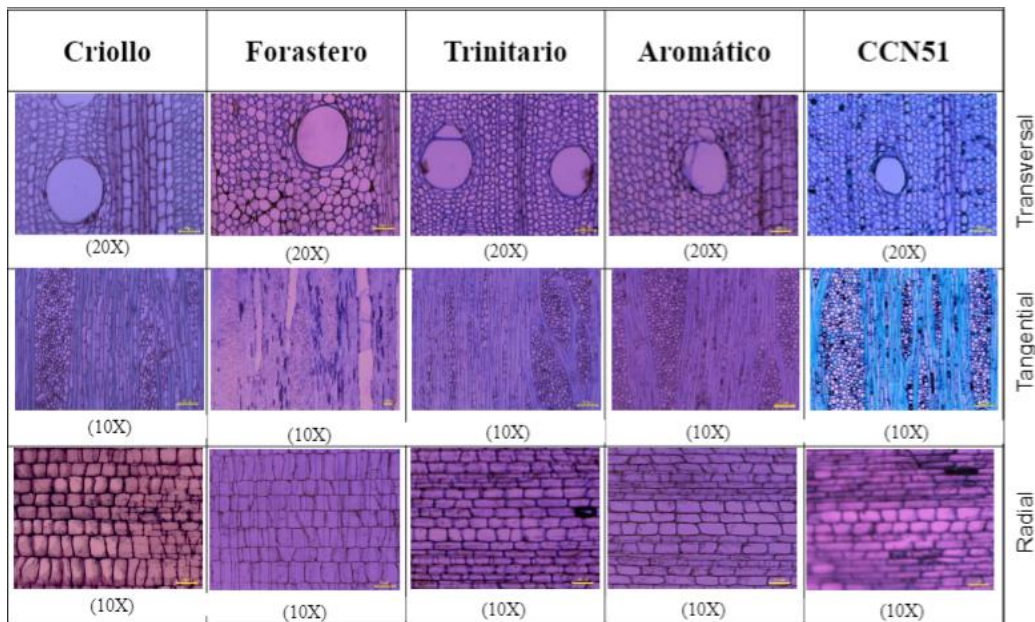


Figure 9 Microscopic images of the wood of five *T. cacao* biotypes in their three anatomical planes (From top to bottom: transversal (20X), tangential (10X) and radial (10X)) (Zhinin et al., 2019).

Similarly to the descriptions found in IAWA and those from other authors, Zhinin, et al. (2019) described distinct and indistinct ring boundaries, simple perforation plates, axial parenchyma diffuse rays with multiseriate portions as wide as uniseriate. Furthermore, the presence of prismatic crystals was only found in the Piuntza site, the site most northwest. The microscopic wood characteristics seem to reflect the morphological variability of the varieties studied by Zhinin et al. (2019).

Quantitative features:

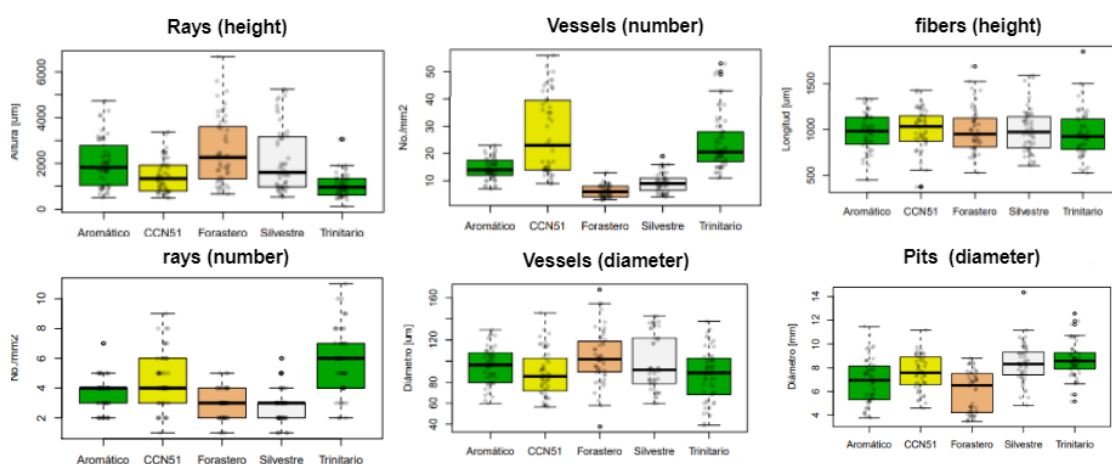


Figure 10 Box plots showing the variability of quantitative characteristics (Zhinin et al., 2019).

A more detailed tree-ring analysis of cacao trees, through dendrochronological methods, can provide more information about their growth, reaction to climatic trends and extremes.

Furthermore, even the influence of cacao swollen shoot virus (CSSV), ecological site conditions and the geographical location have on their health and physiological processes might be better examined through tree-rings analysis. Dry seasons between December and March mark a seasonality peculiar of West Africa, which might be reflected in cacao tree rings. Such studies may help in the selection of cacao's varieties or ecotypes most resistant and resilient to drought.

1.4 Research objectives

Dendroclimatological and dendroecological studies can provide insight into the way cacao trees reacted in the past and give hints about potential reactions in the future, which might depend on site, farming practice, variety and many other factors still under research. How cacao trees will respond to a changing climate is currently still unclear (Lahive et al., 2019). By exploring the wood anatomy of cacao trees, their structure, ring formation, influence of climatic factors and spatial differentiation, the understanding of cacao's resilience towards climate change can be improved.

The main research question under investigation is: do cacao tree rings deliver information about the reactions of cacao trees to climate change?

The aims of this master thesis are to:

- Investigate the wood anatomical properties of cacao trees and their spatial variability
- Understand whether cacao trees have annual tree rings and whether these are more visible at certain sites
- Identify and describe cacao tree rings with anatomical features
- Detect seasonality in the wood structure
- Understand how climatic conditions influence tree growth
- Understand cacao trees' resilience towards a changing climate and the related spatial differentiation
- Investigate the impact of drought on tree growth

With a case study in Ivory Coast and the collaboration between Barry Callebaut, WSL research institute and the University of Zurich, this master thesis will address the above-mentioned topics.

2 Material and methods

The tree samples were indispensable components for this thesis, since the whole project relies on their availability and quality. The samples were collected during two different sampling trips. This chapter describes the sampling trips, procedures and the preparation in the lab.

2.1 Sampling trips

2.1.1 First sampling trip

Before starting a master thesis on a species where dendroecological studies done so far are very few, a first insight into cacao trees' wood anatomy was needed, for better structuring the project. This was attempted in a first sampling trip which took place in July 2019. In company of another research group doing research for Barry Callebaut some samples were collected. The tour was from Abidjan to the central part of southern Ivory Coast where most of the cocoa is produced, passing by Divo, Issia, Gagnoa, Oumè and up to Daloa.

Also the city of Man was reached, which is almost the most northern region where cocoa is still produced before the northern savannah area starts. This is also one of the mountainous regions and the northern Muslim conflictual area during the civil war. The tour continued towards Soubre, ending up in San Pedro which is by the sea in the southwest. From San Pedro the way back to Abidjan was on a street parallel to the sea. The sea was not visible due to the surrounding palm plantations that seemed never-ending. On the last day, also some farms in the northeast near Abengourou were visited.

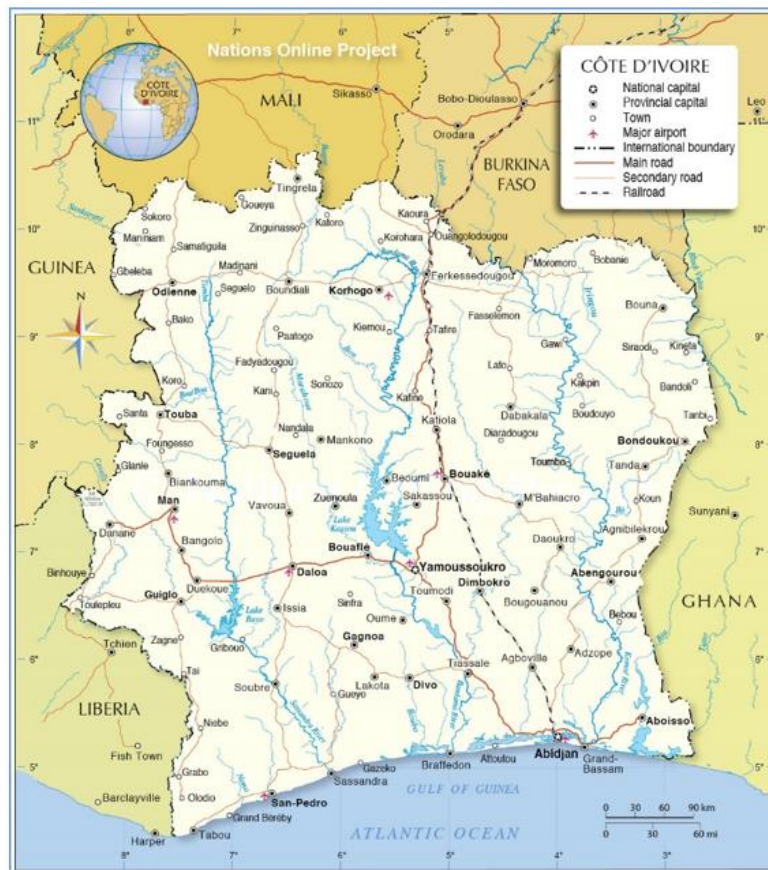


Figure 11 Political map of Ivory Coast. Source: nationsonline.org

The other research group had to visit more than 100 farms in 8 days, which meant only 5-10 minutes time per farm visit. Most of the roads in Ivory Coast are muddy or dusty and full of holes, which makes the mobility quite difficult even with an off-road vehicle. Despite spending many hours of the day in the car, the time for taking samples was severely limited and dependent on Barry Callebaut’s research group. This was further complicated since many farms had to be visited. Sometimes a disk was cut from a dead tree which took longer than 10 minutes, so to compensate, other sites would not be sampled. During this trip, a lot about cacao tree farms, the related details and differences were noticed and observed. The samples were collected far away from each other, scattered on the southern Ivorian area, yet they could still give a good first insight. There was not enough time to describe the farm or the tree sampled, neither to ask some farmers about their management practices. Therefore, to strengthen the research a second more concrete sampling trip was planned. More details on these samples are listed in the sampling description chapter.

2.1.2 Second sampling trip

Thanks to the samples from the first trip, areas of higher interest were identified and a second more focused sampling trip was planned. This time the supervisor of this thesis Dr. Paolo Cherubini joined the sampling, accompanied by the same driver as in the first sampling trip Mr. Franck Bernard Lago. The entire trip was planned with the help of Barry Callebaut's sustainability team and their Katchile database. Four different locations were selected. The aim was to visit the farms at the very north of the cocoa belt and in the central areas. Using the mapped farm-polygons of Katchile's database, some farms were identified in Vavouà, a small village between Daloa and Seguela. This was the first location and it took more than 8 hours to get there from Abidjan. Then a few farms near Daloa city were selected, some near Gagnoa city and some in Kouameziankro, a village nearby Abengourou. Barry Callebaut's local team in Ivory Coast informed the farmer coaches, about the visit and shared their contacts. Before arriving at the locations, the coaches were contacted via phone to agree on a meeting point which would sometimes be at the cooperative where the coaches worked, other times in the middle of a village. The coaches were always ready to show the cooperative or warehouse where the cocoa beans are collected from the farmers, then cleaned and further transported to ports for shipment to Europe.



Figure 12 Cocoa warehouse in Ivory Coast.

As soon as arrived, the coaches usually invited us to sit down on some chairs together with the farmers and during a short conversation all the attendees presented themselves. We

were then taken to the farm where we could ask the farmers several questions. A survey had been prepared on a mobile phone using the application Survey123 from ESRI. The location of the farm was recorded as well as all the answers the farmers could give to the questions. Unfortunately, they were not very sure about the age of the plantation or the specific age of any tree. Also regarding the fertilizer application and pruning activities the farmers were not sure when exactly certain things were done, because they are often not the only ones working on the farm. In fact, they usually have several helpers, which were sometimes present during our visit. Moreover, cacao farmers in West Africa are often extremely poor. The communities they live in struggle with many problems including transport limitation and availability of clean water.



Figure 13 Cocoa farm with farmers and helpers in Ivory Coast.

About 10 to 15 samples per location were collected and stored with the farmers' answers to the survey. The coaches, the farmers and the helpers as well as others working in the cooperative were always extremely nice and welcoming. On some farms, they were so interested in the research that they participated and helped to sample. After explaining to them about this research, even contacts were exchanged with those who were interested in the results.

More pictures can be found in the appendix; sampling trips picture gallery.

2.2 Sampling methods

There are two different kinds of wood samples useful for dendrochronological analyses; cores and disks. The easiest samples to get are cores, because to take these, the tree is only injured and not felled. The sampling with a corer on cacao trees is quite easy, as the wood is not very hard. Since cacao trees are quite small and have a small diameter, only one core per tree was sampled at about one meter height.



Figure 14 Corer in a cacao tree and an extracted core from Ivory Coast.

More difficult is taking disks, also called cross sections. Wood disks contain more information, because the tree rings can be compared along different radii. However, a tree must be already cut or be felled to get a tree disk.



Figure 15 Cacao tree disk from a tree which was already cut in Ivory Coast and the same disk after polishing/ sanding it in the workshop.

2.2.1 Sampling sites

The set of samples, coming from the first trip contains samples from locations far away from each other. The sampling took place in the end of July 2019 during the wet season, in fact, it was raining on some farms and only the northern areas seemed very dry.



Figure 16 Sample set 1 with samples collected during the first sampling trip.

The second set of samples contains samples from the four selected locations. In each location two to three farms were visited and about five samples per farm were collected. The four locations are Vavouà, Daloa, Gagnoa and Abengourou. Vavouà was selected because it is the most northern place where Barry Callebaux' Katchile mapping database has mapped farms and it serves to see how northern trees differ from central ones. Daloa is also important for the northern area and useful to compare with Gagnoa which represents the central area. These three locations made also logistically sense since we had to pass through Gagnoa and Daloa anyway to get to Vavouà. To also have some samples from the eastern part we went to a village called Kouameziankro near Abengourou, which is also the area with farms mapped at the most northern part of the eastern side.



Figure 17 Sample set 2 with samples collected during the second sampling trip.

This second trip took place in February 2020 during the dry season. In fact, it never rained on the farms and the northern farms were often extremely dry.

2.2.2 Samples descriptions

The first data set consists of 50 samples, 40 cores, 7 stem disks and 3 branch disks. The table below shows a summary of the samples classifying them between alive and dead, a number of samples with swollen shoot (SS*) and a number of samples that are hybrids.

Unfortunately, some of the samples were not useful for analysis, due to wood decay or breaking during the trip, yet luckily most of them were in good condition.

Table 1 Summary of first data set.

Type/Status	alive	dead	hybrid	SS*	Total
core	38	2	6	2	40
disk	4	3			7
branch	3				3

Most of the cores were retrieved from living trees, whereby only trees with a robust stem to ensure minimal injury were sampled. The disks and branches of living trees were retrieved from trees that had already been cut, a whole healthy tree was never felled. Hybrid trees were easy to identify since they have red pods in comparison to Forastero, the typical West

African variety with green pods. Trees with swollen shoot are extremely hard to detect for non-experts. Either the stem or upper branches are swollen but it could also be in the roots, which makes its identification challenging (Oro et al., 2012). The other research group or farmers met on the ground helped to find trees attacked by swollen shoot. Experts from Barry Callebaut's team revealed that many affected trees with swollen shoot can be found between Oumé and Issia. As visible on the map (figure 16) all the samples are very far away from each other making the comparison very difficult. Nevertheless, they give an insight into some of the areas and a first impression of cacao trees' wood in Ivory Coast.

The second sampling trip was more tailored to the needs of this research. A total of 56 samples, 52 cores and 4 disks of only living trees were collected. Again, no living trees were killed and the disks came from trees that had already been cut. Although no trees were sampled with identified swollen shoot, at least the farmers were asked some questions about their farm.

Table 2 Summary of second data set.

ID	LOCATION	Hectares	Climate	Year	Pruning	Fertilizer	Diseases	Cores	Disks
LOC4B	KOUAMEZIAMKRO			2000	yearly	yes		5	0
LOC4A	KOUAMEZIAMKRO	3	Dry	2000	yearly	yes	Black pod	7	1
LOC3C	GAGNOA	2.5		1990	yearly	yes	Laurentis	9	0
LOC3B	GAGNOA	1	Dry	1997	2/year	yes	Laurentis	4	0
LOC3A	GAGNOA	1		1997	yearly	no	Laurentis	4	0
LOC2C	DALOA	3.5	Dry	2006	2/year	yes	Myrid	5	0
LOC2B	DALOA	2	Dry	2006	2/year	yes	Some dead	5	0
LOC2A	DALOA	2	Dry	2006	yearly	yes	Not many	5	0
LOC1B	VAVOUÀ	4	Same	2008		no		5	3
LOC1A	VAVOUÀ					no	Swollen shoot	3	0

The table 2, summarizes the farmers' answers to the survey questions and the number of samples collected per farm. There are some gaps because asking the farmers was sometimes challenging, either due to cultural or language barriers. Some of the farmers have never been asked some of these questions and are either not sure about the answer, do not understand the question or simply do not know the response. Almost all of the farmers said that last

years' wet season was quite short and that they do have the feeling it is getting drier. This will need to be proved with the available climatic data.

Table 3 Further comments on the second data set.

ID	Fertilizer	Comments	Cores	Disks
LOC4B			5	0
LOC4A	yes		7	1
LOC3C	yes	Good soil	9	0
LOC3B	yes		4	0
LOC3A	no	Good soil, trees grow differently	4	0
LOC2C	yes	Trees die due to drought	5	0
LOC2B	yes	A lot of fertilizer, one sick tree unknown illness	5	0
LOC2A	yes	A lot of fertilizer, not all trees produce equally	5	0
LOC1B	no	Insecticide, stress due to drought, bigger trees produce more	5	3
LOC1A	no	Good soil, when it rains more branches	3	0

Some farmers did share some further details regarding the soil conditions of their farms and the way cacao trees grow and produce cacao pods (table 3). Farms without fertilizer applied usually are farms commented as with fertile soil. Some farmers highlighted the fact that some trees died due to drought and others due to diseases. Moreover, some farmers apply more insecticide than fertilizer. Information on production patterns or performance about specific trees was not shared, probably because the farmers did not know or remember exactly every tree, since their farms are between 1 and 3 hectares large. However, some said that not all of the trees produce equally and trees that grow more seem to also produce more. Dendroecological analyses might be an added value to this assumption.

2.3 Samples' preparation

In this section the exact methods of samples' preparation are described. Almost all samples underwent a cleaning of the upper part of the core or disk in order to make ring-structures clearer. Then some were used for chemical analyses, others were embedded and for others, only the ring width was measured. An overview of the samples that underwent those

process can be found in the appendix. Only the clearest, most intact or most interesting samples were prepared for further analysis.

2.3.1 Preparation for ring width measurements

For ring width measurements the cores and disks must be polished. The wood sanding machine can polish at different grades. In the case of cacao trees, polishing too much may make it harder to identify tree rings (personal observation). If a sample is polished, material from one ring is mixed up with material from neighbouring rings, therefore, after polishing, it is unreasonable to perform chemical analyses such as stable isotopes analyses. To prepare the surface to be clearer for chemical analyses, the microtome was used to cut the upper part without mixing wood dust from and into different rings (figure 18).



Figure 18 Cutting the upper surface of a core with microtome. Left is before cutting and right is after it.

Once the rings were visible, their width was measured using the software TSAPWin. The samples were placed on the measuring table, i.e., a table that can be shifted from ring to ring while measuring the distance.

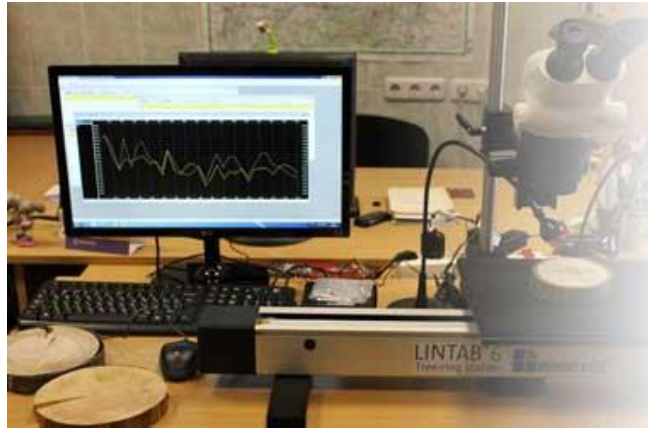


Figure 19 Measuring ring width with TSAPWin. On the right, the microscope and moving table and on the left, the monitor showing ring width values on a plot. Source: <https://hidrolab.lv/tree-wood-analysis-products/>

Another innovative option to measure tree rings, was by taking high-resolution pictures of the samples and measuring the ring width on the WINDendro software directly. Loïc Schneider (WSL) has developed a prototype program that takes pictures and moves the table automatically depending on the users' needs. These high-resolution pictures were then stitched with PTGui and the result was one picture of the whole core as shown below.

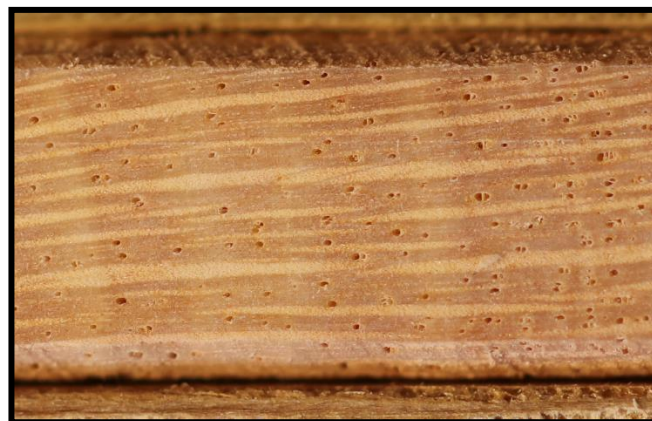


Figure 20 Sample core of a cacao tree from Ivory Coast. The first picture is the entire core and the second is a zoomed in area.

2.3.2 Preparation for wood anatomical analyses

For wood anatomy analyses the samples were embedded in paraffin and cut with the rotatory microtome or directly cut with the microtome.

The embedding procedure took significantly more time but ensured that the cells remained intact and made the cutting procedure easier and faster. Initially, the samples were split into smaller pieces of wood.



Figure 21 Cacao tree core split into smaller pieces.

These small pieces were inserted in a machine and bathed for 24 hours in paraffin and alcohol at different percentage degrees for washing. This process is important to make sure that the paraffin enters the cells. The next step was to get the small pieces embedded in paraffin holders to ensure stability.

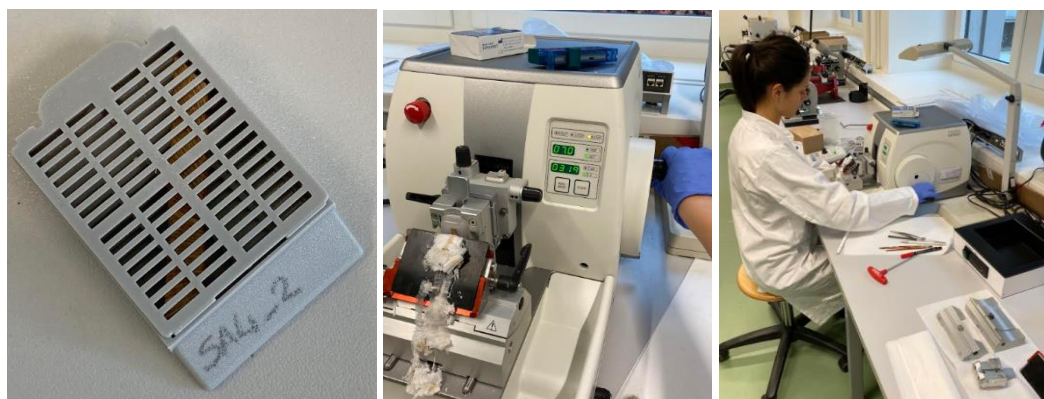


Figure 22 Embedding samples in paraffin and cutting with the rotatory microtome.

Once the samples were embedded, they could be cut with the rotatory microtome as seen in figure 22. With the rotatory microtome, very thin sections can be cut up to 7 micrometers. This is possible thanks to the paraffin which helps stabilizing. Once the samples were cut, they were placed in the oven for the paraffin to melt. They were then bathed in 9 different liquids for 15 minutes each. The first two baths were in xylol and the next two in alcohol to wash away the remaining paraffin. Then in safranin and astrablue where the cells are stained, followed by again two baths in alcohol and two last baths in xylol, to get rid of

water rests. The stained samples are usually then covered with Canada balsam and a thin transparent glass and placed in the oven to dry for 12 hours. The Canada balsam with the glass on top and a magnet to increase the pressure, makes sure that the sample properly dries and stabilizes in the oven. Such microslides or microsections can then be kept forever.

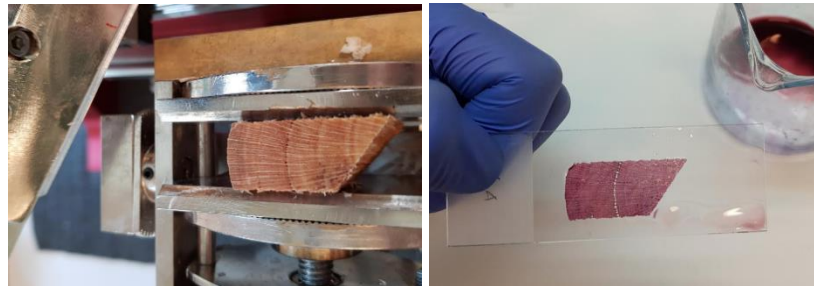


Figure 23 Cutting directly with the microtome and staining with safranin and astrablue.

It was not necessary to embed all samples. In the case of cacao, most samples could also be nicely cut with the microtome directly, depending on the wood quality of the sample and the presence of decaying parts. After splitting and a quick bath in water to make the sample a bit softer, microslides can be cut on the microtome with a thickness of 15 to 20 micrometers. The thinner the cut, the better the visibility of wood structures. After cutting, the samples were placed on glass holders with glycerin until they were stained (figure 23). The staining process is slightly different than the one for the embedded samples. First safranin and astrablue were poured on the sample. After 60 seconds the excess of the staining and glycerin were washed away with water. Then with different alcohol degrees and finally with xylol, water rests were washed away. As with the embedded samples, they were then covered with Canada balsam and placed in the oven. If these processes were done properly, the results were perfectly stained cell structures with no air bubbles. These could then be scanned and used for wood anatomy analysis on WINCell or ROXAS.

2.3.3 Samples preparation for radiocarbon analyses

In order to perform ^{14}C dating and ^{13}C stable isotope analyses, it was important to split the rings as accurately as possible. As explained above the surface can be prepared with a microtome rather than a sanding machine to avoid mixtures. If the rings were visible enough, they could be split directly with a scalpel. If necessary, the microsections,

previously prepared for wood anatomy, would provide help in identifying tree rings. The samples were stored in small capsules for cellulose extraction and isotope measurements.



Figure 24 Cutting tree rings for chemical analysis.

2.3.4 Samples preparation for stable isotope analyses

As explained in the section above, the splitting for ^{14}C and stable isotope analyses is the same. However, for stable isotope analyses, it is not always necessary to extract cellulose. The extraction of cellulose gives a clear environmental signal, especially when not only ^{13}C is of interest but also ^{18}O . This is due to the fact that wood contains multiple components that have different isotope ratios and their relative proportion can change over the lifetime of a tree (Saurere et al., 2017). However, in the case of young trees, like the cacao samples, this fact loses importance. For cellulose extraction more material is needed, about 5-10 mg. The alternative is to analyse the wood directly without extracting cellulose, whereby 1 mg of material is enough. The final decision was to perform wood analyses of stable isotopes of selected samples with clearer rings.

2.4 Samples' measurements and analyses

After preparing the samples, the ones with clearer structures and of best quality were further measured. Disks were put under a microscope to measure the ring widths, or using the microsections to measure the ring widths and also cell lumen. Then with TSAP crossdating was attempted, yet turned out to be extremely hard especially due to the young age of the trees. The samples with clearer rings and showing patterns with relation to climatic data or good correlation with other trees were further investigated into more detail

and some even underwent chemical analyses such as ^{14}C dating and stable isotope measurements.

All the samples with ring width measurements were fed into an R-Script developed by Dr. Laurens Valentin Michiels van Kessenich. After visiting EMPA, an interdisciplinary Swiss research institute for applied materials sciences and technology, together with informatics experts and physicists the possibility of using machine learning for tree-ring recognition was discussed. Since the collected cacao tree samples have unclear rings, a new innovative approach for recognizing or analysing tree rings was explored by using R-Studio. The created R-Script takes the ring width measurements per sample and the related climatic data and initially checks the correlation. Assuming each tree ring is an annual ring and the climatic data is also per year, the correlation is calculated. Due to the uncertainty on whether all rings are indeed annual rings, the script performs permutations whereby rings are merged or added up together to improve the correlation with climatic data. Precipitation data was used, whereby some samples resulted in a considerably improved correlation between ring width and precipitation when merging two rings together. Other samples improved the correlation when merging twice two rings together at different years. These observations helped to understand which rings have a higher chance to be annual tree rings and which rings might be caused by intra-annual density fluctuations. Moreover, detecting which rings merged together to better correlate with precipitation, gave a clue on which border needed further investigation.

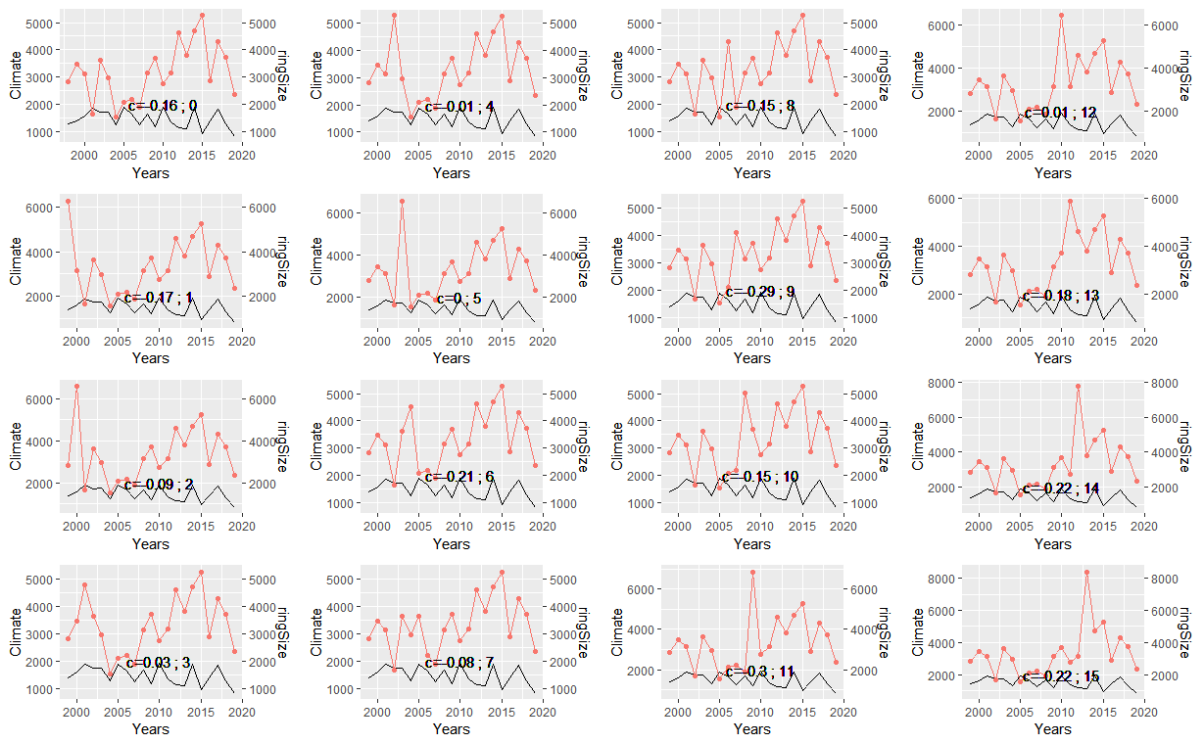
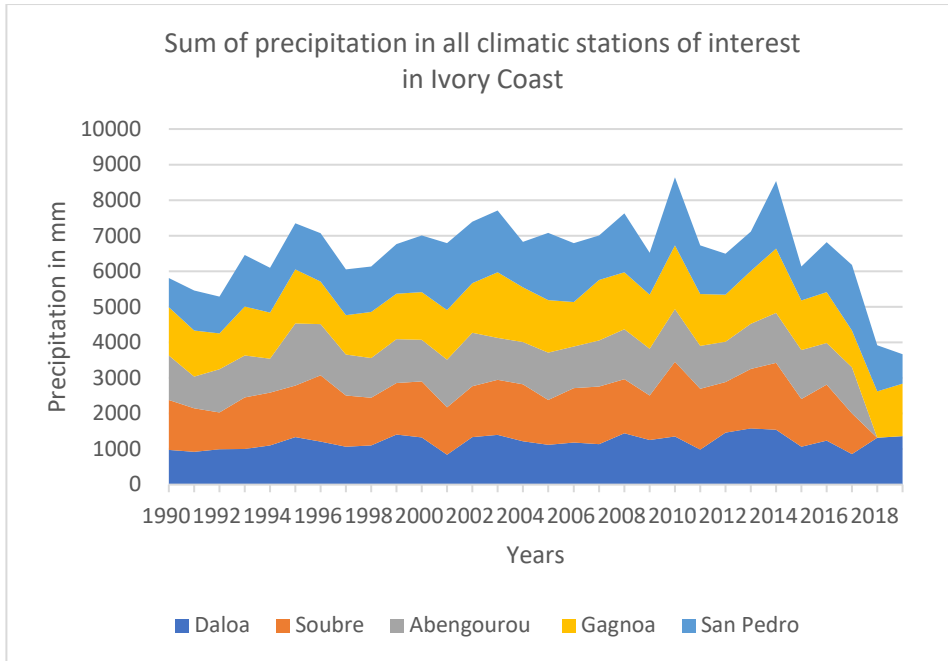


Figure 25 Grid of permutations. The first graph shows the data without any permutations, the following graphs show different permutations and the corresponding correlation with precipitation data. Source: an example of an R-Script output.

The image above shows a grid of permutations resulting from the R-Script. The red line represents the ring width of a specific core and the black line the precipitation data of the region where the core was taken from. The first graph shows no permutation, so all the rings identified in the core and their width, the correlation is of 0.16 and therefore weak. The rest of the graphs show how the correlation changes when combining different couples of rings. The highest correlation reached is 0.29 and it is reached by putting the ring width of ring number 9 together with the one of number 10.

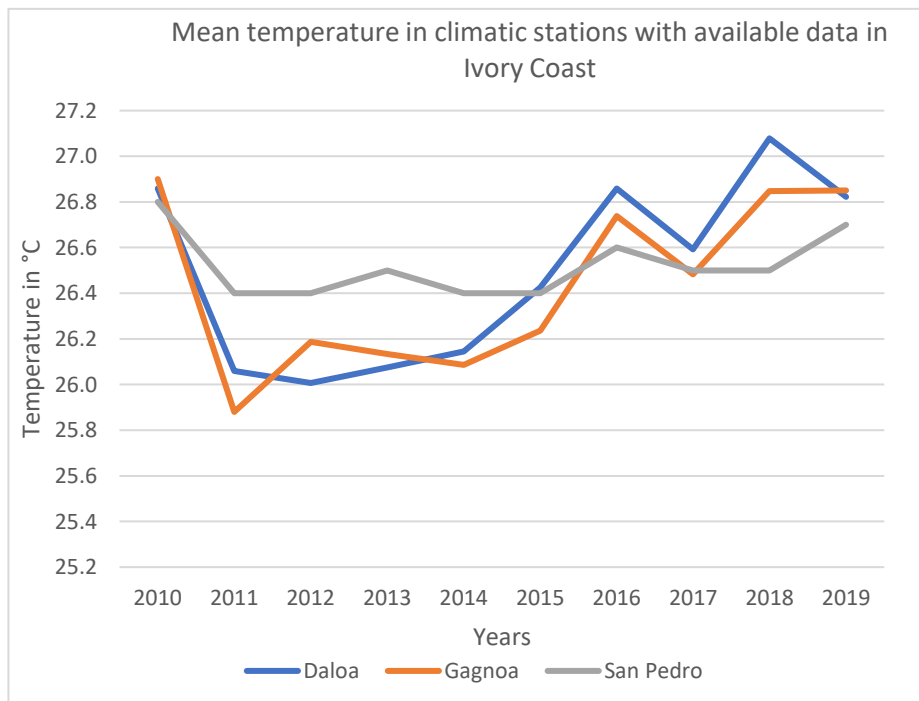
2.5 Climatic data

There are regional climatic stations in Ivory Coast for almost all regions which were visited for this project except for the city of Man due to the past conflicts, which made data collection difficult. A local researcher, Dr. Agathe Dié (University Cocody-Abidjan, Ivory Coast) shared precipitation data for Gagnoa, Daloa, Abengourou, Soubre and San Pedro for the years 1981 up to 2017 and in some cases even for the year 2019. Moreover, she also shared some location temperature data for the past 10 years.



Graph 1 Sum of the precipitation for the different climatic stations of interest for this study in Ivory Coast. Source: data from Dr. Agathe Dié.

The graph above shows the annual changes of precipitation in Ivory Coast at different climatic stations. For Abengourou and Soubre the data is only available until the year 2017. From this graph, we can see that there are some years which were clearly wetter than others.



Graph 2 Mean temperature in climatic stations of interest for this study in Ivory Coast. Source: data from Dr. Agathe Dié.

Since the climatic data from Dr. Agathe Dié does not include all regions of interest, TRMM (Tropical Rainfall Measuring Mission) data was also collected. TRMM is a joint mission of NASA and the Japan Aerospace Exploration Agency aiming to study rainfall for weather and climate research purposes (TRMM, NASA, 2015). NASA Earth Data provides an online platform called Giovanni which allows users to visualize geophysical parameters and retrieve data for a selected location of the Earth (Giovanni v4.33, NASA).

All the coordinates of the locations of the samples were plotted in QGIS, a Geographic Information Systems platform for viewing, editing and analysis of spatial data. After creating a grid on top of all the samples, the grid boundaries were used to retrieve climatic measurements. On the Giovanni NASA platform TRMM precipitation measurements in mm per month were selected, then using the bounding box coordinates and monthly data average for the selected area were retrieved.

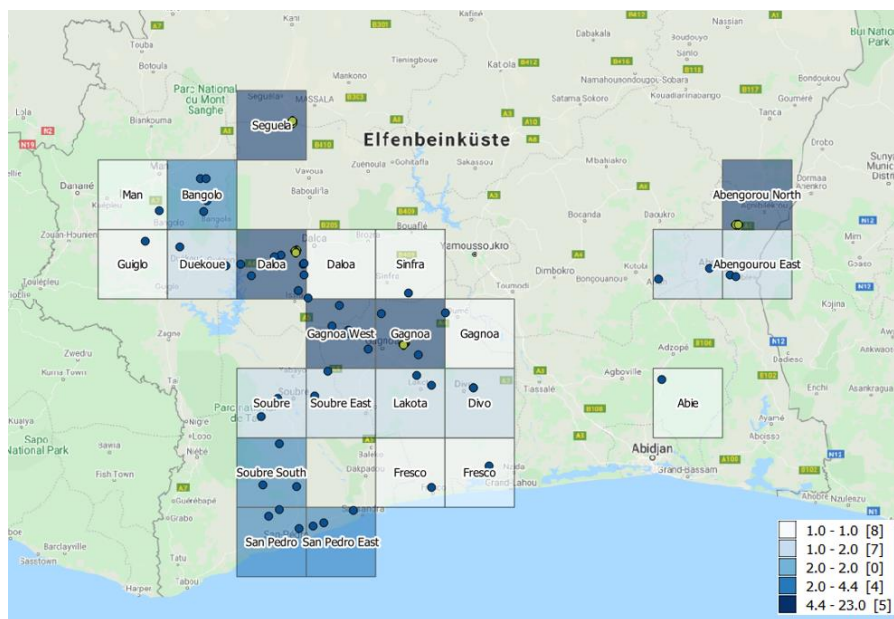


Figure 26 Tree samples collected in Ivory Coast and a grid of about 50 km on top. The darker the grid square the higher the number of samples within it.

3 Analyses and results

In an initial part of the analysis, investigations of the wood anatomical properties of cacao trees were made to identify whether cacao trees have annual tree rings and whether these are more visible in certain locations. This part of the analysis is considered to be qualitative, since it is mainly about the description of cacao wood samples.

The second part of the analysis is more quantitative. Ring widths were measured, correlations with climatic data were calculated and even mass spectrometer measurements were performed, with the intention of validating qualitatively described features of cacao trees' wood. This part covers the identification of intra-annual density fluctuations, ring boundaries, seasonality in the wood structure and how climatic conditions influence cacao trees' growth.

3.1 Qualitative analyses

3.1.1 Feature identification

This section presents wood anatomical properties identified and qualitatively analysed from cacao tree samples. In order to identify the wood structures, the samples were first looked at macroscopically and then microscopically, using microsections. By removing a thin layer of wood from the cores or by slightly polishing the disks, the wood surface structures became clearer. In some samples the ring borders were clearly visible when looking at the polished core or disk, in others, it was more complicated.

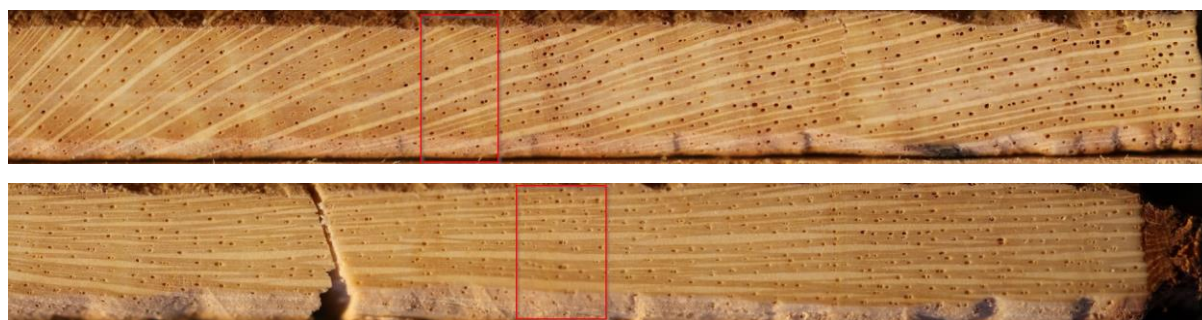


Figure 27 The first core (LOC3A4) has rings which appear to be very clear, especially in comparison to the second core, below (LOC4A5) which has extremely unclear rings.

Some samples were further investigated by cutting thin slices of the cores and disks of about 15 μm . How these sections were prepared is explained in the materials and methods section above. Most of the samples had clear vessels of varying sizes. Ring borders were very different between samples and also showed differences within a single sample. In some cases, it seemed like the cells were smaller in the late wood before the ring border and bigger in the early wood. Most of the rings are made out of early wood and the late wood is often only a smaller part of the rings, whereby cell walls get thicker and the cell lumen gets smaller. Some of these cells are even hard to recognize. Parenchyma rays were abundant and often very large, and detected as multiseriate as well as uniseriate in all samples. At some ring borders, the parenchyma rays seemed to expand as they reached the ring borders and shrank again after.

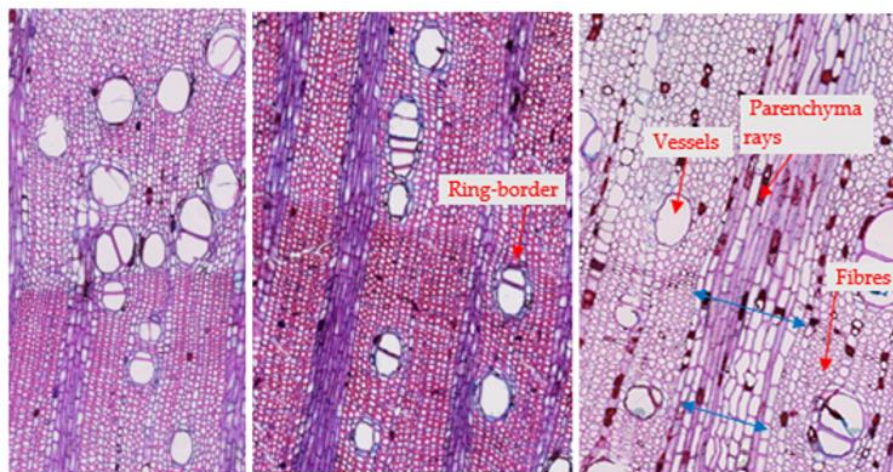


Figure 28 On the left figure, the early wood, ring-border and late wood are displayed. The vessels are smaller in the late wood than in the early wood. On the middle figure, another clear tree-border is displayed, whereby the fibre cells are thicker in the late wood. The third figure shows broader parenchyma bands at a structure similar to a ring-border (AB2 left and middle, DI9 right).

An interesting feature detected were prismatic crystals, which were only visible in the microsections, yet often very abundant. Figure 29 is a rotated picture of a stained microsection with a polar filter polarizing the light and emphasizing the crystals. All of the crystals are found within the parenchyma rays, sometimes in uniseriate rays and sometimes in multiseriate rays.

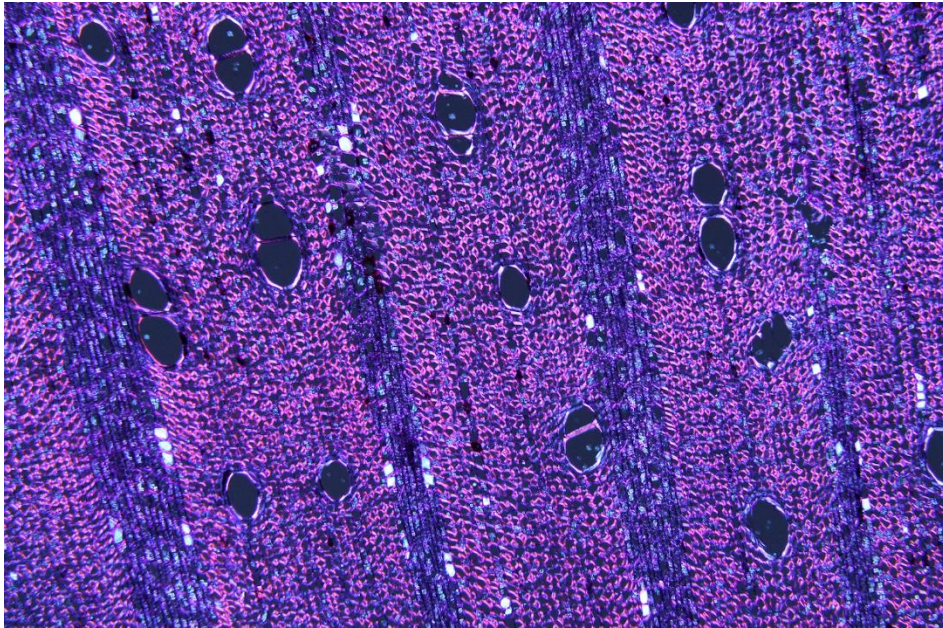


Figure 29 Scanned microsection with polarized light filters with visible prismatic crystals in cacao tree core (AB2).

In some samples gum-ducts were found, similarly to the samples analysed by León in 2015. Such conducts are formed when the tree is disturbed. Not all trees have this kind of reaction. In some cases, the gum-ducts were not through the entire circumference of the disk and some samples also had significantly more gum-ducts than others.

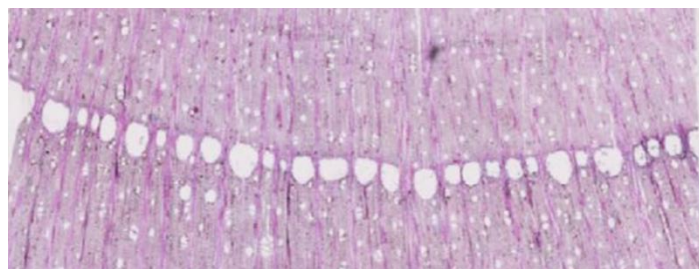
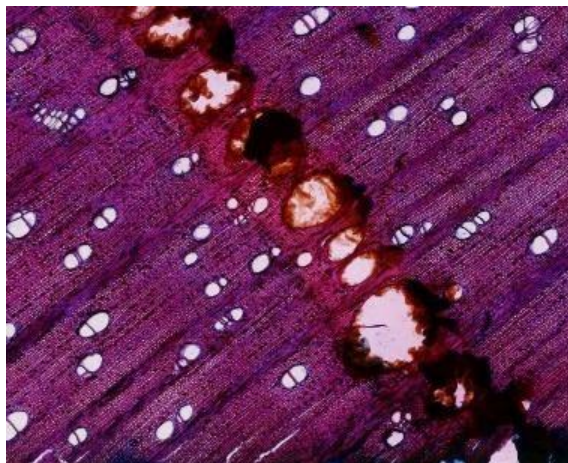


Figure 30 Gum-duct in sample (IS1 top, SP1 bottom).

The gum-ducts were usually easy to identify, even without a microscope. The only difficulty was that some cores were broken and it was hard to tell whether there had been a gum-duct before the core broke or not.

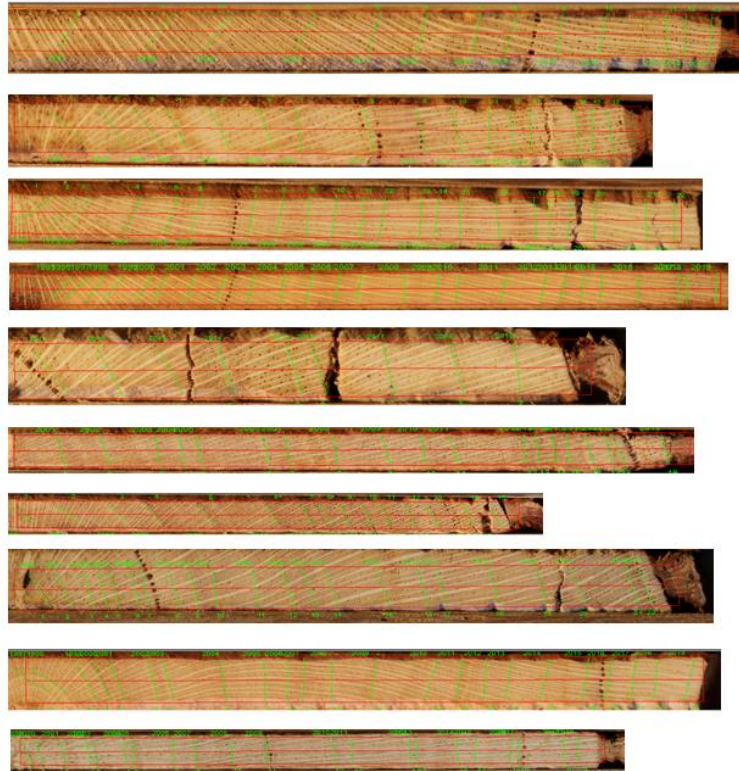
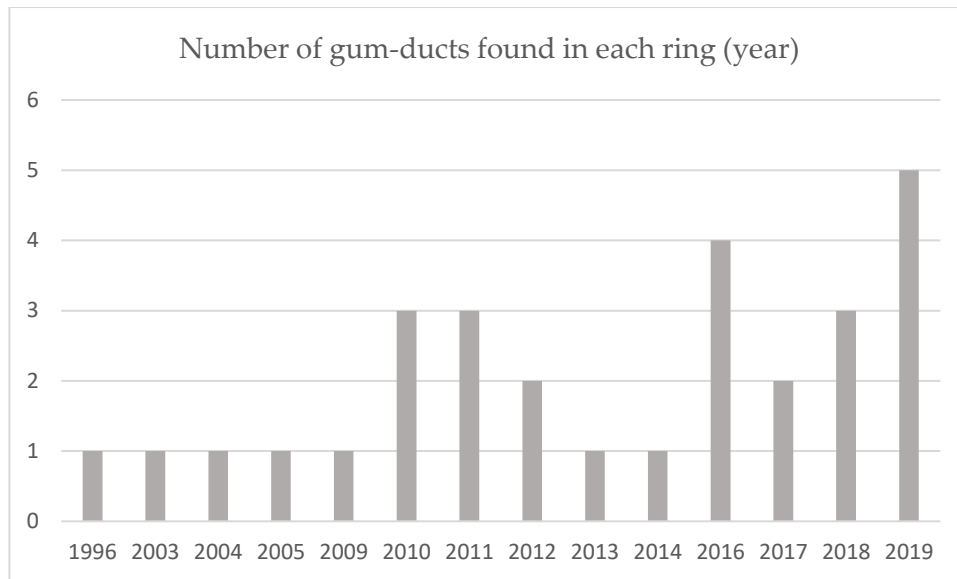


Figure 31 Ring detection with DendroWin and identification of gum-ducts per ring.

Assuming that all rings are actual annual rings, the number of gum-ducts per year were summarized, considering only cores with clear gum-ducts. Most of the gum-ducts were found in the latest or youngest rings.



Graph 3 Number of gum-ducts found in each ring.



Figure 32 Cacao tree stem disk from Abengourou (LOC4dA), many gum-ducts are visible and most of them are not visible through the whole circumference.

3.1.2 Growth rings description

The samples collected for this thesis that were prepared in the laboratory, showed different kinds of ring borders. Some had very clear rings like the one in figure 33. Despite even having clearly visible rings, it remains difficult to assess whether all are growth rings, whether they are annual, seasonal or even intra-annual density fluctuations.



Figure 33 Macroscopic view of a cacao tree core (LOC3B2) from Gagnoa, with very clear rings.

A qualitative score was given to describe how clear most of the rings within the core are. The score “very clear” was for very clear rings, followed by “clear”, “normal” and “unclear” rings. Very clear and clear were assigned to rings that were clear through the whole core. Normal was assigned to rings that were clear in some areas and less clear in others, which was the case in the majority of the cores and unclear were rings that were confusing and hard to see. For some samples, the wood anatomy was further investigated by preparing microsections. This was not done for all cores due to the time limitation. It ended up being quicker and easier to identify tree rings on the tree cores directly instead of using their microsections. Nevertheless, looking at the microsections helped to understand more about the ring boundaries and related anatomical features.

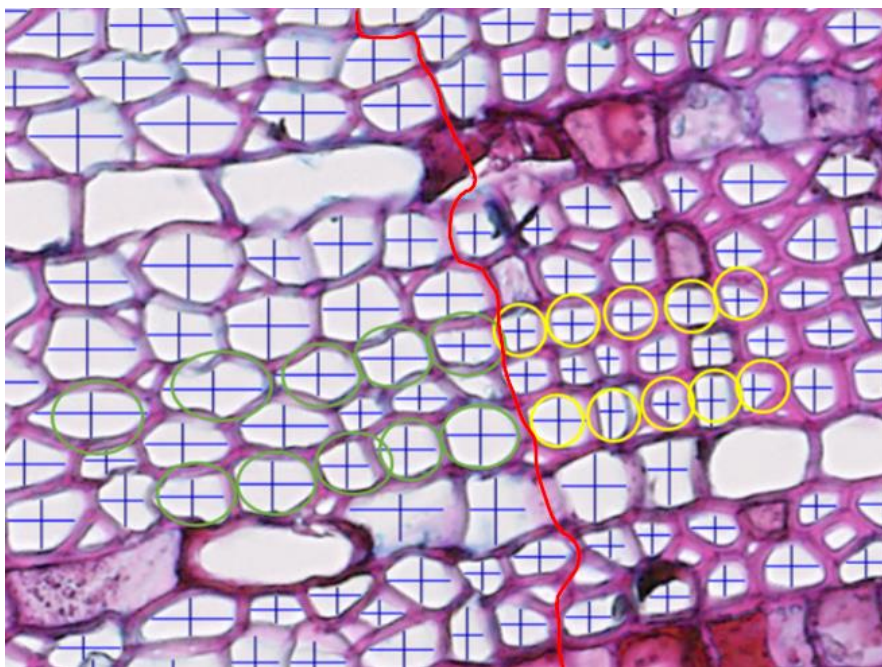


Figure 34 Zoom in ring boundaries of a microsection of a cacao tree disk (MA2).

The qualitative characteristics of cacao tree-ring boundaries show that in most cases the early wood is made up of bigger cells of thinner walls contrary to the late wood, which is also a significantly smaller part of the ring. The border between late wood and early wood (red line in figure 34) can be at times extremely hard to identify, since it is not an abrupt change but often more a continuous shift from bigger to smaller cells. In order to quantify this qualitative assessment, the lumen of late wood cells and early wood cells was measured. Following similar methods used in the literature, three microsections were loaded into WINCell, three ring borders per core were selected and for each border paths through cells in the early and late wood were drawn. A path measured and stored parameters of cells in the early wood (green circles in figure 34) and following the same path for the late wood (yellow circles). For each ring border, eight paths or rows of cells were measured, following numbers that have proven to be effective in the literature (Axelson et al., 2014; Seo et al., 2014). The result was that in most of the cases early wood cells are indeed bigger than late wood cells. The final ratio calculated showed that early wood cells are between 1.57 and 1.83 times bigger than late wood cells.

Samples of tree that had swollen shoot or that were hybrid did not show any differences in the wood anatomy. They did not either show any specific characteristic in the wood anatomy that differs from other trees with no swollen shoot or of Forastero variety. There were some tree cores and disks that had fungi or decayed wood making certain analyses impossible, but these were not necessarily samples with diseases.

3.1.3 Spatial comparison

Samples from the first sampling trip were collected quite far away from each other. The qualitative assessment of the tree rings of these samples was crucial for the preparation of the second sampling trip. Visible as points in the map below (figure 35), most of the samples with clear or even very clear rings are in the northern and central areas. Each point is a sample and its colour reflects the qualitative description of its tree rings. The areas with most samples of clear and very clear rings are the areas selected for sampling the second dataset: Vavouà or Seguela, Daloa, Gagnoa and Kouameziankro or Abengourou. The

samples from the second dataset were gathered from only these four locations and are displayed as pie charts (figure 35).

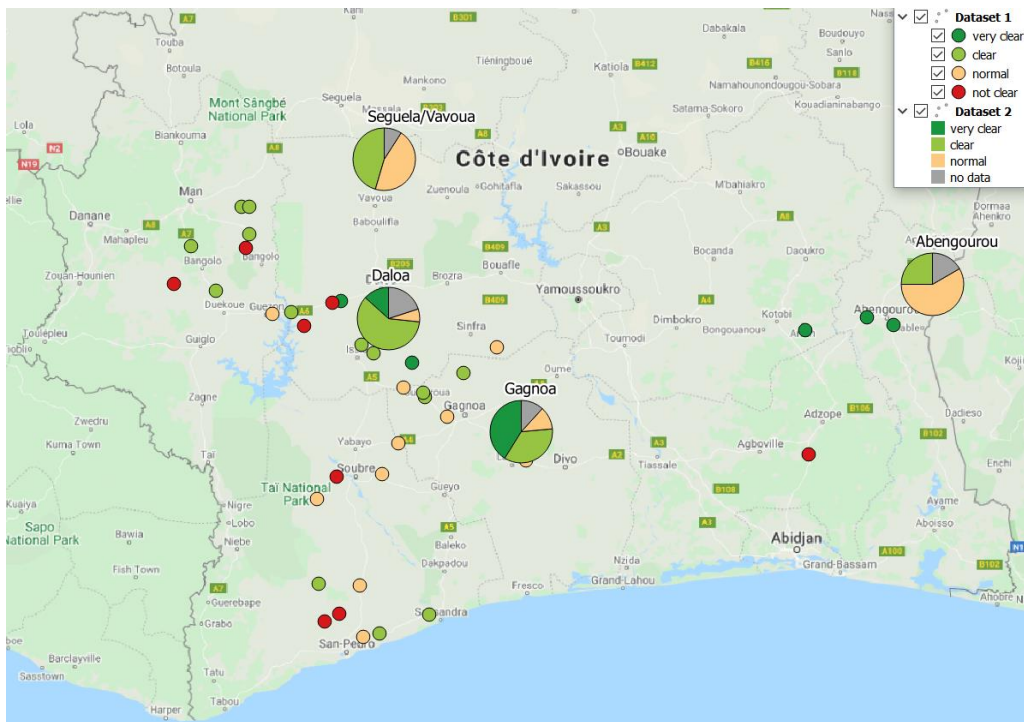


Figure 35 Map of the samples collected and their qualitative assessment. The single points are samples from the first sampling trip and the pie charts summarize the samples of the second sampling trip. The colours reflect the qualitative assessment of the tree rings.

The locations that showed less clear rings were not considered in the second sampling trip, the focus was set on areas with clearer rings. The pie charts summarize the descriptive analyses of the tree rings of all samples collected in those four locations, about 15 samples per location including cores and sometimes even disks. Areas around Daloa showed in both sample sets many trees with clear rings and even some with very clear rings. The area of Gagnoa showed only some normal tree rings from the first sample set. However, almost half of the 15 samples from the second sample set revealed very clear rings, about a third had clear rings and only a small portion showed normal rings. Seguela and Abengourou were selected because they are in the northern areas where cocoa is still produced and nearer to drier climatic zones. Samples from both of these areas showed more normal tree rings than clear ones, especially in Abengourou.

3.2 Quantitative analyses

3.2.1 Ring width measurements

The tree rings did not seem to be clearer when looking at the wood anatomy. In fact, it often seemed easier to look at the rings from further away and without polishing the surface too much. Therefore, the WinDendro tool was used to measure the ring width of the cores and TSAP was used for the disks. The distance between all rings per sample was measured and then samples were compared with each other, depending on their location.



Figure 36 Pictures of the polished cacao tree disks collected during the first sampling trip and their geographical location.

The different disks from the first dataset were collected in different areas in Ivory Coast. Two came from the northwest (GA3 and MA2), most from the central areas (IS1, DI2, SO4, SO5) and only one from the southwest (SP4). Also worthy of note is that not all disks were alive when retrieved, all details of the samples are in the appendix. After polishing and following the tree rings around the whole perimeter of the disks, the ring widths were measured at various radii per disk.

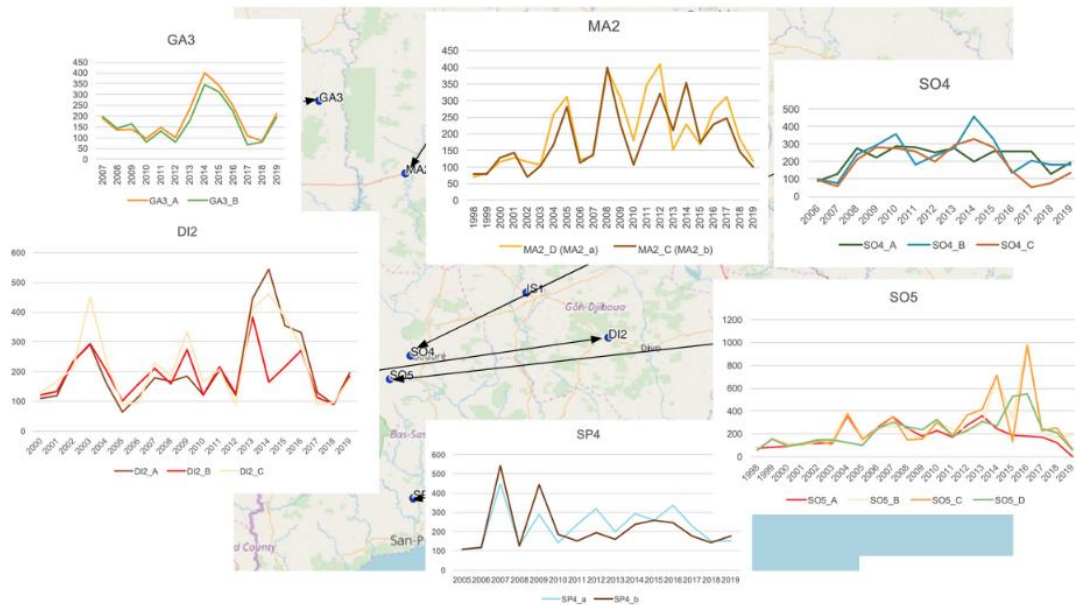
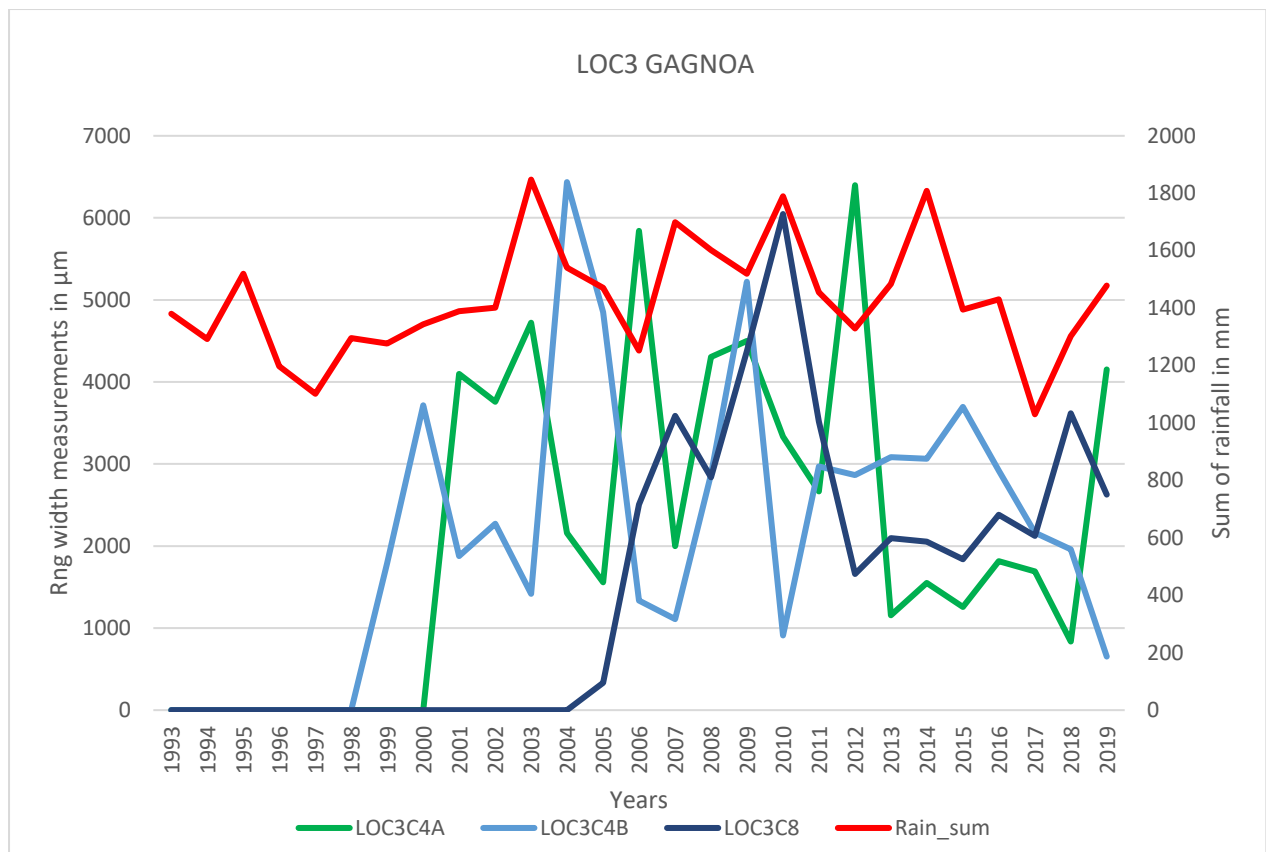


Figure 37 Ring width measurements of the polished tree disks from the first sampling trip. Each sample has a graph and the lines correspond to tree-ring width measurements along different radii of the disk.

The ring width measurements per radii are displayed in the figure above (figure 37). The samples in the northern areas have radii ring width measurements that match better than some samples in southern areas. For instance, the sample in San Pedro (SP4) shows that the ring widths measured in one radius do not correspond to the ones measured in the other radius. In contrast radii of the samples GA3, MA2 and DI2 seem to nicely crossdate.

The ring widths were also measured for tree cores and disks from the samples of the second sampling trip. All of the measurements were then compared with each other to check if they crossdate and if correlations can be found. The qualitative analyses revealed that northern and central areas like Gagnoa had tree rings which seemed clearer than in other locations. In fact, when looking at the correlation between ring width measurements and precipitation, it seemed higher in Gagnoa than in other locations. All the ring width measurements can be found in the appendix.



Graph 4 Ring width measurements of 3 cores collected nearby the city of Gagnoa and the sum of precipitation in mm for this location.

Despite not being able to crossdate as well as in conventional dendroecological studies, the ring width measurements displayed in the graph 4 show differences between the rings. Although these differences might not be annual, they could still show a seasonality reflecting the trees' reaction towards climatic changes.

3.2.2 Ring-width permutations

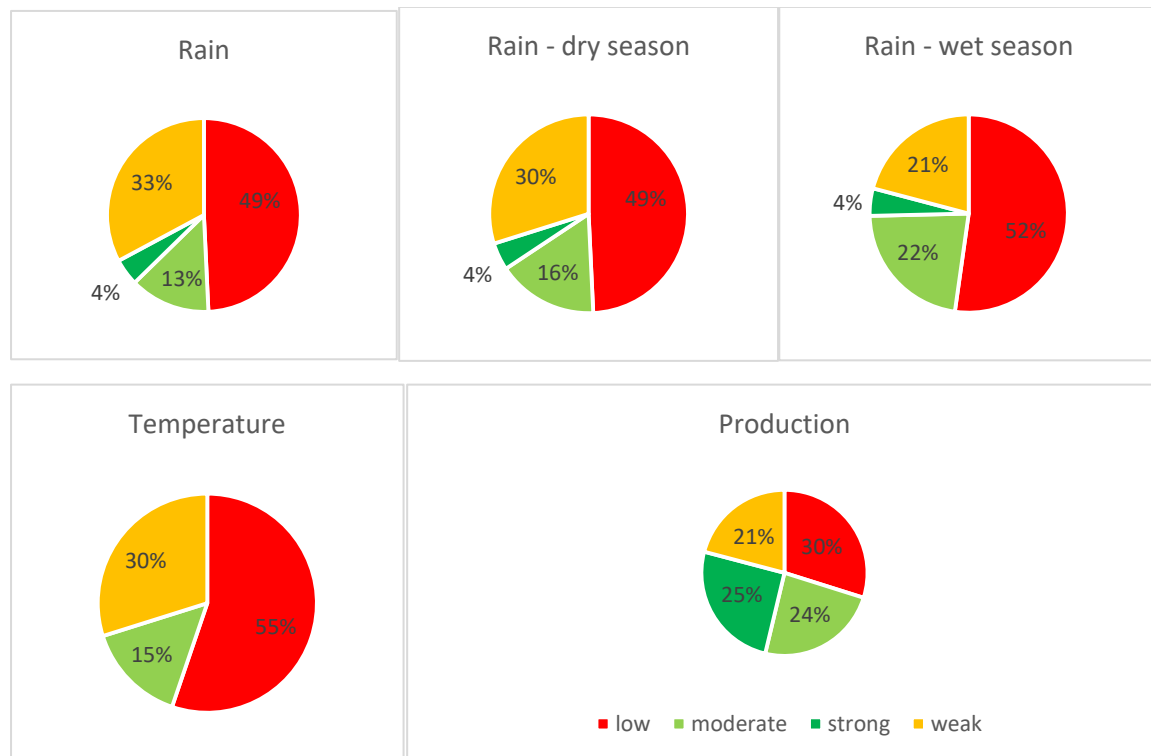
Dendrochronological studies usually use tree-ring data to reconstruct past climatic conditions. In the tropics, tree ring structures vary depending on species and regional environment (Brienen et al., 2016; Cherubini et al., 2003). In the case of cacao trees, it is quite complex to understand whether the ring structures formed are annual or seasonal. Moreover, these structures might change depending on the geographic location, since northern areas are often drier than southern areas. It is possible that per year two or even more ring structures are formed and a potential way to investigate this is through machine learning techniques. The technique used for such investigation in this research is with an R-

Script which takes all the ring width measurements per sample and finds the best combination of tree rings that reach a maximal correlation with climatic data. Given the higher seasonal and yearly variations in precipitation in Ivory Coast, most of the permutations on tree rings were done searching for the best correlation with the sum of rainfall per year. When feeding ring width measurements in the script the output reveals the best combinations and the respective highest correlation with climatic data. This gives in return an idea of which rings might be formed in the same year. There are different kinds of permutation possibilities integrated into the script and all of them call for cautious interpretation and further validation. For instance, the measurements of a sample might have extremely low or almost no correlation at all with the climatic data from its location. Yet when putting two rings together for a specific year, the correlation significantly increases, suggesting that in that specific year the tree might have formed two rings. The permutation could be of two couples of two rings at different years which, when merged together, increase correlation. With a bit longer running time, the script can even check a combination of three rings merged per year. The table below (table 4) shows the possible permutations available in the script. All of them with the aim of improving the correlation between climatic data and tree-ring data, instead of the conventional way which does the opposite.

Table 4 Permutation options for the Tree Ring R-Script, with the aim of identifying the best tree ring combination with highest correlation to climatic data.

Short name	Permutation type	Computational time
2	Two rings for one year are merged together.	Short
22	Two couples of two rings for two different years are merged together.	Short
222	Three couples of two rings for three different years are merged together.	Extremely long
3	Three rings for one year are merged together.	Medium
33	Three rings for two years are merged together.	Medium
23	Two rings for one year and three rings for another year are merged together.	Medium

All the samples with measured tree-ring width were connected to the corresponding climatic data and inserted into the script. For an initial test, the ring widths were compared to yearly national climatic and cocoa production data. The correlation between tree-ring widths and national climatic and production data was investigated with the script and resulted in some first impression outcomes showed in the pie charts below (graph 5).



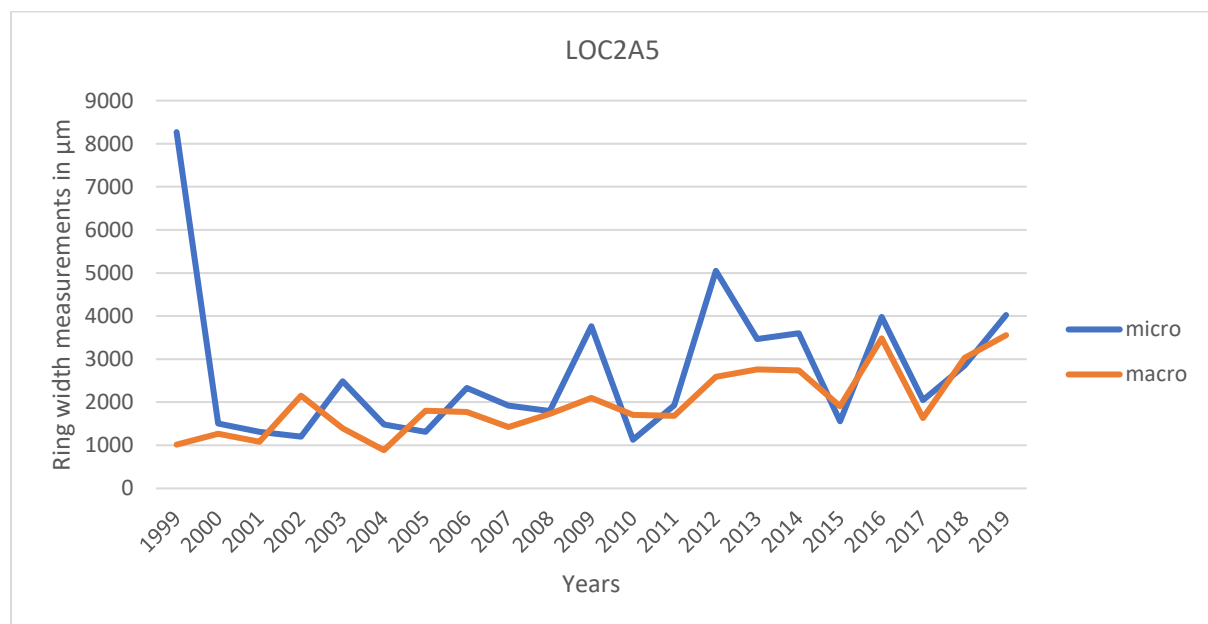
Graph 5 Maximized correlations, after using the R-Script and data permutation, between ring width measurements and yearly rain, dry season rain, wet season rain, yearly temperature and yearly production (strong $R > 0.7$, moderate $R > 0.5$, weak $R > 0.3$ and low $R < 0.3$).

After entering the ring-width measurements into the R-Script which combines the rings together to reach maximum correlation, the result was classified between low, weak, moderate and strong correlation. In all cases most of the data had no correlation at all, even after permutation (low, $R < 0.3$). The weakest correlations were between ring width and temperature, suggesting that despite permutation, there is still no clear relationship. The correlation with rain slightly differed between annual rain and the dry and wet season rain. The wet season rain had slightly more moderate correlations but also some more low correlations. The correlation between ring width and production were almost equally divided between low, weak, moderate and strong correlation. 25% of the samples seemed to strongly correlate with production data (ICCO.org), after undergoing permutation by the

script. Since the data is national for the whole country of Ivory Coast, it remains challenging to understand whether the tree rings are annual, whether larger rings are formed in years with more rain and what impact this has on the cocoa production.

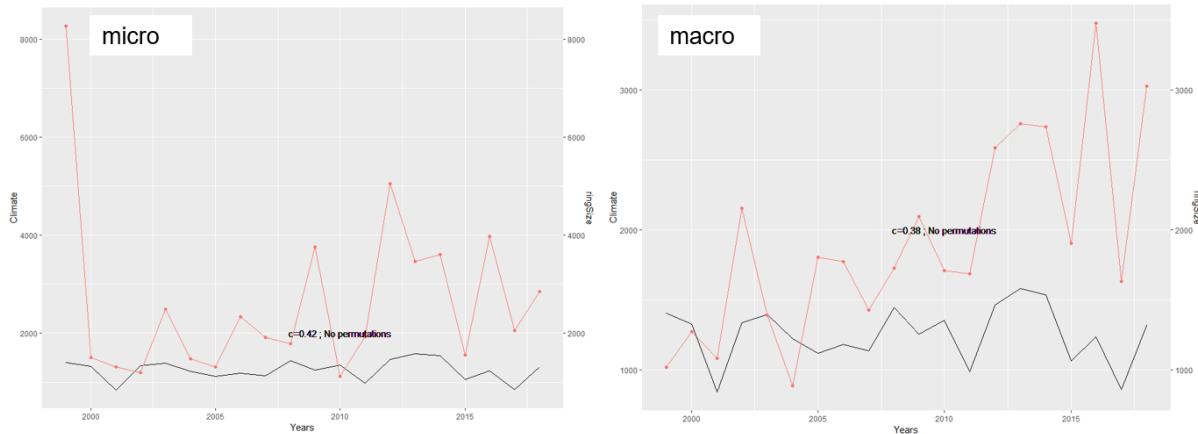
The regional climatic data available stemmed from two different sources. One was shared by Dr. Agathe Dié, yet not for all regions where our samples were located. The other one was from NASA's Giovanni platform, TRMM measurements of global coverage, the areas were selected and measurements were averaged per area and downloaded. The zones which had data from both sites were compared with each other and they showed extremely similar results. Therefore, in order to have more zones analysed, the TRMM data was used.

There was one particular sample that showed exceptionally nice correlations and good concurrence with rainfall in Daloa. This particular sample was further investigated and the ring width was measured using the core and also using its microsections. There were slight differences between the core and the microsections. The graph 6 shows the micro measurements using the thin microsections prepared in the lab and the macro measurements using the core. The first years' measurement and the oldest measurement, was not clearly measured because the pith border was slightly decayed.



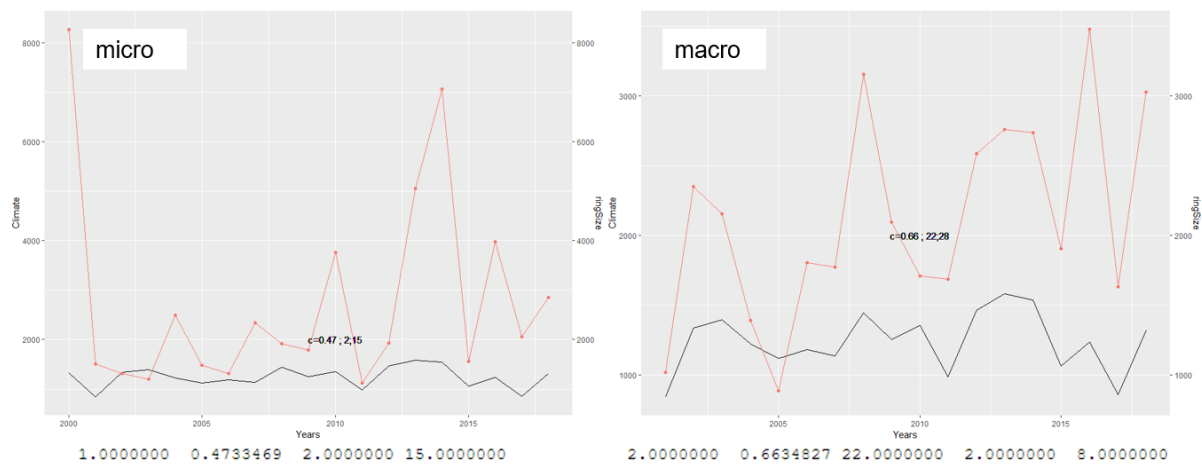
Graph 6 LOC2A5 cacao tree core ring width measurements in μm per year (although it is not clear yet if they are really annual tree rings).

Both measurements micro and macro were fed into the script. The first output of the script shows the ring width measurements in μm , the sum of precipitation per year in mm and their correlation.



Graph 7 Tree Ring R-Script output showing the raw ring width measurements of LOC2A5 microsection and macro version and their correlation with annual sum of rainfall (the black line).

Both of the measurements show a weak positive correlation with precipitation, when including the youngest year with the pith. The micro version shows a slightly higher correlation (0.42) than the macro version (0.38). Interestingly, when running the script aiming at the maximum correlation, the macro version performs much better.



Graph 8 Tree Ring R-Script output showing the permutations of ring width measurements of LOC2A5 microsection and macro version and their correlation with annual sum of rainfall (the black line).

The output suggests for the microsection version to only couple up the 15th tree ring with the 16th and so increase the correlation to 0.47. For the macro version, the maximum correlation is achieved by merging two couple of rings. The 2nd ring with the 3rd and the 8th ring with the

9th, decreasing the age of the tree by two years, yet reaching a moderate almost strong correlation with precipitation of 0.66.

Similar observations were made with all other samples and the script's outputs were summarized in tables that can be found in the appendix. Using the zones created (figure 26) as explained in the materials and methods chapter, all rings were assigned a zonal location and the maximized correlation with precipitation data retrieved with the R-Script were summarized per zone.

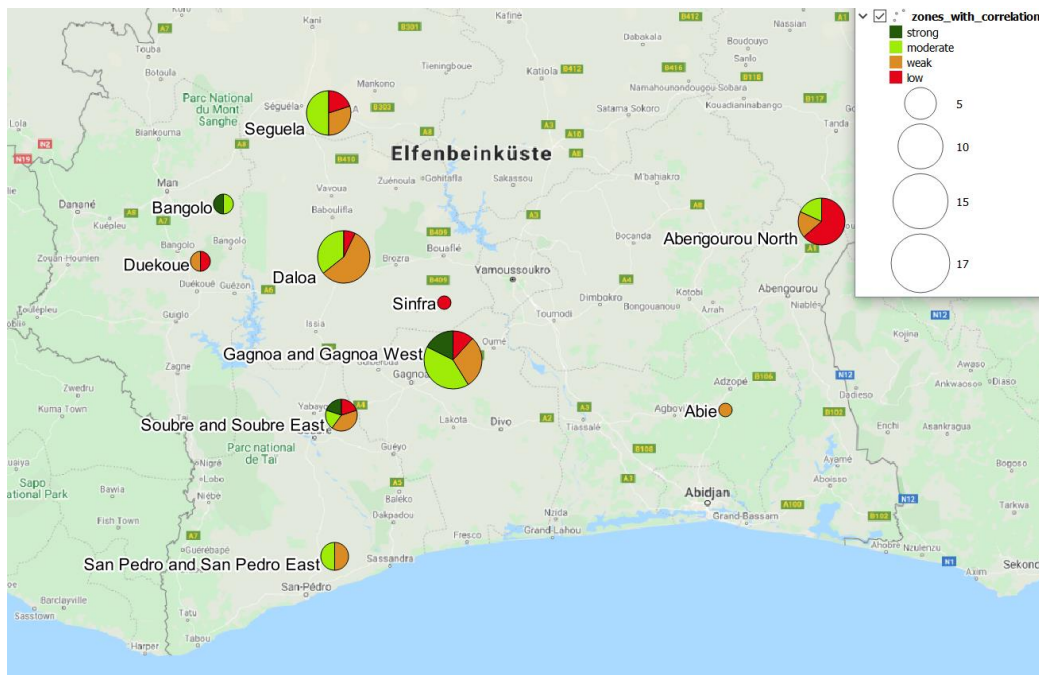


Figure 38 Map of the samples collected and their quantitative assessment based on the permutations with maximized correlation with climatic data. The size of the pie charts represents the number of samples collected in that zone and the colours show the level of correlation with precipitation data (strong $R > 0.7$, moderate $R > 0.5$, weak $R > 0.3$ and low $R < 0.3$).

The map above (figure 38) shows, similarly to the one for the qualitative assessment, the way different samples seem to correlate with the yearly regional precipitation data. In some zones the number of samples is significantly lower, shown by the size of the chart. Moreover, the correlations reached through the permutations suggested by the script are not enough evidence. Nevertheless, the map gives an idea of which zones have mostly moderate correlations and which mostly low correlations. Abengourou seems to have many samples with low or no real correlation with the climatic data. Seguela is the zone with most moderate correlations, followed by Gagnoa and Daloa, these are also the areas with most samples. Strong correlations are mostly found in central areas like Gagnoa, Soubre and

Bangolo. Nevertheless, understanding which trees really grow more depending on precipitation remains challenging, because the exact age of the tree is unknown and the increasing correlation through permutations is not a robust evidence.

3.2.3 Chemical analyses results: radiocarbon dating and stable isotopes

In order to investigate the age of the trees and better understand the number of tree rings formed per year and what their growth might depend upon, ^{14}C dating methods were applied to only some samples due to time and cost limitations. The first few rings of some disks were analysed. The qualitative and quantitative analyses helped in choosing which samples to analyse. MA2 and GA3 were two disk samples of living trees that had previously already been felled but still had new flowers and leaves on the stem. They were found between Daloa and Man around the area of Bangolo, in the northwest part of Ivory Coast. The last few rings or the youngest ones nearby the bark were analysed macroscopically and microscopically using stained microsections. Then they were split and sent to ETH for ^{14}C dating. IS1 was also a living sample from Issia, a village near Gagnoa in central-western Ivory Coast. For this sample, all the rings were split and sent for both, ^{14}C dating and for stable isotopes analysis at ETH.

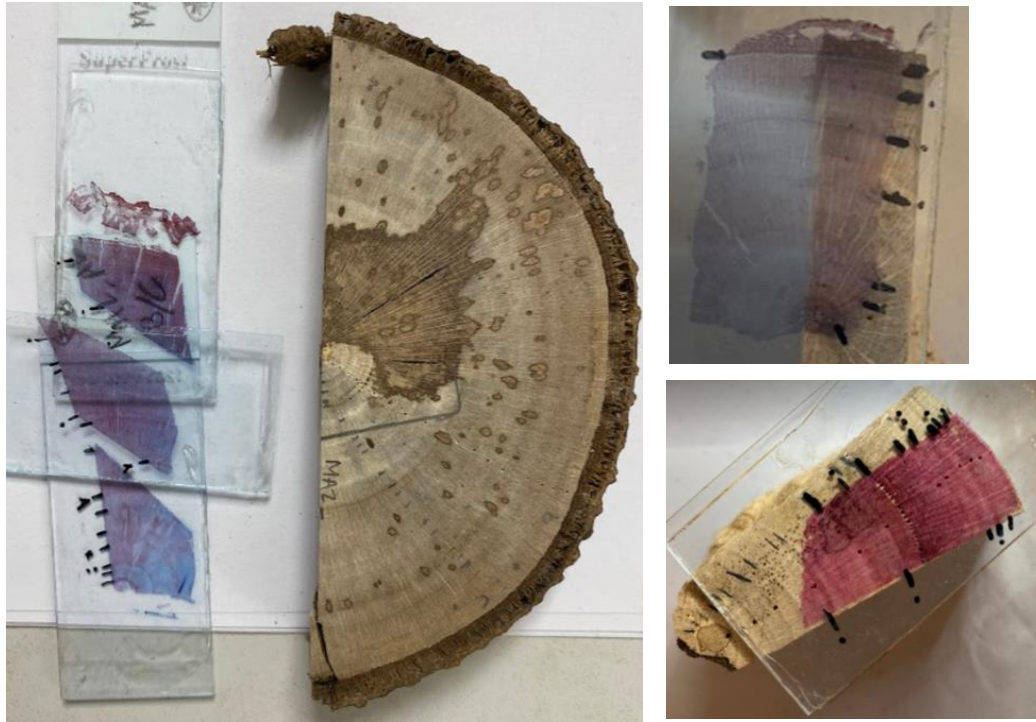


Figure 39 Three cacao tree disks and their microsections, MA2 on the left, GA3 on the top right and IS1 on the bottom right.

All the rings identified were split, even if classified as unclear rings, with the aim of understanding the age and related growth per year or season.

IS1_1 2019	IS1_2 2018	IS1_3 2017	IS1_4 2016	IS1_5 2015	IS1_6G 2015	IS1_6 2014	IS1_7 2013	IS1_8 2012
Very clear with IADFs near	Clear, flattened cells	Very clear, flattened cells, can be seen from far	Not clear, few flat cells	Big gum-duct in this tree ring	Normal, clear from far, less clear when zooming	Unclear	Normal, clearer from far	

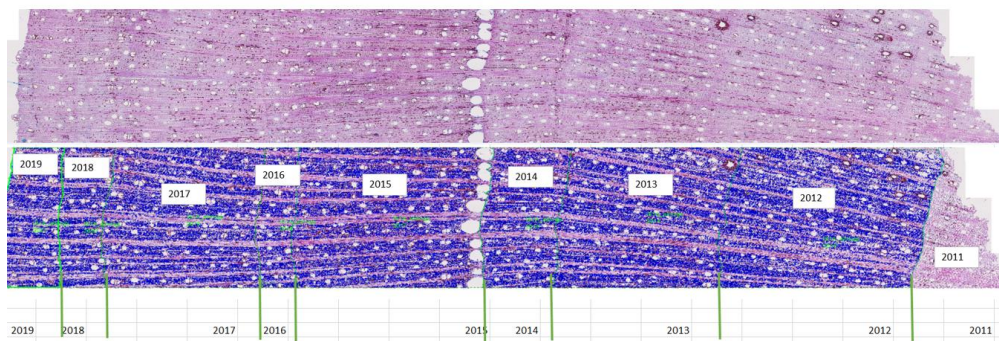
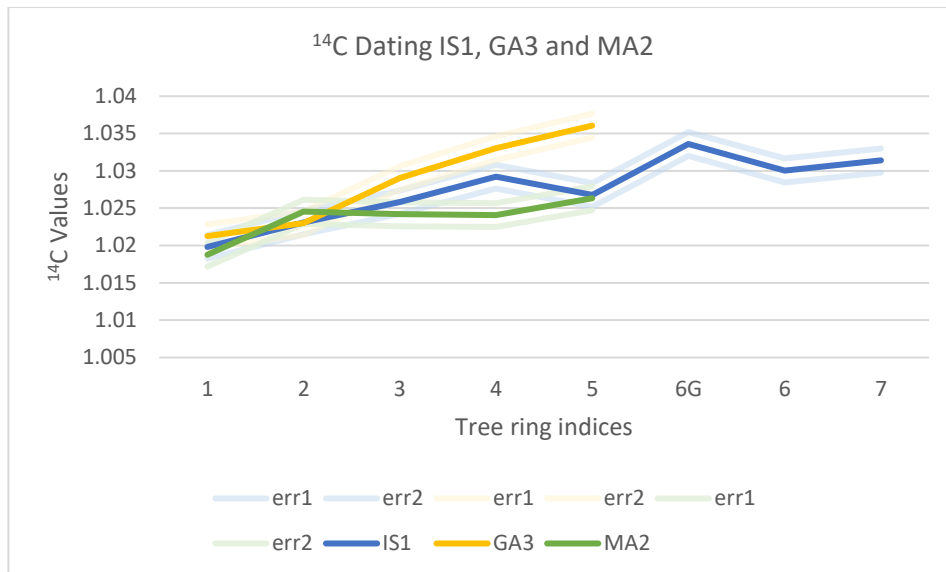


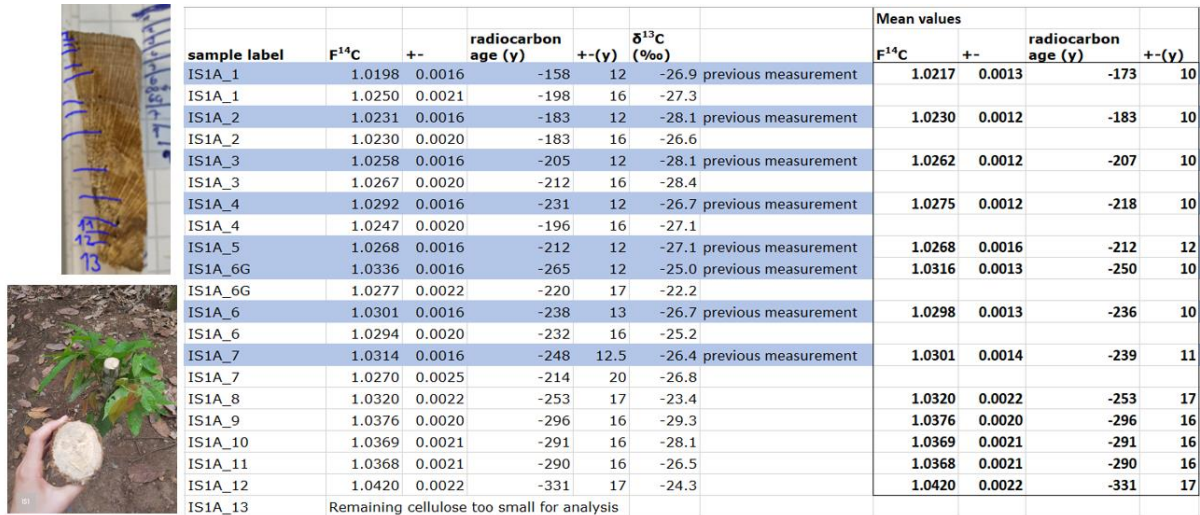
Figure 40 IS1 microsection and identified tree rings and their description.

The carbon dating results for the three disks are displayed in the graph below. The small number of tree rings and marginal space for errors must be taken into consideration when interpreting these measurements. The values of ^{14}C seem to increase from the younger rings towards older tree rings.



Graph 9 Radio carbon dating results for three cacao tree disk samples; IS1, GA3 and MA2 and their corresponding errors.

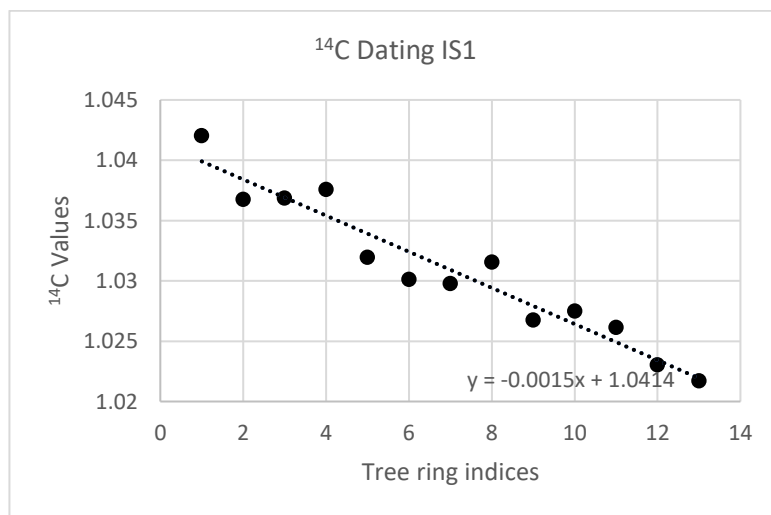
The difference between the rings in MA2 is minimal and difficult to interpret, it could even be that the five tree rings measured only represent the growth of two years. Similarly for GA3, although the steepness is higher and therefore the five rings might as well correspond to three to five years. IS1 is more interesting to analyse because exactly in between the 5th and 7th ring there is a gum-duct (see figure 40). It might be that younger material is transported through the gum-duct, possibly explaining the oscillations in ¹⁴C values at ring 5, 6G and 6. IS1 sample was measured a second time but including all tree rings; from the youngest to the oldest, attempting to better approximate the age of the tree. The results are displayed in the table below. Some of the samples were measured twice (the first and second time) and new samples (ring 8 to 13) were only measured during the second time. The mean was looked at for those measured twice.



sample label	F ¹⁴ C	+/-	radiocarbon age (y)	+/(y)	δ ¹³ C (‰)		Mean values			
							F ¹⁴ C	+/-	radiocarbon age (y)	+/(y)
IS1A_1	1.0198	0.0016	-158	12	-26.9	previous measurement	1.0217	0.0013	-173	10
IS1A_1	1.0250	0.0021	-198	16	-27.3					
IS1A_2	1.0231	0.0016	-183	12	-28.1	previous measurement	1.0230	0.0012	-183	10
IS1A_2	1.0230	0.0020	-183	16	-26.6					
IS1A_3	1.0258	0.0016	-205	12	-28.1	previous measurement	1.0262	0.0012	-207	10
IS1A_3	1.0267	0.0020	-212	16	-28.4					
IS1A_4	1.0292	0.0016	-231	12	-26.7	previous measurement	1.0275	0.0012	-218	10
IS1A_4	1.0247	0.0020	-196	16	-27.1					
IS1A_5	1.0268	0.0016	-212	12	-27.1	previous measurement	1.0268	0.0016	-212	12
IS1A_6G	1.0336	0.0016	-265	12	-25.0	previous measurement	1.0316	0.0013	-250	10
IS1A_6G	1.0277	0.0022	-220	17	-22.2					
IS1A_6	1.0301	0.0016	-238	13	-26.7	previous measurement	1.0298	0.0013	-236	10
IS1A_6	1.0294	0.0020	-232	16	-25.2					
IS1A_7	1.0314	0.0016	-248	12.5	-26.4	previous measurement	1.0301	0.0014	-239	11
IS1A_7	1.0270	0.0025	-214	20	-26.8					
IS1A_8	1.0320	0.0022	-253	17	-23.4		1.0320	0.0022	-253	17
IS1A_9	1.0376	0.0020	-296	16	-29.3		1.0376	0.0020	-296	16
IS1A_10	1.0369	0.0021	-291	16	-28.1		1.0369	0.0021	-291	16
IS1A_11	1.0368	0.0021	-290	16	-26.5		1.0368	0.0021	-290	16
IS1A_12	1.0420	0.0022	-331	17	-24.3		1.0420	0.0022	-331	17
IS1A_13	Remaining cellulose too small for analysis									

Figure 41 Picture of IS1 sample when sampled in the plantation, when prepared in the lab and the results.

Online available datasets show past carbon values which can be used to understand the age of trees. A compilation of northern and southern hemisphere datasets (Hua et al., 2013) can be used to calculate a regression line of the approximate decrease of radiocarbon even after 2010. Ivory Coast is in the NH zone 3, an area bounded in the north by the mean summer intertropical convergence zone and in the south by the equator (see figure 7). Therefore, the monthly data points provided by Hua et al. (2013) can be extrapolated and the slope can be used to estimate the age of the IS1 cacao tree sample.

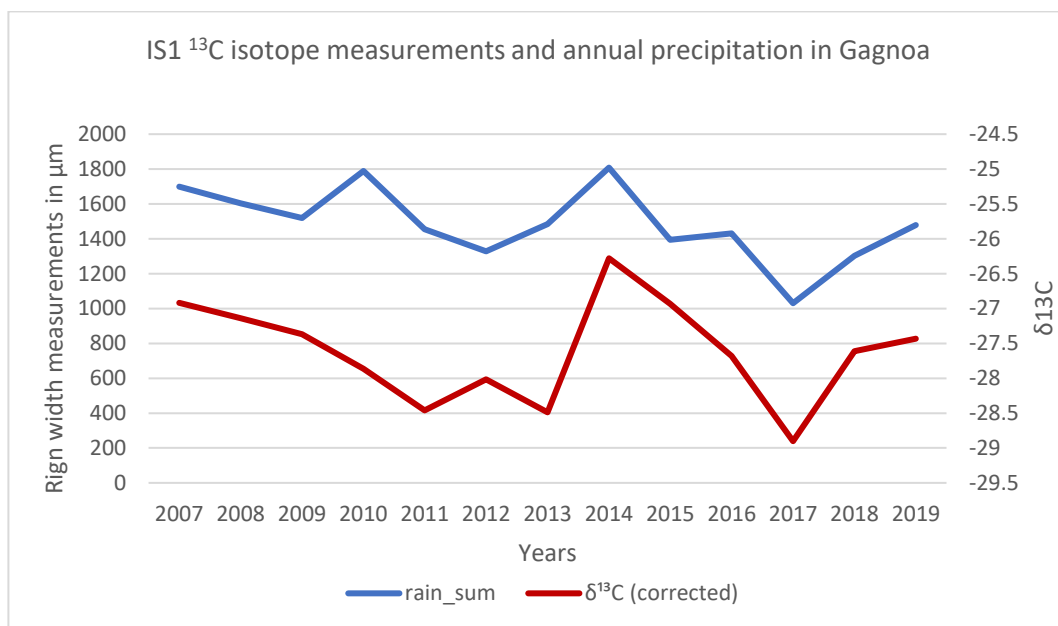


Graph 10 Radiocarbon dating of all the tree rings identified in IS1 and its linear regression line.

The graph above shows the ¹⁴C values for 14 tree rings identified in the IS1 sample. The difference between the radiocarbon values of the oldest ring (1.0217) and the youngest ring measured (1.0420) is of 20.3 ‰. This value, divided by the slope of the NH zone 3

radiocarbon values, gives an estimation of the age of IS1, which resulted to have an age between three to six years. Given more than double the number of rings, the question rises on whether cacao trees form two or more rings per year.

The sample IS1 was also sent to ETH for isotopes analyses, which revealed interesting results. The ^{13}C measurements seemed to nicely correlate with the annual precipitation as visible in the graph below. Assuming, however, that the tree rings are annual, a minimal age of the tree of twelve years would be estimated. Yet, the carbon dating on this sample resulted in a contradicting age of three to six years. This led to further investigation on an older sample or one with even more tree rings.



Graph 11 ^{13}C measurements per tree ring of sample IS1 and annual precipitation data from Gagnoa.

The cacao tree core LOC2A5 from Daloa showed a particularly nice concurrence and correlation even before the ring permutation through the R-script, as discussed above, where 22 tree rings had been identified on it. Therefore, one of the oldest, the youngest and two middle tree rings were split and sent to ETH for radiocarbon analyses.

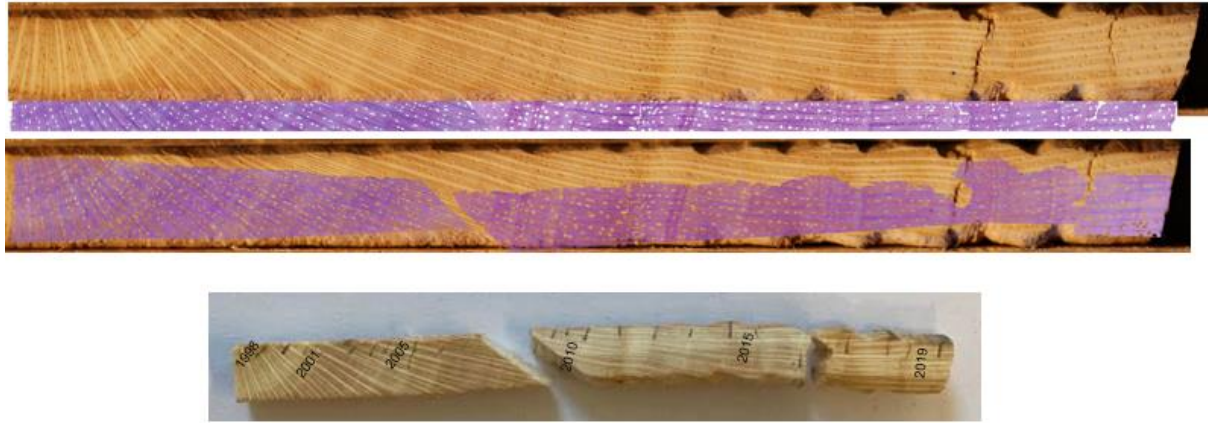
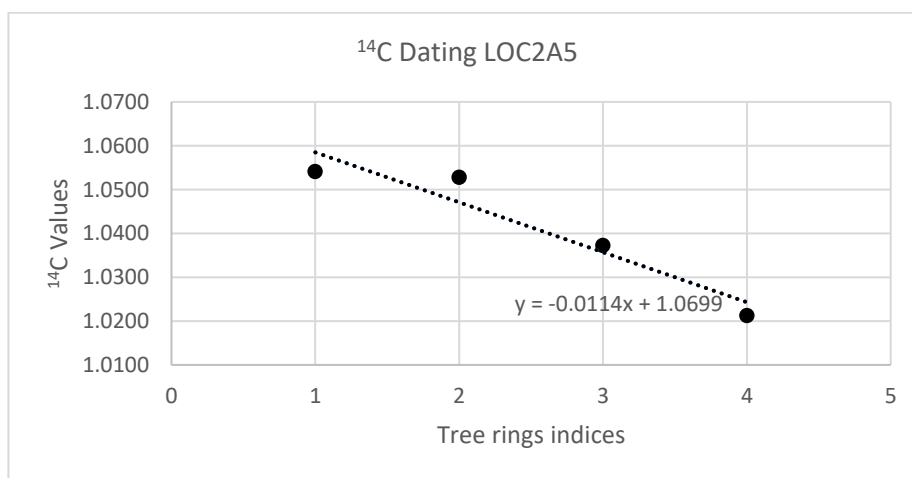


Figure 42 Tree core LOC2A5 and its microsection. Below the tree core and the marked rings that were sent for radiocarbon dating.

The results showed a difference between the oldest and the youngest tree ring measured of 32.8 ‰, using Hua et al. (2013) data the age estimation was of seven to ten years old.

Radiocarbon measurements do have errors and when splitting the samples material, the rings might get mixed, results must therefore be carefully interpreted. The oldest sample sent for analysis might well be older than what the ^{14}C measurements suggest and so better fit the line visible below. Most of the ^{14}C measurements and analyses were done in Europe or in the upper northern hemisphere where clearer seasonality is visible between winter and summer even in the ^{14}C values. These values are higher in summer than in winter.

Furthermore, the anthropogenic activities also influence the radiocarbon values measured (Levin et al., 2013; Svetlik et al., 2019). In tropical areas like Ivory Coast, the measurements are generally more vague and uncertain.



Graph 12 Radiocarbon dating of all the tree rings identified in IS1 and its linear regression line.

Assuming due to these results that the age of LOC2A5 sample is of seven to ten years, the 22 identified tree rings cannot be annual. They might be seasonal and to further investigate this, the tree ring R-Script was used. Since the last ring was extremely small and too near to the pith, it was removed from the analysis. The output results of the script are listed in the table 5.

Table 5 LOC2A5 permutations with maximum correlation with annual rainfall.

Short name	Maximized correlation	Index of rings to be merged
No permutation	0.2 (original data, without the ring at the pith)	-
2	0.53	11
22	0.61	3,10
222	0.64	2,7,9
3	0.51	10
33	0.67	6,8
23	0.17	7,9

Despite the nice concurrence of the ring width of LOC2A5 and the sum of precipitation, discussed in the previous section, when removing the ring at the pith the correlation is of only 0.2. All other types of permutations significantly improve the correlation, except for the type 23 combining one couple with 2 rings and another with 3 rings. The highest correlation is achieved by coupling the 3rd ring with the 4th and the 10th with the 11th. Other ring combinations also achieve a quite high correlation, like the type 222 combining three times couples of rings together. Furthermore, the ¹⁴C dating measurements suggested a maximal age of ten years. Given this information, the core was examined again to see if it could be that per year several tree rings are formed.



Figure 43 Ring width measurement of all rings identified for LOC2A5.

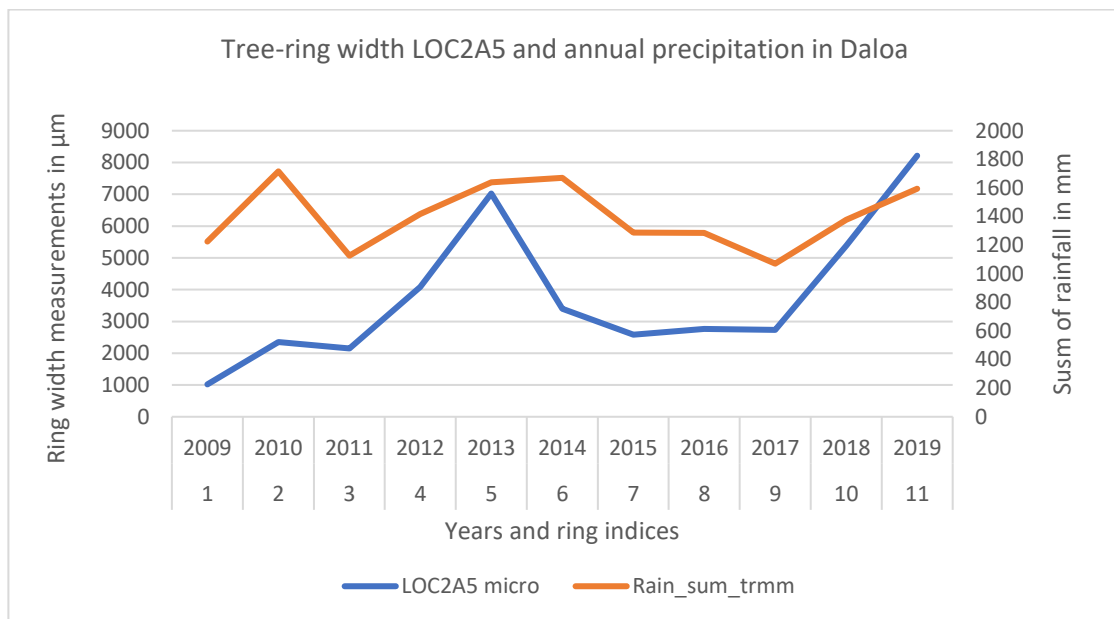
Using the permutations suggested by the script and the qualitative assessment, the rings were coupled up resulting in 12 rings. Some rings made up of single rings and others made up of 2 or even more rings. The 12 rings identified are the ones that also had the sharpest

borders which were macroscopically visible.



Figure 44 Tree ring classification of LOC2A5.

The outcome of this final examination of the sample LOC2A5 resulted in tree rings that nicely concur with the annual precipitation in Daloa, with a moderate correlation of 0.51. Therefore, it could be that cacao rings form more than one ring per year and have intra-annual density fluctuations.



Graph 13 Final tree ring identification and width measurements of the core LOC2A5 with the corresponding annual precipitation.

4 Synthesis

According to previous research on tropical trees' wood anatomy and the impact of climate on tree growth, cacao trees were expected to form ring boundaries during the dry season (van der Sleen et al., 2017; Alvim, 1957; Bressan-Smith et al., 1997). Given Ivory Coast's north to south climatic gradient; drier northern areas and wetter coastal zones, it was also expected to see spatial differences depending on where the samples were taken.

In the qualitative analyses it resulted that the collected cacao trees' samples showed the same characteristics described by Zhanin et al. (2019) and León (2015). The prismatic crystals were also detected by León (2015) but were not mentioned by Zhanin (2019) nor by Alvim (1957). Since in some cases, the gum-ducts were not through the entire circumference of the disk, these features can probably not be used as markers. In the literature, gum-ducts in cacao trees are a sign of disturbance (León, 2015), yet the cause remains unclear. Without evidence one could suggest to further investigate whether cacao tree gum-ducts are the reaction to pruning activities by the farmers or the attack of mirids, which would explain why gum-ducts are found also on only some sides of the stem and not always around the whole disk samples.

Cacao trees are dicotyledonous trees and their wood has vessels or pores (Schoch, 2004). The wood is described as diffuse-porous, with simple perforation plates and uniseriate and multiseriate parenchyma rays (León, 2015). Growth-ring boundaries have been described as indistinct or absent by León (2015) who looked at samples from Venezuela. Avim (1957) looked at trees from Costa Rica and revealed the existence of concentric circles similar to growth rings. While analysing hydraulic patterns of cacao trees and neighbouring shading trees, Kotowska et al. (2015) also looked at the wood anatomy. They found considerable differences between the wood anatomy of the shade trees and the wood anatomy of cacao trees. The vessel diameters of cacao trees were among the smallest and did not change much between stem and branch. The ring description analysis took into consideration the studies done so far in cacao tree wood anatomy and resulted in differences in ring borders that might depend on geographical location or management practices, such as pruning or the addition of fertilizers. The ratio calculated at ring border using early wood and late wood

cells measurements could be a quantitative guideline for the identification of tree-ring borders. Nevertheless, it must be noted that the ratio was calculated using rows in ring borders already identified as such and that rows were manually drawn, therefore the room for potential errors and overestimation remains. The tree-ring width measurements differ between the different rings and seem to have clear peaks in some areas, e.g., Gagnoa. Since the crossdating was extremely hard and statistically not significant, due to the young age of the trees, it might as well be that the differences in width reflect seasonality rather than annual oscillations. These trees are from tropical areas with low-temperature oscillations throughout the year, yet bigger differences in rainfall mark a quite clear wet and dry season. Therefore, it remains unclear whether all the ring structures detected and measured are really annual tree rings or seasonal oscillations. In order to further explore this, innovative machine learning techniques have been applied. The analyses with the R-Script did show important correlations with climatic data when combining ring widths. However, knowing the age of the tree would help approximating the number of rings formed per year. In fact the radiocarbon dating showed for all measured samples that the identified tree ring are most probably not annual. Therefore, it is possible that cacao trees in Ivory Coast form several seasonal tree rings. LOC2A5 was the sample analysed most in detail. After merging several rings through the script outputs and the ^{14}C dating results suggesting an age of around ten years, the ring width measurements did seem to correlate with precipitation. Moreover, this sample came from the farm labelled as LOC2A in Daloa and the farmer said that the plantation was established in 2006, therefore the estimated age of ten years seems to make sense. Most of the couples of seasonal rings per year had a total width lower than 4 mm, reflecting the annual growth also measured by Alvim (1957). Nevertheless, to validate that the tree rings are seasonal and need to be paired in couples of two or even three per year, carbon and oxygen stable isotopes per ring should be measured. Variations in stable isotopic composition should be driven by changes in stomatal activity induced by climatic variability, i.e., changes in precipitation. The results of such analyses could then be compared to monthly or seasonal precipitation and confirm true correlation.

Despite the qualitative and quantitative analyses performed on the collected cacao tree samples, the interpretation remains challenging. Both assessments revealed a spatial

difference between the samples, suggesting that the regional location of cacao trees in Ivory Coast does reflect a difference in the wood structure.

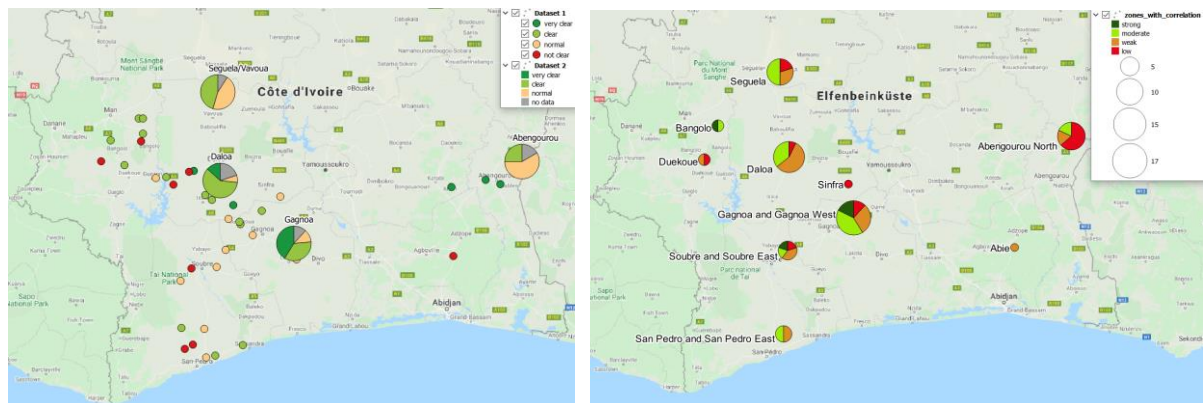


Figure 45 Comparison of the qualitative analyses describing the tree-ring borders clarity and the quantitative analyses measuring widths and checking correlations with climatic data.

The samples from the first sampling trip gave an aid to identify regions where rings seem to be clearer and where not. This was then confirmed with the samples from the second sampling trip, because most of these showed clear tree rings.

The map on the left in figure 45 shows the qualitative assessment of the first sample set as points and the second sample set as pie charts. Some samples from the first sample set are coloured red, meaning that the tree rings were not clear and hard to identify. The majority of the samples with clear rings seem to be in the northern and western areas. In fact, the second sample set retrieved from Seguela, Daloa, Gagnoa and Abengourou as pie charts show no tree rings marked as not clear. Therefore, the qualitative description of the second sample set resulted in clearer tree rings in those areas. The northern sites, especially Abengourou show the least amount of very clear and clear tree rings. In contrast, Daloa and Gagnoa show a good portion of clear and even some very clear tree rings, especially in Gagnoa.

The map on the right in figure 45 shows the quantitative assessment results and here too, the samples with the best performance (highest correlation with climatic data) are from Gagnoa. The size of the circle reflects the sample size per location, therefore, the smaller pie charts for Bangolo, Duekoue, San Pedro and Soubre are harder to interpret. Nevertheless, most of these areas do not show many samples with moderate or strong correlation, except for Bangolo and Soubre with some samples with even a strong correlation between ring width and annual precipitation. There might be more regional factors like a small mountain nearby where regional rain is transported or a small river influencing the growth.

The correlations visualised on the maps above are the maximized correlations achieved through permutations by the R-Script. However, ¹⁴C measurements have shown for a couple of samples that the tree rings are not annual. Therefore, coupling 1 or 2 pairs of tree rings might not be enough.

Schroth et al. (2016) published maps showing the “relative climatic suitability (in percent) for cocoa of the West Africa cocoa belt under current and projected 2050s climatic conditions, as well as suitability change, according to a Maxent model based on 24 climate variables”. When overlaying the sample zones with their correlation on these suitability maps, it is visible that according to these projections Seguela and Abengourou will clearly no longer be suitable for cocoa.

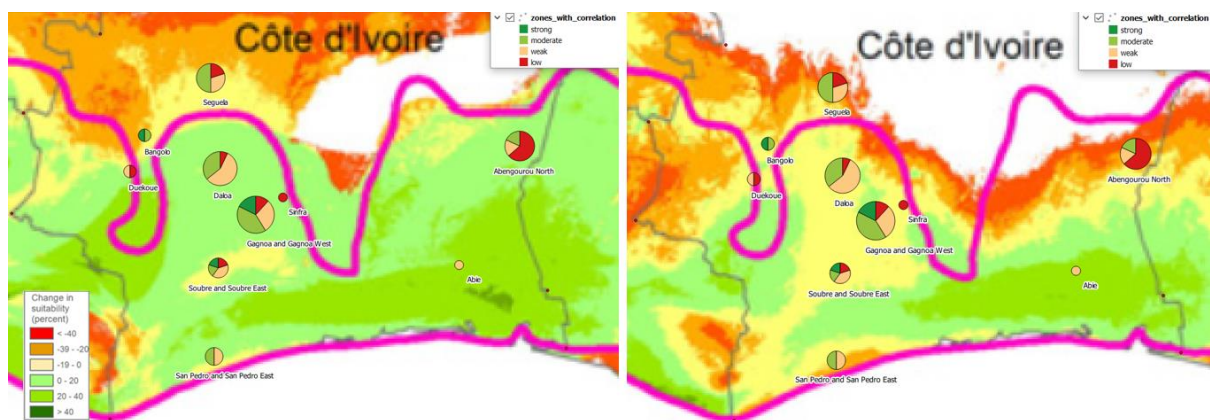


Figure 46 “Relative climatic suitability (in percent) for cocoa of the West Africa cocoa belt under current (left) and projected 2050s climate conditions (right). The red lines show areas of cocoa production.” (Schroth et al., 2016).

Gagnoa and Daloa, which are currently suitable areas for cocoa where big amounts of cocoa are globally sourced from, might as well no longer be suitable by 2050 (right map figure 46). The quantitative analyses done on cacao tree cores around this central zone of Ivory Coast suggested that more than one tree ring per year is created and that it probably depicts a seasonal change. If seasonal changes influence tree growth, especially precipitation and future climatic projections suggest significant changes resulting in shifting areas of suitability, it is worthwhile to further investigate on these wood features to fully understand annual trends and limiting factors.

Differences in cacao tree-ring widths are recognizable when looking at individual tree rings or when coupling tree rings at sharper ring boundaries with the help of a script. When then compared to temperature data, most of the samples showed no correlation, yet when

compared with precipitation data, the results seemed more promising. Also compared to other researches, it seems like cacao trees' growth is affected by drought, depending on the location of the samples. For this research, only national cocoa production data was used, which still showed a positive correlation with ring widths. However, further and more detailed research is needed to understand the relationships between ring width and cocoa production.

5 Conclusion

This research was the first research collecting such an amount of cacao tree samples from so different areas within the cocoa belt in Ivory Coast. The vast variety of the samples is extremely interesting. Most of the samples were Forastero type and only a few hybrid, and no wood structure differences between these two were identified. However, the reaction of the tree-rings growth and precipitation resulted to be different depending on the location of the sample. The most promising areas turned out to be Gagnoa and Daloa, which are also areas where high amounts of cocoa are sourced from and which are susceptible to future change according to climatic projections. Some tree cores from these areas were investigated in more detail and have revealed the possibility that cacao trees form more than one tree ring per year and that the identified tree rings probably reflect seasonality changes. These findings will lead to further analyses on these samples, using not only wood anatomy and dendrochronological methods, but also ^{14}C dating methods to determine age and stable isotope analyses to detect seasonality. Similarly to other species like some mediterranean or tropical ones, where double rings were found (Cherubini et al., 2003; Santos et al., 2020), cacao trees probably form two or even three rings per year. The R-Script played an important role in identifying which rings should be coupled up, such promising and innovative methods can prove to be extremely useful in future research. Therefore, wood anatomical and conventional dendrochronological analyses are not enough to analyse cacao trees. A combination of radiocarbon, stable isotopes but also statistical permutations with climatic data are needed to investigate such complex ring structures and even when combining all of these methods, the interpretation must be cautious. Additionally, measuring the trunk growth with a dendrometer and then comparing it with tree ring formation should provide further evidence and validation. Once it becomes clearer, in which areas cacao trees create what kind of rings, the resilience towards climate change and even the relationship between ring growth and cocoa production can further be investigated.

The wood anatomical properties of cacao trees were thoroughly investigated and the result was that cacao trees do not form one ring per year, but two and at times even more. These intra-annual density fluctuations probably reflect seasonal changes between wet and dry

seasons. Spatial differences in the clarity of tree-ring borders have been identified and the areas with clearer rings seem to be Daloa and Gagnoa. According to the correlation analyses, cacao tree rings seem to correlate with precipitation, yet the seasonal changes need further investigation. The impact of drought and resilience towards climate change of cacao trees can only be revealed when tree rings are correctly coupled up per years. Only by combining the different suggested methods and using the permutation script created for this purpose, cacao tree rings can be correctly allocated and provide insight into how climatic conditions affect the growth. This research provides a first insight into the wood features of cacao trees in Ivory Coast, regional differences and helpful methods, which will help future research in this field.

6 References

- Alvim, P. d. T. (1957). Estudos sobre o crescimento do tronco do cacauero.
- Axelson, J., Bast, A., Alfaro, R., Smith, D. and Gärtner, H. (2014). Variation in wood anatomical structure of Douglas-fir defoliated by the western spruce budworm: a case study in the coastal-transitional zone of British Columbia, Canada. *Trees*, 28(6), pp.1837-1846.
- Battipaglia, G., De Micco, V., Brand, W., Saurer, M., Aronne, G., Linke, P. and Cherubini P. (2013). Drought impact on water use efficiency and intra-annual density fluctuations in *Erica arborea* on Elba (Italy). *Plant, Cell & Environment*, 37(2), pp.382-391.
- Battipaglia, G., De Micco, V., Brand, W. A., Linke, P., Aronne, G., Saurer, M. and Cherubini, P. (2010). Variations of vessel diameter and $\delta^{13}\text{C}$ in false rings of *Arbutus unedo* L. reflect different environmental conditions. *New Phytologist*, 188(4), pp. 1099-1112.
- Beer, J., Muschler, R., Kass, D. and Somarriba, E. (1998). Shade management in coffee and cacao plantations. *Agroforestry systems*, 38, pp. 136-164.
- Bhattacharjee, R. and Akoroda, M. (2018). Taxonomy and classification of cacao. *Achieving sustainable cultivation of cacao*. Burleigh Dodds Science Publishing. DOI: 10.19103/AS.2017.0021.01
- Bhattacharjee, R., and Kumar, P. L. (2007). Cacao. *Technical crops*. Springer, Berlin, Heidelberg: Springer, pp. 127-142.
- Bressan-Smith, R., Silva, E. A. M., Alvim, P. D. T. and Maestrp, M. (1997). Periodicidade do crescimento do tronco em cinco espécies no sul da Bahia, Brasil.
- Brienen, R., Schöngart, J. and Zuidema, P. (2016). Tree Rings in the Tropics: Insights into the Ecology and Climate Sensitivity of Tropical Trees. *Tree Physiology*, pp.439-461.
- Butler, R.A. (2006). Cote D'Ivoire, Mongabay, Tropical forests. Retrieved from: <https://rainforests.mongabay.com/20cotedivoire.htm> [08.11.2019]
- Cailleau, G., Braissant, O. and Verrecchia, E. P. (2011). Turning sunlight into stone: the oxalate-carbonate pathway in a tropical tree ecosystem. *Biogeosciences*, 8(7), 1755-1767.
- Carr, M. K. V. and Lockwood, G. (2011). The water relations and irrigation requirements of cocoa (*Theobroma Cacao* L.): A review. *Experimental Agriculture*, 47(4), pp. 653-676.
- Cherubini P., Fontana G., Rigling D., Dobbertin M., Brang P., Innes J.L. (2002). Tree-life history prior to death: two fungal root pathogens affect tree ring growth differently. *Journal of Ecology*, 90, 5, 839-850.

Cherubini P., Gartner B.L., Tognetti R., Bräker O.U., Schoch W., Innes J.L. (2003). Identification, measurement and interpretation of tree rings in woody species from Mediterranean climates. *Biological Reviews of the Cambridge Philosophical Society*, 78, 1, 119-148.

Cherubini, P., Humbel, T., Beeckman, H., Gärtner, H., Mannes, D., Pearson, C., Schoch, W., Tognetti, R. and Lev-Yadun, S. (2013). Olive Tree-Ring Problematic Dating: A Comparative Analysis on Santorini (Greece). *PLoS ONE*, 8(1).

Colombaroli, D., Cherubini, P., De Ridder, M., Saurer, M., Toirambe, B., Zweifel, N., Beeckman, H. (2016). Stable carbon and oxygen isotopes in tree rings show physiological responses of *Pericopsis elata* to precipitation in the Congo Basin. *Journal of Tropical Ecology*, 15, 32(3), pp. 213-225.

Cote D'Ivoire Geography. Landforms - World Atlas (2019). Retrieved from: <https://www.worldatlas.com/webimage/countrys/africa/cotedivoire/ciland.htm> [08.11.2019]

"Côte d'Ivoire". The World Factbook. CIA Directorate of Intelligence. 24th July 2008. Archived from the original on 5th February 2010. Retrieved from: <https://www.cia.gov/library/publications/the-world-factbook/geos/iv.html> [08.11.2019]

David, E. T., Chhin, S. and Skole, D. (2014). Dendrochronological Potential and Productivity of Tropical Tree Species in Western Kenya. *Tree-Ring Research*, 7, 70(2), pp. 119-135.

De Ridder, M., Toirambe, B., Van den Bulcke, J., Bourland, N., Van Acker, J., Beeckman, H. (2014). Dendrochronological potential in a semi-deciduous rainforest: The case of *Pericopsis elata* in central Africa. *Forests*, 5(12), pp. 3087-3106.

Dié, A., De Ridder, M., Cherubini, P., Kouamé, F. N., Verheyden, A., Kitin, P., Toirambe, B., Van den Bulcke, J., Van Acker, J., Beeckman, H. (2015). Tree rings show a different climatic response in a managed and a non-managed plantation of teak (*Tectona grandis*) in West Africa. *IAWA Journal*, 36(4), 409-427.

Farquhar, G.D., Ehleringer, J.R. and Hubick, K.T. (1989). Carbon isotope discrimination and photosynthesis. *Annual review of plant biology*, 40(1), pp.503-537.

Fichtler, E., Clark, D.A. and Worbes, M. (2003). Age and long-term growth of trees in an old-growth tropical rain forest, based on analyses of tree rings and ^{14}C . *Biotropica*, 35(3), pp.306-317.

Fritts, H.C. and Swetnam, T.W. (1989). Dendroecology: a tool for evaluating variations in past and present forest environments. In *Advances in ecological research* (Vol. 19, pp. 111-188). Academic Press.

Fritts, H. C. (1971). Dendroclimatology and dendroecology. *Quaternary Research*, 1(4), 419-449.

- Gebrekirstos, A., Bräuning, A., Sass-Klassen, U. and Mbow, C. (2014). Opportunities and applications of dendrochronology in Africa. *Current Opinion in Environmental Sustainability*, 6, pp.48-53.
- Gidoin, C., Avelino, J., Deheuvels, O., Cilas, C. and Bieng, M.A.N. (2014). Shade tree spatial structure and pod production explain frosty pod rot intensity in cacao agroforests, Costa Rica. *Phytopathology*, 104(3), pp.275-281.
- Gil Restrepo, J. P., Leiva-Rojas, E. I. and Ramírez Pisco, R. (2017). Phenology of cocoa tree in a tropical moist forest. *Científica*, 67, 45(3), p. 240.
- Giovanni v 4.33, NASA. Retrieved from: <https://giovanni.gsfc.nasa.gov/giovanni/> [29.05.2020]
- Giraldo, J. A., del Valle, J. I., Sierra, C. A., Melo, O. (2020). Dendrochronological Potential of Trees from America's Rainiest Region. In: Latin American Dendroecology. *Springer International Publishing*, pp. 79-119.
- Gourlay, I.D. and Grime, G.W. (1994). Calcium Oxalate Crystals in African Acacia Species and Their Analysis by Scanning Proton Microprobe (Spm). *Iawa Journal*, 15(2), pp.137-148.
- Gray, A. (2000). The world cocoa market outlook. Ghana Conference Paper.
- Gro Intelligence (2019). As cocoa harvest begins, risks emerge from major producing countries. Retrieved from: <https://gro-intelligence.com/insights/articles/as-cocoa-harvest-begins-risks-emerge-from-major-producing-countries> [25.05.2020]
- Groenendijk, P., Bongers, F. and Zuidema, P. A. (2017). Using tree-ring data to improve timber-yield projections for African wet tropical forest tree species. *Forest Ecology and Management*, 159, Band 400, pp. 396-407.
- Häkkinen R, Linkosalo T, Hari P. (1998). Effects of dormancy and environmental factors on timing of bud burst in *Betula pendula*. *Tree Physiol.* 18(10):707-712.
doi:10.1093/treephys/18.10.707
- Hartl-Meier, C., Dittmar, C., Zang, C. and Rothe, A. (2014). Mountain forest growth response to climate change in the Northern Limestone Alps. *Trees - Structure and Function*, 28(3), pp. 819-829.
- Hua, Q., Barbetti, M. and Rakowski, A. Z. (2013). Atmospheric Radiocarbon for the Period 1950–2010. *Radiocarbon*, 55(4), pp. 2059-2072.
- Hughes, M. K., Swetnam, T. W., and Diaz, H. F. (Eds.). (2010). *Dendroclimatology: progress and prospects* (Vol. 11). Springer Science & Business Media.
- Humphries, E. C. (1944). Dormancy of cacao bush. III. The relationship between bud-bursting and growth of the whole tree. *Cacao Research Annual Report*: 11:37-39.

International Cocoa Organization ICCO (2013). Growing cocoa. Retrieved from: <https://www.icco.org/about-cocoa/growing-cocoa.html> [08.11.2019]

Jacoby G.C. (1989). Overview of tree ring analysis in tropical regions. *IAWA Bull.*, 10, 99-108.

Kotowska M.M., Herttel D., Anou Rajab Y., Barus H., Schuldt B. (2015). Patterns in hydraulic architecture from roots to branches in six tropical tree species from cacao agroforestry and their relation to wood density and stem growth. *Frontiers in Plant Science*, 6, 191.

Laboratory of Tree-Ring Research, University of Arizona (1999). Dendrochronology. Retrieved from: <https://www.ltrr.arizona.edu/~sheppard/ltrrweb/dendrochronology.htm>[27.05.2020]

Lahive, F., Hadley, P. and Daymond, A. J. (2019). The physiological responses of cacao to the environment and the implications for climate change resilience. A review. *Agronomy for sustainable development*, 39(1), 5.

León, W. (2015). Anatomía xilemática de tronco y ramas de *Theobroma cacao* L.(Malvaceae: byttnerioideae). *Ernstia*, 25(1), pp.1-17. Levin, I., Kromer, B. and Hammer, S. (2013).

Levin, I. Kromer, B. and Hammer, S. (2013). Atmospheric $\Delta^{14}\text{CO}_2$ trend in Western European background air from 2000 to 2012. *Tellus B: Chemical and Physical Meteorology*, 65(1), p.20092.

Lovelock, C.E., Sorrell, B., Hancock, N., Hua, Q, Swales, A. (2010). Mangrove forest and soil development on a rapidly accreting shore in New Zealand. *Ecosystems* 13(3):437–51.

Nicolini, G., Tarchiani, V., Saurer, M. and Cherubini, P. (2010). Wood-growth zones in *Acacia seyal* Delile in the Keita Valley, Niger: Is there any climatic signal? *Journal of Arid Environments*, 3, 74(3), pp. 355-359.

Nishimura, P. H. (2009). *Dendroclimatology, dendroecology and climate change in western Labrador, Canada* (Doctoral dissertation, Mount Allison University).

Oro, F.Z., Bonnot, F., Ngo-Bieng, M.A., Delaitre, E., Dufour, B.P., Ametefe, K.E., Mississo, E., Wegbe, K., Muller, E. and Cilas, C. (2012). Spatiotemporal pattern analysis of Cacao swollen shoot virus in experimental plots in Togo. *Plant pathology*, 61(6), pp.1043-1051.

Poussart, P. M., Myneni, S. C. and Lanzirotti, A. (2006). Tropical dendrochemistry: A novel approach to estimate age and growth from ringless trees. *Geophysical Research Letters*, 1 9.33(17).

Poussart, P.F., Schrag, D.P. (2005). Seasonally resolved stable isotope chronologies from northern Thailand deciduous trees. *Earth and Planetary Science Letters* 235(3– 4):752–65

Reimer, P. J., Brown, T. A. and Reimer, R. W. (2004). Discussion: Reporting and calibration of post-bomb ¹⁴C data. *Radiocarbon*, 46(3), pp.1299-1304.

Richter, H.G., and Dallwitz, M.J. (2000). Commercial timbers: descriptions, illustrations, identification, and information retrieval. Retrieved from: <https://www.deltaintkey.com/wood/en/www/morbrali.htm> [28.10.2019]

Rodríguez-Ramírez, E. C., Terrazas, T. and Luna-Vega, I. (2019). The influence of climate on the masting behavior of Mexican beech: growth rings and xylem anatomy. *Trees - Structure and Function*, 13 2, 33(1), pp. 23-35.

Rozendaal, D. M. and Zuidema, P. A. (2011). Dendroecology in the tropics: A review. *Trees*, 25(1), pp.3-16.

Ruf, F. and Schroth, G. (2015). Introduction—economic and ecological aspects of diversification of tropical tree crops. In *Economics and Ecology of Diversification* (pp. 1-40). Springer, Dordrecht.

Santos, G. M. et al. (2020). Radiocarbon analysis confirms annual periodicity in *Cedrela odorata* tree rings from the equatorial Amazon. *Quaternary Geochronology*, 4.p. 101079.

Sauchyn, D. (2000). Ecosite mapping and dendroclimatology, Duck Mountains, west central Manitoba.

Saurer M., Borella S., Schweingruber, F., Siegwolf, R. (1997). Stable carbon isotopes in tree rings of beech: climatic versus site-related influences. *Trees*, 11(5), 291-297.

Saurer, M.; Cherubini, P.; Bonani, G.; Siegwolf, R. (2003). Tracing carbon uptake from a natural CO₂ spring into tree rings: an isotope approach. *Tree Physiology*, 23, 14: 997-1004. doi: 10.1093/treephys/23.14.997

Schoch, W., Heller, I., Schweingruber, F.H., Kienast, F. (2004): Wood anatomy of central European Species. Online version: www.woodanatomy.ch [08.06.2020]

Schroth, G., Läderach, P., Martinez-Valle, A. I., Bunn, C., Jassogne, L. (2016). Vulnerability to climate change of cocoa in West Africa: Patterns, opportunities and limits to adaptation. *Science of the Total Environment*, 556, 231-241.

Schwendenmann, L., Veldkamp, E., Moser, G., Hölscher, D., Koehler, M., Clough, Y., Anas, I., Djajakirana, G., Erasmí, S., Hertel, D. and Leitner, D. (2010). Effects of an experimental drought on the functioning of a cacao agroforestry system, Sulawesi, Indonesia. *Global Change Biology*, 16(5), pp.1515-1530.

Seo, J. W., Smiljanić, M. and Wilmking, M. (2014). Optimizing cell-anatomical chronologies of Scots pine by stepwise increasing the number of radial tracheid rows included-Case study based on three Scandinavian sites. *Dendrochronologia*, 32(3), pp. 205-209.

- Sultan, B., Roudier, P., Quirion, P., Alhassane, A., Muller, B., Dingkuhn, M., Ciais, P., Guimberteau, M., Traore, S. and Baron, C. (2013). Assessing climate change impacts on sorghum and millet yields in the Sudanian and Sahelian savannas of West Africa. *Environmental Research Letters*, 8(1), p.014040.
- Svetlik, I., Jull, A.J.T., Molnár, M., Povinec, P.P., Kolář, T., Demján, P., Brabcova, K.P., Brychova, V., Dreslerová, D., Rybníček, M. and Simek, P. (2019). The Best possible Time resolution: How precise could a Radiocarbon dating method be? *Radiocarbon*, 61(6), pp.1729-1740.
- Tondoh, J.E., Kouamé, F.N.G., Guéi, A.M., Sey, B., Koné, A.W. and Gnessougou, N. (2015). Ecological changes induced by full-sun cocoa farming in Côte d'Ivoire. *Global Ecology and Conservation*, 3, pp.575-595.
- TRMM, NASA (2015). Retrieved from: <https://gpm.nasa.gov/trmm> [29.05.2020]
- Van der Sleen, P., Zuidema, P.A. and Pons, T.L. (2017). Stable isotopes in tropical tree rings: theory, methods and applications. *Functional ecology*, 31(9), pp.1674-1689.
- Vieira Aragao J.R., Groenendijk P., Lisi C.S. (2019). Dendrochronological potential of four neotropical dry-forest tree species: Climate-growth correlations in northeast Brazil. *Dendrochronologia*, 53, 5-16.
- Wittig, R., König, K., Schmidt, M. and Szarzynski, J. (2007). A study of climate change and anthropogenic impacts in West Africa. *Environmental Science and Pollution Research-International*, 14(3), 182-189.
- Wood, G.A.R. and Lass, R.A. (2008). *Cocoa*. John Wiley & Sons.
- Woods, D. (2003). The tragedy of the cocoa pod: rent-seeking, land and ethnic conflict in Ivory Coast. *The Journal of Modern African Studies*, 41(4), 641-655.
- Worbes M, Junk WJ. (1989). Dating tropical trees by means of ¹⁴C from bomb tests. *Ecology* 70(2):503-7
- Zardo, R. N. and Henriques, R. P. B. (2011). Growth and fruit production of the tree *Caryocar brasiliense* in the Cerrado of central Brazil. *Agroforestry Systems*, 5, 82(1), pp. 15-23.
- Zhinin, H., Retete, C., Angamarca, E., Enrique, N., Bryan, M., Darwin, P.C. (2019). Wood anatomical features of five types of *Theobroma Cacao* (L.) from Southern Ecuador. DOI: 10.13140/RG.2.2.28778.26565

7 List of Tables

Table 1	Summary of first data set. Source: first sampling trip, data can be found in the appendix.
Table 2	Summary of second data set. Source: second sampling trip, data can be found in the appendix.
Table 3	Further comments on the second data set. Source: second sampling trip, data can be found in the appendix.
Table 4	Permutation options for the Tree Ring R-Script, with the aim of identifying the best tree ring combination with highest correlation to climatic data.
Table 5	LOC2A5 permutations with maximum correlation with annual rainfall.

8 List of Graphs

Graph 1	Sum of the precipitation for the different climatic stations of interest for this study in Ivory Coast. Source: data from Dr. Agathe Dié.
Graph 2	Mean temperature in climatic stations of interest for this study in Ivory Coast. Source: climatic data from Dr. Agathe Dié.
Graph 3	Number of gum-ducts found in each ring.
Graph 4	Ring width measurements of 3 cores collected nearby the city of Gagnoa and the sum of precipitation in mm for this location.
Graph 5	Maximized correlations, after using the R-Script and data permutation, between ring width measurements and yearly rain, dry season rain, wet season rain, yearly temperature and yearly production (strong $R > 0.7$, moderate $R > 0.5$, weak $R > 0.3$ and low $R < 0.3$).
Graph 6	LOC2A5 cacao tree core ring width measurements in μm per year (although it is not clear yet if they are really annual tree rings).
Graph 7	Tree Ring R-Script output showing the raw ring width measurements of LOC2A5 microsection and macro version and their correlation with annual sum of rainfall (the black line).
Graph 8	Tree Ring R-Script output showing the permutations of ring width measurements of LOC2A5 microsection and macro version and their correlation with annual sum of rainfall (the black line).

- Graph 9 Radio carbon dating results for three cacao tree disk samples; IS1, GA3 and MA2 and their corresponding errors.
- Graph 10 Radiocarbon dating of all the tree rings identified in IS1 and its linear regression line.
- Graph 11 ¹³C measurements per tree ring of sample IS1 and annual precipitation data from Gagnoa.
- Graph 12 Radiocarbon dating of all the tree rings identified in IS1 and its linear regression line.
- Graph 13 Final tree ring identification and width measurements of the core LOC2A5 with the corresponding annual precipitation.

9 List of Figures

- Figure 1 World cocoa production (gross) 2014/15 forecast: 4.232 million tonnes. Source: ICCO. Retrieved from: <https://www.confectionerynews.com/Article/2015/04/29/What-is-the-future-of-cocoa-growing-in-Asia> [05.11.2019]
- Figure 2 Relative climatic suitability (in percent) for cocoa of the West Africa cocoa belt under current and projected 2050s climate conditions, as well as suitability change, according to a Maxent model based on 24 climate variables. The red lines show areas of cocoa production (Schroth et al., 2016).
- Figure 3 Conifer tree ring visualisation (Laboratory of Tree-Ring Research Arizona, 1999).
- Figure 4 Above: Stem disc from sample E3 overlaid by a SXFM-profile. Content of calcium and strontium increases at the tree-ring borders. Below: Neutron Image of a section of the same sample (E3). Higher density peaks should reflect tree-ring borders but can also be induced by Intra-Annual-Density-Fluctuations, making tree-ring dating impossible (Cherubini et al., 2013).
- Figure 5 Radial growth of the trunks of five different tropical species from Brazil and the precipitation curve (Bressan-Smith et al., 1997).
- Figure 6 Radiocarbon in tree rings at different lo cations. Data representing the 4 different zones defined by Hua and Barbetti (2004) include NE Hungary (Hertelendi and Cson gor 1982) in NH zone 1; Agematsu, Japan (Muraki et al., 1998) in NH zone 2; Doi Inthanon, Thailand (Hua et al., 2000, 2004) in NH zone 3; and Armidale (Hua et al., 2003) and Ta smania (Hua et al., 2000)

from Australia in the SH zone. The new tree ring data are from Muna Island, Indonesia (Hua et al., 2012b). Error bars are 1σ . (Hua et al., 2013).

- Figure 7 World map showing zonal atmospheric bomb 14 C. The mean positions of the summer and winter ITCZ are adapted from Linacre and Geerts (1997) (Hua et al., 2013).
- Figure 8 Microscopical images of cross-sections of different parts of cacao tree: branch (left), root (middle) and stem (right). These pictures were taken in cacao tree grown in Sulawesi, Indonesia, by Kotowska et al. (2015).
- Figure 9 Microscopic images of the wood of five T. cacao biotypes in their three anatomical planes (From top to bottom: transversal (20X), tangential (10X) and radial (10X)) (Zhinin et al., 2019).
- Figure 10 Box plots showing the variability of quantitative characteristics (Zhinin et al., 2019).
- Figure 11 Political map of Ivory Coast. Source: nationsonline.org
- Figure 12 Cocoa warehouse in Ivory Coast. Source: sampling trip.
- Figure 13 Cocoa farm with farmers and helpers in Ivory Coast. Source: sampling trip.
- Figure 14 Corer in a cacao tree and an extracted core from Ivory Coast. Source: sampling trip.
- Figure 15 Cacao tree disk from a tree which was already cut in Ivory Coast and the same disk after polishing/ sanding it in the workshop. Source: sampling trip and lab work.
- Figure 16 Sample set 1 with samples collected during the first sampling trip.
- Figure 17 Sample set 2 with samples collected during the second sampling trip.
- Figure 18 Cutting the upper surface of a core with microtome. Left is before cutting and right is after it. Source: lab work.
- Figure 19 Measuring ring width with TSAPWin. On the right, the microscope and moving table and on the left, the monitor showing ring width values on a plot. Source: <https://hidrolab.lv/tree-wood-analysis-products/>
- Figure 20 Sample core of a cacao tree from Ivory Coast. The first picture is the entire core and the second is a zoomed in area. Source: lab work.
- Figure 21 Cacao tree core split into smaller pieces. Source: lab work.

- Figure 22 Embedding samples in paraffin and cutting with the rotatory microtome. Source: lab work.
- Figure 23 Cutting directly with the microtome and staining with safranin and astrablue. Source: lab work.
- Figure 24 Cutting tree rings for chemical analysis. Source: lab work.
- Figure 25 Grid of permutations. The first graph shows the data without any permutations, the following graphs show different permutations and the corresponding correlation with precipitation data. Source: R-Script output.
- Figure 26 Tree samples collected in Ivory Coast and a grid of about 50 km on top. The darker the grid square the higher the number of samples within it. Source: sampling trip, map created with QGIS.
- Figure 27 The first core (LOC3A4) has rings which appear to be very clear, especially in comparison to the second core, below (LOC4A5) which has extremely unclear rings. Source: lab work.
- Figure 28 On the left figure, the early wood, ring-border and late wood are displayed. The vessels are smaller in the late wood than in the early wood. On the middle figure, another clear tree-border is displayed, whereby the fibre cells are thicker in the late wood. The third figure shows broader parenchyma bands at a structure similar to a ring-border (AB2 left and middle, DI9 right). Source: lab work.
- Figure 29 Scanned microsection with polarized light filters with visible prismatic crystals in cacao tree core (AB2). Source: lab work.
- Figure 30 Gum-duct in sample (IS1 top, SP1 bottom). Source: lab work.
- Figure 31 Ring detection with DendroWin and identification of gum-ducts per ring. Source: lab work.
- Figure 32 Cacao tree stem disk from Abengourou (LOC4dA), many gum-ducts are visible and most of them are not visible through the whole circumference. Source: sampling trip and lab work.
- Figure 33 Macroscopical view of a cacao tree core (LOC3B2) from Gagnoa, with very clear rings. Source: sampling trip and lab work.
- Figure 34 Zoom in ring boundaries of a microsection of a cacao tree disk (MA2). Source: sampling trip and lab work.
- Figure 35 Map of the samples collected and their qualitative assessment. The single points are samples from the first sampling trip and the pie charts summarize

the samples of the second sampling trip. The colours reflect the qualitative assessment of the tree rings. Source: sampling trip, map created with QGIS.

- Figure 36 Pictures of the polished cacao tree disks collected during the first sampling trip and their geographical location. Source: sampling trip, map created with QGIS.
- Figure 37 Ring width measurements of the polished tree disks from the first sampling trip. Each sample has a graph and the lines correspond to tree-ring width measurements along different radii of the disk. Source: sampling trip.
- Figure 38 Map of the samples collected and their quantitative assessment based on the permutations with maximized correlation with climatic data. The size of the pie charts represents the number of samples collected in that zone and the colours show the level of correlation with precipitation data (strong $R > 0.7$, moderate $R > 0.5$, weak $R > 0.3$ and low $R < 0.3$). Source: sampling trip, map created with QGIS.
- Figure 39 Three cacao tree disks and their microsections, MA2 on the left, GA3 on the top right and IS1 on the bottom right. Source: sampling trip and lab work.
- Figure 40 IS1 microsection and identified tree rings and their description. Source: sampling trip and lab work.
- Figure 41 Picture of IS1 sample when sampled in the plantation, when prepared in the lab and the results. Source: sampling trip and lab work.
- Figure 42 Tree core LOC2A5 and its microsection. Below the tree core and the marked rings that were sent for radiocarbon dating. Source: lab work.
- Figure 43 Ring width measurement of all rings identified for LOC2A5. Source: lab work.
- Figure 44 Tree ring classification of LOC2A5. Source: lab work.
- Figure 45 Comparison of the qualitative analyses describing the tree-ring borders clarity and the quantitative analyses measuring widths and checking correlations with climatic data. Source: lab work, map created with QGIS.
- Figure 46 “Relative climatic suitability (in percent) for cocoa of the West Africa cocoa belt under current (left) and projected 2050s climate conditions (right). The red lines show areas of cocoa production.” (Schroth et al., 2016). Map created with QGIS.

10 Appendix

10.1 Samples tables

Table with all the details of the first sample set from the first sampling trip:

Index	ID	Location	Status	Type	Labor analysis	Tree-rings	Gum-ducts	Correlation with precipitation	Comments
1	DI1	#N/A	alive	core	no	no	no		bad quality, decayed, broken or lost
2	DI2	Lakota	dead	disk	microsection	normal			DI2_C2 DI2_A after ring or gum-duct serie of crystals in parenchyma band
3	DI3	Lakota	alive	core	microsection	normal			perfect slides
4	DI4	Gagnoa	alive	core	microsection	clear			no location!, thicker parenchyma bands at ring
5	DI5	Gagnoa	alive	branch	no	no	no		bad quality, decayed, broken or lost
6	DI6	Gagnoa West	alive	core	microsection	clear			
7	DI8	Sinfra	alive	core	microsection, ring width	normal	2010, 2014	low	has SS, pith
8	DI9	Gagnoa	alive	core	microsection	clear			big tree, many pods, maybe thick slice
9	IS1	Gagnoa West	alive	disk	microsection, ring width	normal		strong	
10	IS2	Gagnoa West	alive	core	ring width	normal	2003	moderate	
11	IS3	Gagnoa West	alive	core	microsection	clear/normal			small/short, almost pith
12	IS4	Gagnoa West	alive	core	microsection	very clear			is a hybrid, red pods, very broad parenchyma band full of crystals 1.2, very thick slices
13	IS5	Daloa	alive	core	microsection	clear			redo IS5_1 and 5
14	IS6	Daloa	alive	branch	microsection	clear			
15	IS7	Daloa	alive	branch	no	no	no		bad quality, decayed, broken or lost, fallen

16	IS8	Daloa	alive	core	microsection	very clear			nice rings! IS8_6 wavy rings! measure them IS8_1 45
17	IS9	Daloa	alive	core	ring width	normal	1999, 2017	weak	whole inside, almost broken
18	MA 1	Daloa	alive	core	microsection	very clear			marked red, no pods, rainy, pith, flowers, very blue, maybe MA1_1 redo
19	MA 2	Daloa	alive	disk	microsection	not clear			with flowers, humidity soil moisture 51%, all redo
20	MA 3	Daloa	alive	core	?	clear			wet area, neat Sassandra, soil moisture 40.3%
21	MA 4	Duekoue	alive	core	ring width	normal	2007, 2019	weak	almost pith
22	MA 5	Duekoue	alive	core	ring width	clear	none	low	is a hybrid, small, many flowers, near beautiful farm
23	MA 6	Guiglo	alive	core	microsection	not clear			small tree, no pith, very bad wood, funghi, bad slides, too thick, redo all
24	MA 7	Man	alive	core	?	clear			is a hybrid, fruits below and on top
25	GA 1	Bangolo	alive	core	microsection	clear			maybe not straight, short, only 1 pod, thick, redo all
26	GA 2	Bangolo	dead	core	microsection	clear			is a hybrid, dead, almost straight, poor quality slides, redo all
27	GA 3	Bangolo	alive	disk	microsection, ring width	clear		moderate	probably broken, GA3_A: from pith onwards, 1 ring, followed by 1 intra-annual fluctuation, GA3_A
28	GA 4	Bangolo	alive	core	ring width	not clear	none	strong	more stems merged, core broke, almost 2 piths (only 1 measured ring widths), neat protected area

29	GA 5	Daloa	alive	core	ring width	not clear	2006, 2008, 2009	weak	cut tree, perfect pith and beyond
30	SO 1	Soubre East	alive	core	ring width	normal	2018	weak	has SS, big tree, almost points, with black pods
31	SO 2	Soubre	alive	core	ring width	not clear	2006, 2011, 2013	low	with farmers permission, many IADFs
32	SO 3	Soubre East	alive	core	ring width	normal	2009, 2016	weak	is a hybrid, half broken core
33	SO 4	Soubre	dead	disk	microsection, ring width	not clear		strong	insect holes on lower stem, took upper one, redo all
34	SO 5	Soubre	alive	disk	microsection, ring width	normal		moderate	cut by Kipre with machete, redo all
35	SO 6	Soubre South	alive	core	no				small tree, high core
36	SP1	Soubre South	alive	core	microsection	normal			near rubber trees, no pith, maybe interesting rings, too thick, redo all
37	SP2	San Pedro	alive	core	ring width	normal	2016	moderate	bad plantation, almost no pods, if then sick, old big tree with only 1 rotten pod sampled
38	SP3	San Pedro	alive	core	ring width	not clear	2004, 2008, 2012, 2018	weak	not many pods, with pith
39	SP4	San Pedro	dead	disk	microsection, ring width	not clear		moderate	dead tree pile, very dry wood, no location!, redo all
40	SP6	Soubre South	alive	core	microsection	clear/normal			small tree, whole pith
41	SA 1	San Pedro	alive	core	microsection	normal			broken/split core, confused with IS3, redo all, thick
42	SA 2	San Pedro East	alive	core	microsection, ring width	clear	none	weak	some pods and flowers, no pith, some parts are bad, redo
43	SA 3	San Pedro East	alive	core	?	?			old tree, many pods, young farm (12 years)
44	SA 4	San Pedro East	alive	core	microsection	clear			cored tree no pods, nice farms with many green pods, bad quality, bad blade

45	SA 5	Fresco	alive	core	?	?				nice farm, farmer says 12 years old, no rain past 4 weeks, less rain than past years
46	SA 6	Fresco	alive	core	no	no	no			bad quality, decayed, broken or lost, few pods, 2 piths
47	AB 1	Abie	alive	core	microsection, ring width	not clear	2005, 2006, 2015	weak		big tree, almost pith
48	AB 2	Abengourou West	alive	core	microsection	very clear				is a hybrid, small, red pods
49	AB 3	#N/A	alive	core	microsection	very clear				some too thick
50	AB 4	Abengourou East	dead	core	microsection	very clear				half dead, pith, very bad

Table with all the details of the second sample set from the second sampling trip:

Index	ID	Location	Type	Status	Labor analysis	Tree-rings	Gum-ducts	Correlation with precipitation	Comments
53	LOC1A1	Seguela	core	alive	ring width	normal	none	moderate	
54	LOC1A2	Seguela	core	alive	no	no	no		bad quality, decayed, broken or lost
55	LOC1A3	Seguela	core	alive	ring width	normal	none	moderate	
56	LOC1B1	Seguela	core	alive	ring width	clear	maybe/broke	moderate	a bit decayed
57	LOC1B2	Seguela	core	alive	microsection, ring width	clear	none	weak	
58	LOC1B3	Seguela	core	alive	ring width	normal	2019	moderate	
59	LOC1B4	Seguela	core	alive	ring width	normal	none	moderate	a bit decayed
60	LOC1B5	Seguela	core	alive	ring width	normal	2014	no correlation	
61	LOC1Ad A	Seguela	disk	alive	ring width	clear	?	weak	
62	LOC1Ad B	Seguela	disk	alive	ring width	clear	?	no correlation	
63	LOC1Ad C	Seguela	disk	alive	ring width	clear	?	weak	
64	LOC2A1	Daloa	core	alive	ring width	clear	none	weak	
65	LOC2A2	Daloa	core	alive	ring width	clear	2012	moderate	
66	LOC2A3	Daloa	core	alive	ring width	clear	2004	moderate	

67	LOC2A4	Daloa	core	alive	ring width	clear	maybe/broke	weak	
68	LOC2A5	Daloa	core	alive	ring width	very clear	none	moderate	
69	LOC2B1	Daloa	core	alive	ring width	clear	none	weak	
70	LOC2B2	Daloa	core	alive	ring width	normal	none	moderate	
71	LOC2B3	Daloa	core	alive	ring width	clear	2003	weak	
72	LOC2B4	Daloa	core	alive	ring width	clear	none	moderate	
73	LOC2B5	Daloa	core	alive	microsection, ring width	very clear	none	weak	
74	LOC2C1	Daloa	core	alive	no	no	no		bad quality, decayed, broken or lost
75	LOC2C2	Daloa	core	alive	ring width	clear	2011	no correlation	
76	LOC2C3	Daloa	core	alive	ring width	clear	none	weak	
77	LOC2C4	Daloa	core	alive	no	no	no		bad quality, decayed, broken or lost
78	LOC2C5n	Daloa	core	alive	no	no	no		bad quality, decayed, broken or lost
79	LOC3A1	Gagnoa	core	alive	no	no	no		bad quality, decayed, broken or lost
80	LOC3A2	Gagnoa	core	alive	no	no	no		bad quality, decayed, broken or lost
81	LOC3A3	Gagnoa	core	alive	microsection, ring width	very clear	none	strong	
82	LOC3A4	Gagnoa	core	alive	ring width	very clear	none	strong	
83	LOC3B1	Gagnoa	core	alive	ring width	very clear	none	moderate	
84	LOC3B2	Gagnoa	core	alive	ring width	very clear	maybe/broke 2016	weak	
85	LOC3B3	Gagnoa	core	alive	ring width	very clear	none	weak	
86	LOC3B4	Gagnoa	core	alive	ring width	clear	none	moderate	
87	LOC3C1	Gagnoa	core	alive	ring width	clear	none	no correlation	many IADFs
88	LOC3C2	Gagnoa	core	alive	ring width	clear	none	no correlation	many IADFs

89	LOC3C3	Gagnoa	core	alive	ring width	normal	none	weak	
90	LOC3C4 A	Gagnoa	core	alive	ring width	normal	2019	moderate	
91	LOC3C4 B	Gagnoa	core	alive	ring width	very clear	none	moderate	
92	LOC3C5	Gagnoa	core	alive	ring width	clear	none	moderate	many IADFs
93	LOC3C6	Gagnoa	core	alive	ring width	very clear	none	weak	some IADFs
94	LOC3C7	Gagnoa	core	alive	ring width	clear	none	weak	some IADFs
95	LOC3C8	Gagnoa	core	alive	ring width	clear	2018	moderate	
96	LOC4A1	Abengourou North	core	alive	no	no	no		bad quality, decayed, broken or lost
97	LOC4A2	Abengourou North	core	alive	ring width	clear	2005	no correlation	
98	LOC4A3	Abengourou North	core	alive	no	no	no		bad quality, decayed, broken or lost
99	LOC4A4	Abengourou North	core	alive	ring width	clear	none	no correlation	
100	LOC4A5	Abengourou North	core	alive	microsection, ring width	unclear	none	no correlation	
101	LOC4A6 A	Abengourou North	core	alive	ring width	normal	none	moderate	
102	LOC4A6 B	Abengourou North	core	alive	ring width	normal	none	no correlation	
103	LOC4B1	Abengourou North	core	alive	ring width	clear	2016	moderate	some IADFs, wrong namiong loc3b1
104	LOC4B2 A	Abengourou North	core	alive	ring width	normal	2010	weak	
105	LOC4B2 B	Abengourou North	core	alive	ring width	normal	none	no correlation	not well cut
106	LOC4B3	Abengourou North	core	alive	ring width	normal	2010, 2018	weak	not well cut
107	LOC4B4	Abengourou North	core	alive	ring width	normal	1996, 2012, 2019	no correlation	
108	LOC4Ad A	Abengourou North	disk	alive	ring width	normal	?	no correlation	

10.2 Samples ring width measurements

Seguela or Vavouà

Year	LOC1 A1	LOC1 A3	LOC1B 1	LOC1B 2	LOC1B 3	LOC1B 4	LOC1B 5	LOC1Ad A	LOC1A dB	LOC1Ad C
1998	0	0	0	0	936	0	0	0	0	0
1999	1013	790	0	0	1729	0	0	0	0	0
2000	2216	3851	1053	0	1273	0	0	0	0	0
2001	4198	5965	2663	0	4192	0	0	0	0	0
2002	1961	4244	2903	0	3419	0	0	0	0	0
2003	3337	3769	2165	0	1058	0	0	0	0	0
2004	3419	3661	2008	1106	1700	0	0	0	0	0
2005	2115	5256	2312	1310	2099	0	0	0	0	0
2006	2449	2765	2057	2674	4908	0	0	0	1350	1720
2007	8612	2331	1649	1969	2680	1102	13314	2000	2450	2320
2008	996	3253	3311	2234	1554	3346	4826	4500	3080	2640
2009	4674	1073	2784	3431	2570	4532	3286	2990	2090	2350
2010	6124	3340	2846	5387	1863	952	5219	2930	1500	2020
2011	4573	2492	2299	2967	2641	3651	4518	2990	1670	4140
2012	3939	3024	2095	3284	2738	2740	3257	2750	2510	3050
2013	1684	3369	3213	3163	1919	2201	3653	5060	1730	3240
2014	2602	3560	1821	3184	2021	3156	2352	3190	2350	3090
2015	2293	6975	1942	2896	3078	5600	3276	7530	5880	4050
2016	3298	2549	1797	3898	3827	3582	2916	5390	3220	3830
2017	1125	3599	2152	3730	1169	4768	4415	2600	2710	3570
2018	3298	6328	2919	3995	3665	4021	1306	2790	4990	1280
2019	764	2165	3264	2468	1955	2879	1749	3360	2740	1230

Abengourou North

Year	LOC 4A2	LOC4 A4	LOC4 A5	LOC4A 6A	LOC4 A6B	LOC4 B1	LOC4B 2A	LOC4B 2B	LOC4 B3	LOC4 B4	LOC4A dA
1998	1483	895	0	4211	4431	664	4106	234	0	2319	0
1999	1623	1833	0	3437	1211	2261	3955	2250	641	1817	0
2000	1687	1253	0	2370	2070	979	1947	4737	1361	1721	0
2001	1027	632	0	4119	1380	988	2564	1603	2426	3941	0
2002	798	1239	0	1463	1509	2389	3707	2908	2746	5153	840
2003	1421	889	0	1774	1268	1037	2413	1099	709	1220	1570
2004	768	1280	0	2189	1503	3764	2287	1690	3314	2298	1280
2005	2000	1704	0	2032	1820	2832	1321	1458	852	3202	1640
2006	1400	1431	10	3503	1588	1559	953	1587	4503	3826	2390
2007	1498	1793	3200	1480	1865	1171	2015	762	2353	3186	2840
2008	2873	1659	1283	1314	1873	1930	2285	2079	4065	2899	3560
2009	2196	1238	2059	3271	2123	2835	876	2626	3827	3361	2080
2010	1462	1195	5880	2203	1119	3806	1699	2287	7396	2887	2000
2011	1474	4286	1483	2111	885	1905	1136	1772	2045	2967	4920
2012	3554	1889	2600	5940	1229	1781	1496	1890	6409	6815	1380
2013	2758	2101	2799	4492	2286	1607	2009	4862	734	2694	5880
2014	1293	1581	8376	1889	1101	2406	497	4591	4566	4430	3140
2015	3653	2135	6901	2256	3948	2815	1889	1825	1980	3521	2620
2016	3356	726	4590	963	1569	1549	2031	2085	3830	4528	4730
2017	2387	856	2157	686	2974	1735	618	5708	895	1746	2520
2018	3774	1830	3053	1907	1143	1505	2822	758	5051	1426	2980

2019	879	1323	2745	1893	2850	2245	1492	1134	1571	2044	510
------	-----	------	------	------	------	------	------	------	------	------	-----

Bangolo and Abie

Year (Bangolo)	GA3	GA4	Year (Abie)	AB1
1999	0	0	1999	0
2000	0	0	2000	0
2001	0	0	2001	0
2002	0	0	2002	0
2003	0	0	2003	486
2004	0	0	2004	1523
2005	0	0	2005	1160
2006	0	0	2006	2321
2007	1930	0	2007	3388
2008	1390	0	2008	6544
2009	1530	0	2009	2723
2010	870	620	2010	4219
2011	1390	5615	2011	3526
2012	900	3403	2012	3571
2013	2080	2310	2013	4647
2014	3730	5077	2014	5594
2015	3250	2319	2015	6877
2016	2350	4286	2016	3415
2017	890	2534	2017	5564
2018	820	3244	2018	3745
2019	2020	1763	2019	3384

Daloa

Year	IS9	GA5	LOC2A1	LOC2A2	LOC2A3	LOC2A4	LOC2A5
1992	0	0	0	0	0	0	0
1993	1822	0	0	0	0	0	0
1994	1792	0	0	0	0	0	0
1995	2618	0	0	0	0	0	0
1996	3160	0	0	0	0	0	0
1997	2881	0	0	0	0	0	0
1998	2001	0	0	0	808	0	40
1999	3312	0	0	0	1643	0	1019
2000	2292	0	0	0	919	0	1271
2001	3543	0	0	0	3305	0	1081
2002	3366	0	0	0	2528	0	2154
2003	3406	0	0	0	1642	0	1392
2004	2488	0	0	2175	3791	0	887
2005	2870	0	840	2287	1909	4143	1804
2006	4239	1119	2141	1756	1928	5381	1773
2007	3175	4724	1843	1476	1806	3509	1427
2008	2740	7460	2687	2314	1923	2262	1728
2009	971	4210	1639	2623	1406	1276	2097
2010	4044	5214	771	1973	2585	3870	1708
2011	3267	5233	1504	4110	1127	1216	1686
2012	2260	6301	1551	3101	1623	1334	2587
2013	2380	3827	1209	2114	2607	2067	2761
2014	2479	5589	2958	1941	2596	2180	2737
2015	4034	3312	1350	1351	966	3149	1906
2016	2827	6354	3089	1182	1360	1480	3479
2017	4927	4676	4293	2766	1776	3797	1631

2018	2900	1390	2569	875	3559	4203	3027
2019	860	4601	1691	1109	1933	1647	3556

Year	LOC2B1	LOC2B2	LOC2B3	LOC2B4	LOC2B5	LOC2C2	LOC2C3
1992	0	0	0	0	685	0	0
1993	0	0	0	0	1515	0	2376
1994	0	0	0	0	1305	0	1556
1995	0	0	2986	0	1915	0	1398
1996	0	0	969	0	1198	0	2446
1997	0	0	1399	0	1710	0	1443
1998	1405	0	1219	0	1705	0	2073
1999	444	852	2342	1103	1061	0	2027
2000	1705	1009	1393	1663	1214	0	1144
2001	795	1574	2571	721	813	1576	3242
2002	1027	1615	2706	1289	1283	2613	2758
2003	1868	2438	2655	962	2956	1690	1765
2004	927	1450	2924	1512	2159	2166	2152
2005	1160	1638	2355	3354	3797	1773	3105
2006	1263	1832	2532	2129	1770	2322	2215
2007	1327	2681	2042	2052	773	1863	2770
2008	2446	1343	4180	995	1417	2712	4098
2009	2755	1895	2992	1494	1048	2422	3408
2010	2544	1757	1917	1535	3531	2039	3941
2011	2871	1400	4068	1585	772	2002	3356
2012	1842	1246	3583	5293	2079	849	1274
2013	1884	1760	1760	4465	2034	2317	1649
2014	3371	1650	1785	1701	704	1232	1366
2015	3614	1013	1692	3332	1211	3010	3182
2016	1559	1261	3413	1387	1521	3134	2430
2017	3141	1692	3779	2790	1383	4064	1637
2018	2195	901	790	3553	1666	1720	1697
2019	3796	833	2759	1477	1255	3093	2268

Gagnoa

Year	LOC3A3	LOC3A4	LOC3B1	LOC3B2	LOC3B3	LOC3B4	LOC3C1
1990	0	0	0	0	0	0	185
1991	0	0	0	0	0	0	2575
1992	0	0	0	0	0	0	4408
1993	0	0	0	0	0	0	3016
1994	0	0	0	0	0	0	2607
1995	0	0	0	0	0	0	1710
1996	0	0	0	949	0	0	1211
1997	0	0	2418	1548	0	0	1134
1998	0	0	2800	748	0	2317	1275
1999	0	0	5403	1404	0	1564	1621
2000	0	0	4123	2006	0	2018	2595
2001	0	0	1901	889	962	2234	2827
2002	0	0	1571	726	3801	1951	2937
2003	2197	0	2686	1509	1373	1951	1601
2004	1702	0	1582	3872	4023	1642	3804
2005	1318	0	1016	2023	2205	1894	1756
2006	3377	2830	1827	2290	4147	1652	3342
2007	4273	1344	4120	953	1001	2168	756
2008	3614	2048	2451	1365	2179	992	4087

2009	3594	2205	2411	1786	2356	1978	2423
2010	2512	1587	6225	1884	3211	1497	1403
2011	540	2165	4391	523	1520	601	824
2012	1249	2838	996	2816	3684	1449	2536
2013	2650	1708	2552	627	1511	2081	1242
2014	2883	3069	3997	1877	1612	484	627
2015	2774	1983	579	1647	2686	1160	1576
2016	3304	3501	2091	1960	1486	1547	3506
2017	1878	2051	1094	1886	1609	1388	1082
2018	1258	2393	3880	1931	2809	2860	1842
2019	1659	2160	1224	2123	1057	729	1099

Year	LOC3C2	LOC3C3	LOC3C4A	LOC3C4B	LOC3C5	LOC3C6	LOC3C7	LOC3C8
1990	0	0	0	0	0	3516	0	0
1991	0	0	0	0	0	1137	0	0
1992	0	0	0	0	0	2469	0	0
1993	0	2376	0	0	0	1569	0	0
1994	0	1556	0	0	0	2155	0	0
1995	0	1398	0	0	0	1953	0	0
1996	0	2446	0	0	0	1470	0	0
1997	0	1443	0	0	0	3775	0	0
1998	0	2073	0	0	0	5366	0	0
1999	0	2027	0	1787	0	2022	5644	0
2000	0	1144	0	3715	0	3726	1732	0
2001	1576	3242	4099	1878	0	3122	2614	0
2002	2613	2758	3757	2272	601	4423	3938	0
2003	1690	1765	4723	1419	2191	1697	2042	0
2004	2166	2152	2160	6436	4016	3700	1948	0
2005	1773	3105	1559	4852	2386	2914	1845	333
2006	2322	2215	5840	1337	4927	1752	1873	2508
2007	1863	2770	1999	1110	1438	3479	2274	3585
2008	2712	4098	4305	2873	3788	1366	1511	2837
2009	2422	3408	4500	5223	2093	3404	1813	4375
2010	2039	3941	3332	911	2605	2554	2353	6047
2011	2002	3356	2667	2972	3111	3760	1796	3517
2012	849	1274	6398	2867	2961	2178	1954	1659
2013	2317	1649	1155	3084	4092	2036	1915	2095
2014	1232	1366	1550	3064	2431	1082	4246	2052
2015	3010	3182	1256	3696	3517	2904	4080	1841
2016	3134	2430	1817	2919	2486	1791	3761	2382
2017	4064	1637	1690	2161	845	3253	4674	2125
2018	1720	1697	836	1961	1466	1595	2826	3618
2019	3093	2268	4154	652	3893	2443	1160	2626

Duekoue, Gagnoa West and Sinfra

Year (Duekoue)	MA4	MA5	Year (Gagnoa West)	IS1	IS2	Year (Sinfra)	DI8
1990	0	0	1990	0	0	1990	0
1991	0	2054	1991	0	0	1991	0
1992	0	1721	1992	0	400	1992	694
1993	0	3119	1993	0	1732	1993	2275
1994	0	5155	1994	0	1580	1994	674
1995	0	3179	1995	0	1765	1995	1380

1996	0	1528	1996	0	4324	1996	1435
1997	0	2753	1997	0	2196	1997	1923
1998	0	1699	1998	0	3441	1998	2540
1999	810	3264	1999	0	4820	1999	2763
2000	13441	3674	2000	1200	2633	2000	2487
2001	5186	1714	2001	1400	3385	2001	1443
2002	4011	3290	2002	2250	3934	2002	5478
2003	1575	4578	2003	3450	3890	2003	3726
2004	1805	3865	2004	2010	2774	2004	4946
2005	2570	8132	2005	850	4745	2005	2141
2006	2347	1695	2006	1240	6685	2006	4669
2007	6167	2216	2007	2070	3474	2007	2019
2008	4417	3298	2008	1700	5133	2008	2847
2009	2636	2947	2009	2640	2165	2009	3201
2010	3338	2433	2010	1360	1683	2010	4512
2011	4891	4634	2011	2100	2683	2011	2577
2012	3319	3710	2012	1130	7146	2012	3793
2013	3130	3298	2013	4140	4044	2013	5942
2014	5589	4716	2014	3900	5482	2014	3262
2015	5883	2524	2015	3180	6923	2015	3253
2016	5022	3170	2016	2950	1807	2016	6211
2017	4429	1881	2017	1110	7818	2017	6312
2018	3749	2653	2018	920	3230	2018	2371
2019	2584	3881	2019	1850	3156	2019	2062

Soubre and Soubre East

Year (Soubre)	SO1	SO3	Year (Soubre East)	SO4	SO5	SO2
1997	0	3076	1997	0	0	0
1998	0	3426	1998	0	0	0
1999	3287	4108	1999	0	1340	0
2000	5872	3757	2000	0	1020	0
2001	3727	5121	2001	0	1090	0
2002	6885	4495	2002	0	1310	0
2003	2895	3940	2003	0	1300	714
2004	5380	4714	2004	0	3130	5523
2005	3328	3241	2005	0	1350	10640
2006	4398	2555	2006	940	2470	1705
2007	6188	2256	2007	890	3180	3984
2008	7212	1286	2008	2430	2220	1288
2009	3203	2585	2009	2650	1780	2330
2010	3390	2650	2010	3080	2900	2228
2011	4267	2060	2011	2430	1950	5737
2012	4583	1273	2012	2290	2780	3442
2013	3548	2693	2013	2830	3390	2625
2014	4157	1256	2014	3290	4840	3339
2015	3042	3270	2015	2880	2950	3519
2016	3928	2860	2016	1790	6770	4373
2017	6225	1478	2017	1710	2120	2198
2018	3816	1715	2018	1310	1910	3676
2019	3921	2223	2019	1700	770	840

San Pedro and San Pedro

Year (San Pedro)	SP3	SP4	SP2	Year (San Pedro East)	SA2
1996	2350	0	0	1996	0
1997	2731	0	0	1997	0
1998	2939	0	1175	1998	2830
1999	2037	0	7150	1999	3466
2000	3165	0	3939	2000	3132
2001	4084	0	2804	2001	1668
2002	4498	0	1403	2002	3631
2003	2746	0	3018	2003	2970
2004	1434	0	4471	2004	1544
2005	1139	1100	6006	2005	2102
2006	3263	1200	5956	2006	2199
2007	1465	4960	3815	2007	1889
2008	3334	1260	4655	2008	3147
2009	2024	3660	2456	2009	3710
2010	1853	1620	7355	2010	2749
2011	2472	1960	2578	2011	3159
2012	2073	2560	1339	2012	4608
2013	1836	1780	1780	2013	3815
2014	1915	2660	2490	2014	4705
2015	2407	2580	1178	2015	5268
2016	3536	2930	5167	2016	2881
2017	1750	2030	4497	2017	4300
2018	2274	1460	2306	2018	3730
2019	1315	1640	2470	2019	2354

10.3 Climatic and production data

Global climatic data from the World Bank Group. Source:

<https://climateknowledgeportal.worldbank.org/country/cote-divoire> [05.02.2020]

Precipitation in mm per year and temperature in degree Celsius.

Year	Rain_sum	Rain_sum_dry	Rain_sum_wet	Temp_mean
1991	1250.73	1071.965	178.76489	26.423808
1992	1184.3	997.7803	186.51713	26.265917
1993	1271.64	1037.113	234.52343	26.403667
1994	1326.72	1152.754	173.9665	26.347917
1995	1407.65	1193.77	213.88081	26.597033
1996	1400.71	1202.901	197.8102	26.564542
1997	1196.11	1030.628	165.48646	26.606042
1998	1255.34	1101.008	154.329	27.153958
1999	1421.16	1177.956	243.20008	26.494608
2000	1309.57	1155.649	153.92352	26.512033
2001	1426.64	1234.767	191.87	26.651908
2002	1292.22	1129.1837	163.03809	26.817358

2003	1476.06	1230.046	246.0116	26.804733
2004	1348.04	1110.273	237.77057	26.778358
2005	1276.67	1091.946	184.7236	26.962717
2006	1433.06	1264.3135	168.74838	26.744083
2007	1360.06	1170.07	189.98863	26.879017
2008	1407.67	1204.4563	203.20968	26.393108
2009	1445.66	1169.345	276.3117	26.862108
2010	1738.67	1527.287	211.383	27.168258
2011	1347.07	1134.4913	212.57444	26.80155
2012	1291.94	1089.202	202.73482	26.510883
2013	1117.39	909.7996	207.59286	26.768017
2014	1523.75	1291.47	232.28403	26.79395
2015	1119.35	923.8561	195.49787	26.976833
2016	1308.82	1107.0883	201.7362	27.254042

Climatic data received from Dr. Agathe Dié.

Sum of precipitation in mm per year:

Year	Seguela	Abengourou North	Daloa	Gagnoa	Soubre	San Pedro
1990	0	0	1992	1364.2	0	0
1991	0	0	1993	1300.8	0	0
1992	0	0	996.6	1006.4	0	0
1993	0	0	1001.6	1379.9	0	0
1994	0	0	1102	1292.8	0	0
1995	0	0	1334.9	1520	0	0
1996	0	0	1206.2	1197.3	0	1356.8
1997	0	0	1070.1	1101.3	0	1288.7
1998	1100.9	1113.4	1100.9	1295.7	0	1283.2
1999	1403.9	1237.6	1403.9	1276.7	1449.8	1398.7
2000	1329.1	1173.3	1329.1	1343.9	1568.8	1594
2001	841.2	1345.5	841.2	1389.233	1329.8	1881.5
2002	1336.783	1497.6	1336.783	1401	1433.5	1726.6
2003	1396.4	1173.5	1396.4	1847.6	1552.8	1743.1
2004	1222.1	1187.1	1222.1	1540.9	1600.5	1274.4
2005	1120.4	1338	1120.4	1470.7	1258.3	1892.7
2006	1180.1	1170	1180.1	1252.4	1530.3	1654.6

2007	1135.7	1294.6	1135.7	1698.7	1625	1250.9
2008	1443.5	1407.3	1443.5	1602.7	1517.9	1661
2009	1253.8	1315.2	1253.8	1519.9	1249.6	1186.7
2010	1355.2	1484.5	1355.2	1789.1	2100.3	1912.5
2011	984.8727	1207.6	984.8727	1454.8	1712.5	1364.4
2012	1464.3	1129.5	1464.3	1329	1421	1153.6
2013	1582.9	1263.2	1582.9	1484.3	1673.5	1113.9
2014	1538.9	1403.5	1538.9	1808	1886.5	1902.4
2015	1062.1	1383.7	1062.1	1395	1342.7	954.7
2016	1234.7	1175.9	1234.7	1430.7	1575.8	1401.4
2017	858.1	1302.1	858.1	1030.3	1141.1	1849.1
2018	1319.3	0	1319.3	1302.2	0	1295.6
2019	1363.7	0	1363.7	1478.7	0	822.7

Mean temperature per year in degree Celsius:

Year	Seguela	Daloa	Gagnoa	San Pedro
2010	26.9	26.9	26.9	26.8
2011	26.1	26.1	25.9	26.4
2012	26	26	26.2	26.4
2013	26.1	26.1	26.1	26.5
2014	26.1	26.1	26.1	26.4
2015	26.4	26.4	26.2	26.4
2016	26.9	26.9	26.7	26.6
2017	26.6	26.6	26.5	26.5
2018	27.1	27.1	26.8	26.5
2019	26.8	26.8	26.9	26.7

TRMM precipitation data retrieved from Giovanni platform NASA. Source:

<https://giovanni.gsfc.nasa.gov/giovanni/> [27.05.2020]

Year	Seguela	Abengourou North	Abie	Bangolo	Daloa	Gagnoa
1998	1110.782876	1112.441742	0	0	0	0
1999	1464.075865	1345.058402	1275.559094	1772.431901	1642.538198	1448.299193
2000	1093.685713	1051.824074	1526.651541	1503.347623	1413.304496	1311.190457
2001	968.091404	1185.073103	1419.874113	1087.283972	1246.734732	1175.456927
2002	1100.336865	1049.577108	1507.876342	1273.594415	1342.087863	1212.759518

2003	1383.737758	1318.17676	1126.049052	1407.886486	1574.444329	1611.088559
2004	1069.630445	1199.914114	1463.028404	1334.66496	1269.511474	1283.013314
2005	1149.892257	1119.675005	1393.102644	1135.200576	1187.814346	1381.692992
2006	1450.014327	1141.516414	1462.560703	1328.83372	1409.198829	1242.952735
2007	1197.147001	1070.251975	1400.755997	1305.3923	1237.094447	1227.23541
2008	1323.352635	1289.562764	1304.41284	1489.895655	1650.52903	1401.364032
2009	1121.928032	1107.75807	1547.37195	1229.361449	1224.615041	1421.674428
2010	1478.793484	1333.002377	1232.806498	1614.27993	1715.638586	1642.060482
2011	1169.167943	1066.634884	1679.482157	1191.634863	1125.884914	1188.248862
2012	1329.041896	1049.17466	1396.664881	1309.570147	1417.381913	1271.204459
2013	1318.875523	1142.307549	1261.438647	1359.869075	1638.845945	1413.600521
2014	1420.692162	1159.70635	1164.316799	1562.857761	1670.782634	1604.17495
2015	1150.690257	957.6559082	1518.423659	1310.686042	1287.498361	1196.936624
2016	1144.584475	927.0688601	1390.357388	1326.658316	1285.35711	1222.433674
2017	1081.46377	1077.896257	1222.880145	1251.915869	1070.392721	1168.292448
2018	1323.409858	1091.713166	1612.069061	1443.152143	1376.131213	1356.091916
2019	0	0	1446.056415	1446.467503	1593.735575	1379.839735

Year	Gagnoa West	Duekoue	Sinfra	Soubre	Soubre East	San Pedro East	San Pedro East
1998	0	1473.573238	1088.576648	0	1302.492969	0	0
1999	1557.51116	1728.157085	1484.725841	1580.895722	1481.31882	1442.480897	1382.407047
2000	1397.040763	1508.003921	1292.69435	1554.284101	1419.292684	1454.253076	1421.507142
2001	1160.776438	1297.307042	1168.013489	1421.561882	1372.355824	1323.612119	1312.734311
2002	1281.244311	1401.542026	1189.683212	1189.873576	1192.891639	1089.795803	1121.315056
2003	1532.622247	1920.152678	1538.308759	1697.281737	1699.223961	1296.205641	1238.465815
2004	1339.960907	1379.214552	1313.141276	1449.613741	1298.042149	773.5257016	732.0810603
2005	1259.543461	1193.346057	1252.577954	1640.74108	1385.070697	1323.544145	1384.815141
2006	1313.94432	1605.233841	1232.002337	1560.266519	1376.792451	1199.337509	1194.953843
2007	1344.461035	1366.208065	1178.218625	1388.883972	1336.553441	933.9476032	940.1028527
2008	1471.919343	1588.339122	1376.587994	1716.392282	1510.321644	1221.951185	1231.617467
2009	1153.877276	1228.400026	1497.201109	1293.239011	1162.740872	852.6094184	849.1722142
2010	1704.854772	2002.023586	1647.048712	1956.357654	1827.707688	1583.397197	1472.746335
2011	1175.945244	1210.725037	1059.374587	1539.529824	1319.142288	1069.127046	1016.144801
2012	1285.636369	1299.980912	1374.445674	1414.270272	1312.013962	917.7149517	835.8713431
2013	1529.250975	1551.639505	1364.056667	1630.813071	1499.123982	1190.656251	1169.308191
2014	1743.875579	1584.728393	1587.734085	1966.053398	1853.880167	1552.137091	1592.719099

2015	1328.314524	1338.051841	1077.414075	1506.527417	1385.364718	1069.189152	1056.211308
2016	1307.438947	1412.572674	1202.86198	1528.802556	1477.54385	1213.356876	1159.71814
2017	1169.797588	1337.239314	1075.393237	1726.291607	1454.827486	1614.737153	1556.354937
2018	1369.310827	1492.791031	1355.944194	1602.909448	1398.90032	1164.072743	1086.032692
2019	1447.081916	0	0	1573.573454	0	1113.941483	1071.234461

The cocoa production data was confidentially shared by Barry Callebaut, who retrieved it from ICCO.org. Due to confidential agreements this data cannot be further shared.

10.4 Tree Ring R-Script

This script has been written by Dr. Laurens Valentin Michiels van Kessenich following Prof. Dr. Paolo Cherubini and Alice Gargano's indications. It is made out of different components presented below and can be ran on R-Studio.

Functions.R

This component contains the definitions of all functions.

```
#####
#####
#####
#####
#Rscript for Tree-Ring analysis
#####
#####
#####

#import used libraries
library(ggplot2)
library(plyr)
library(reshape2)
library(doParallel)

## Loading required package: foreach

## Loading required package: iterators

## Loading required package: parallel

library(foreach)
library(grid)
```

```

library(gtable)
library(tidyverse)

## -- Attaching packages ----- tidyverse 1.2.1 --

## v tibble 2.1.1    v purrr 0.3.2
## v tidyr 0.8.3    v dplyr 0.8.0.1
## v readr 1.3.1    v stringr 1.4.0
## v tibble 2.1.1    v forcats 0.4.0

## -- Conflicts ----- tidyverse_conflicts() --
## x purrr::accumulate() masks foreach::accumulate()
## x dplyr::arrange() masks plyr::arrange()
## x purrr::compact() masks plyr::compact()
## x dplyr::count() masks plyr::count()
## x dplyr::failwith() masks plyr::failwith()
## x dplyr::filter() masks stats::filter()
## x dplyr::id() masks plyr::id()
## x dplyr::lag() masks stats::lag()
## x dplyr::mutate() masks plyr::mutate()
## x dplyr::rename() masks plyr::rename()
## x dplyr::summarise() masks plyr::summarise()
## x dplyr::summarize() masks plyr::summarize()
## x purrr::when() masks foreach::when()

#Function to plot yearly weather with the monthly together (used to verify that the transistion from
month->year data makes sense)
plotClimate <- function(climate,title){
  pplot <- ggplot(data=climate, aes(x=Year, y=Rain_sum)) + geom_line()
  # add a line layer
  #pplot2 + pplot + geom_line() + ggtitle(title) + labs(y="climate", x = "month")
  pplot
}

#correlations between samples

#Define correlation function
getCorrelation <- function(a,b){
  correlation=ccf(a,b,0, pl = FALSE)
  return(correlation$acf[1])
}

#####
#####
#####
#####

#Function definitions for the search of optimal Permutation to correlate with climate
#from here on the inputs into the functions are one column for both climateData and ringData. Needs

```

to be prepared before passing into the functions

```
#Define some functions
removeZeros <- function(x){
  x=as.data.frame(x[!apply(x == 0, 1, FUN = any, na.rm = TRUE),]) # remove 0 elements form the
column
  x=as.data.frame(as.numeric(as.character(unlist(x))))
  colnames(x) <- c("ringSize")
  return(x)
}

#Reduce the length of the climate data to treeRingData. For correlation function we need the same len
gth
climateSameLengthAsRingData <- function(climateData,ringData){
  return(tail(climateData,nrow(ringData)))
}

#Plots the climate and ring and calculates correlation. Correlation is printed as text on the image
plotClimateAndRingCorrelation <- function(climateData,ringDataIn,labeltext,label_position
, scale){
  ringData=removeZeros(ringDataIn)
  climateData=climateSameLengthAsRingData(climateData,ringData)
  #get correlation
  corr=getCorrelation(climateData[c(2)],ringData)

  ringData$Year <- climateData$Year # align the ringData to 30 years (max of climateData)
  colnames(ringData) <- c("ringSize", "Year")
  pplot <- ggplot(data=climateData, aes(x=Year, y=Rain_sum))
  # add a line layer
  pplot2 <- pplot + geom_line() + xlab("Years") + ylab("Climate")
  pplot2 <- pplot2 + geom_point(data=ringData, aes(Year,ringSize*scale, color='red'), show.le
gend=F) + geom_line(data=ringData, aes(Year,ringSize*scale, color='red'), show.legend=F) +
scale_y_continuous(sec.axis = sec_axis(~.*1/scale, name = "ringSize"))
  #add label
  pplot2 <- pplot2 + geom_text(x=2010, y=label_position, label=paste(c("c=", round(corr,digits
=2)," ; ", labeltext), collapse = ""))
  return(pplot2)
}

#Here follow some permutation functions
#Add two neighbouring points together at position=pos
permutateData2 <- function(ringData,pos){
  if(pos>0){
    ringData[pos,1]=ringData[pos,1]+ringData[pos+1,1]
    return(as.data.frame(ringData[-c(pos+1),]))
  }else{
    return(ringData)
  }
}
```

```

}
}

#Add three neighbouring points together at position=pos
permuteData3 <- function(ringData,pos){
  if(pos>0){
    ringData[pos,1]=ringData[pos,1]+ringData[pos+1,1]+ringData[pos+2,1]
    return(as.data.frame(ringData[-c(pos+1,pos+2),]))
  }else{
    return(ringData)
  }
}

#Runs over multiple permutation positions and visualizes as a grid
plotGridOfPermutations <- function(climateData,ringData,shift=0){
  rows=4
  columns=4

  #create first column
  #create first row
  g0=ggplotGrob(plotClimateAndRingCorrelation(climateData, permuteData2(ringData,
0+shift),0+shift,2000,1))
  column <- rbind(g0, size = "first")
  i=0
  #loop rows
  for(j in 1:(rows-1)){
    gnew=ggplotGrob(plotClimateAndRingCorrelation(climateData, permuteData2(ringD
ata,i*rows+j+shift),i*rows+j+shift,2000,1))
    column = rbind(column,gnew, size = "first")
  }
  g <- cbind(column, size = "first")

  #loop columns
  for(i in 1:(columns-1)){
    #create first column
    #create first row
    j=0
    g0=ggplotGrob(plotClimateAndRingCorrelation(climateData, permuteData2(ringData
,i*rows+j+shift),i*rows+j+shift,2000,1))
    column <- rbind(g0, size = "first")
    #loop rows
    for(j in 1:(rows-1)){
      gnew=ggplotGrob(plotClimateAndRingCorrelation(climateData, permuteData2(ring
Data,i*rows+j+shift),i*rows+j+shift,2000,1))
      column = rbind(column,gnew, size = "first")
    }
    g <- cbind(g,column, size = "first")
  }
}

```

```

}
grid.newpage()
grid.draw(g)
}

#Find the maximal correlation by once adding 2 points
maximizeCorrelation2 <- function(climateData,ringData,plot=TRUE){
  ringData=removeZeros(ringData)
  max=-1

  for(i in 0:nrow(ringData)-1){
    permutedRingData=permuteData2(ringData,i)
    corr=getCorrelation(climateSameLengthAsRingData(climateData,permutedRingData),
permutedRingData)
    if(corr>max){
      max=corr
      maxPos=i
    }
  }
  #Plot the permutation with max correlation
  permutedRingData=permuteData2(ringData,maxPos)
  corr=getCorrelation(climateSameLengthAsRingData(climateData,permutedRingData),p
ermutedRingData)
  if(plot){print(plotClimateAndRingCorrelation(climateData,permuteData2(ringData,ma
xPos),paste(c("2;",maxPos),collapse="")))}

  return(c(corr,2,maxPos))
}

#Find the maximal correlation by twice adding 2 points
maximizeCorrelation22 <- function(climateData,ringData,plot=TRUE){
  ringData=removeZeros(ringData)
  max=-1

  for(i in 0:(nrow(ringData)-1)){
    if(i==0){extra=1}else{extra=0}
    for(j in 0:(nrow(ringData)-2+extra)){
      permutedRingData=permuteData2(permuteData2(ringData,i),j)
      corr=getCorrelation(climateSameLengthAsRingData(climateData,permutedRingData
),permutedRingData)
      if(corr>max){
        max=corr
        maxPosi=i
        maxPosj=j
      }
    }
  }
}

```

```

#Plot the permutation with max correlation
permutatedRingData=permutateData2(permutateData2(ringData,maxPosi),maxPosj)
corr=getCorrelation(climateSameLengthAsRingData(climateData,permutatedRingData),p
ermutatedRingData)
if(plot){print(plotClimateAndRingCorrelation(climateData,permutatedRingData,paste(c("
22;" ,maxPosi,maxPosj),collapse="")))})
return(c(corr,22,maxPosi,maxPosj))
}

#Find the maximal correlation by three times adding 2 points
maximizeCorrelation222 <- function(climateData,ringData,plot=TRUE){
  ringData=removeZeros(ringData)
  max=-1

  for(i in 0:(nrow(ringData)-1)){
    if(i==0){extra=1}else{extra=0}
    for(j in 0:(nrow(ringData)-2+extra)){
      if(j==0){extra=1}else{extra=0}
      for(k in 0:(nrow(ringData)-3+extra)){
        permutatedRingData=permutateData2(permutateData2(permutateData2(ringData,i),j),
k)
        corr=getCorrelation(climateSameLengthAsRingData(climateData,permutatedRingDat
a),permutatedRingData)
        if(corr>max){
          max=corr
          maxPosi=i
          maxPosj=j
          maxPosk=k
        }
      }
    }
  }

  #Plot the permutation with max correlation
  permutatedRingData=permutateData2(permutateData2(permutateData2(ringData,maxPo
si),maxPosj),maxPosk)
  corr=getCorrelation(climateSameLengthAsRingData(climateData,permutatedRingData),p
ermutatedRingData)
  if(plot){print(plotClimateAndRingCorrelation(climateData,permutatedRingData,paste(c("
222;" ,maxPosi,maxPosj,maxPosk),collapse="")))})
  return(c(corr,222,maxPosi,maxPosj,maxPosk))
}

#Find the maximal correlation by once adding 3 points
maximizeCorrelation3 <- function(climateData,ringData,plot=TRUE){
  ringData=removeZeros(ringData)

```

```

max=-1

for(i in 0:nrow(ringData)-2){
  permutedRingData=permutateData3(ringData,i)
  corr=getCorrelation(climateSameLengthAsRingData(climateData,permutedRingData),
permutedRingData)
  if(corr>max){
    max=corr
    maxPos=i
  }
}
#Plot the permutation with max correlation
permutedRingData=permutateData3(ringData,maxPos)
corr=getCorrelation(climateSameLengthAsRingData(climateData,permutedRingData),p
ermutedRingData)
if(plot){print(plotClimateAndRingCorrelation(climateData,permutateData3(ringData,ma
xPos),paste(c("3;",maxPos),collapse="")))}
return(c(corr,3,maxPos))
}

#Find the maximal correlation by twice adding 3 points
maximizeCorrelation33 <- function(climateData,ringData,plot=TRUE){
  ringData=removeZeros(ringData)
  max=-1

  for(i in 0:(nrow(ringData)-2)){
    if(i==0){extra=2}else{extra=0}
    for(j in 0:(nrow(ringData)-4+extra)){
      permutedRingData=permutateData3(permutateData3(ringData,i),j)
      corr=getCorrelation(climateSameLengthAsRingData(climateData,permutedRingData
),permutedRingData)
      if(corr>max){
        max=corr
        maxPosi=i
        maxPosj=j
      }
    }
  }

  #Plot the permutation with max correlation
  permutedRingData=permutateData3(permutateData3(ringData,maxPosi),maxPosj)
  corr=getCorrelation(climateSameLengthAsRingData(climateData,permutedRingData),p
ermutedRingData)
  if(plot){print(plotClimateAndRingCorrelation(climateData,permutedRingData,paste(c("
33;",maxPosi,",",maxPosj),collapse="")))}
  return(c(corr,33,maxPosi,maxPosj))
}

```

```

#Find the maximal correlation by once adding 2 points and once adding 3 points
maximizeCorrelation23 <- function(climateData,ringData,plot=TRUE){
  ringData=removeZeros(ringData)
  max=-1

  for(i in 0:(nrow(ringData)-1)){
    if(i==0){extra=1}else{extra=0}
    for(j in 0:(nrow(ringData)-3+extra)){
      permutedRingData=permuteData3(permuteData2(ringData,i),j)
      corr=getCorrelation(climateSameLengthAsRingData(climateData,permutedRingData
),permutedRingData)
      if(corr>max){
        max=corr
        maxPosi=i
        maxPosj=j
      }
    }
  }

  #Plot the permutation with max correlation
  permutedRingData=permuteData3(permuteData2(ringData,i),j)
  corr=getCorrelation(climateSameLengthAsRingData(climateData,permutedRingData),p
ermutedRingData)
  if(plot){print(plotClimateAndRingCorrelation(climateData,permutedRingData,paste(c("
23;",maxPosi,",",maxPosj),collapse="")))}
  return(c(corr,23,maxPosi,maxPosj))
}

#Function definitions end
#####
#####
#####
#####

```

useFunctions.R

This component of the script calls the functions component and uses the functions on the dataset selected. Outputs are graphs and correlation values.

```

source("functions.R")

## Loading required package: foreach

## Loading required package: iterators

## Loading required package: parallel

```

```

## -- Attaching packages ----- tidyverse 1.2.1 --

## v tibble 2.1.1    v purrr  0.3.2
## v tidyr  0.8.3    v dplyr  0.8.0.1
## v readr  1.3.1    v stringr 1.4.0
## v tibble 2.1.1    v forcats 0.4.0

## -- Conflicts ----- tidyverse_conflicts() --
## x purrr::accumulate() masks foreach::accumulate()
## x dplyr::arrange()    masks plyr::arrange()
## x purrr::compact()   masks plyr::compact()
## x dplyr::count()     masks plyr::count()
## x dplyr::failwith()  masks plyr::failwith()
## x dplyr::filter()    masks stats::filter()
## x dplyr::id()        masks plyr::id()
## x dplyr::lag()       masks stats::lag()
## x dplyr::mutate()    masks plyr::mutate()
## x dplyr::rename()    masks plyr::rename()
## x dplyr::summarise() masks plyr::summarise()
## x dplyr::summarize() masks plyr::summarize()
## x purrr::when()     masks foreach::when()

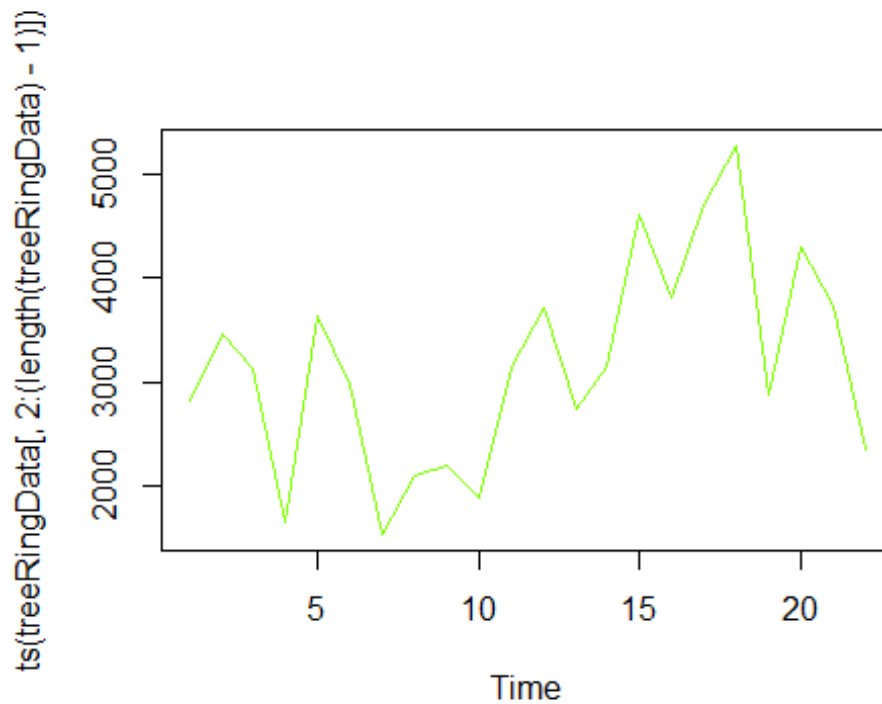
#####
#####
#####

#Import and convert/preprocess the data into easily usable formats

#set the inputFile name. Any file placed in here needs to have exactly yhe same format and header names as the example File Data.csv or else the script will most likely not work
Filename= "data/ad/sanpedro_east.csv"

#Read treeringData from csv file
treeRingData = read.csv(Filename, sep = ";", header = TRUE)
#treeRingData = treeRingData[-nrow(treeRingData),] # removes the last row which for some reason is empty
#plot the treeRing data
plot(ts(treeRingData[,2:(length(treeRingData)-1)],plot.type=c("single"),col=rainbow(ncol(treeRingData)))

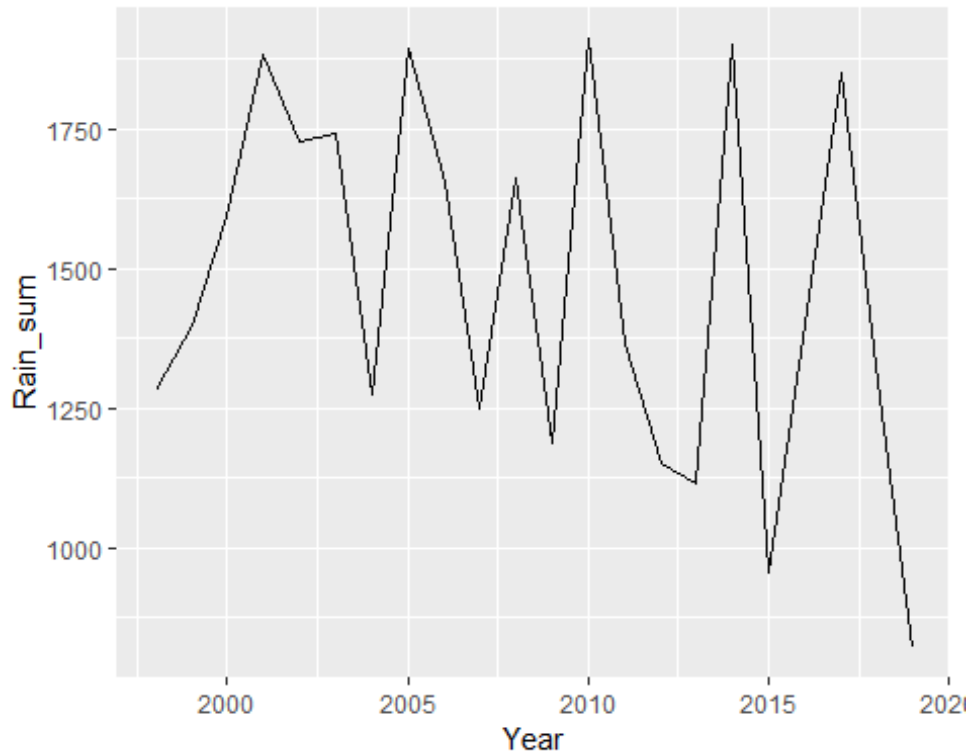
```



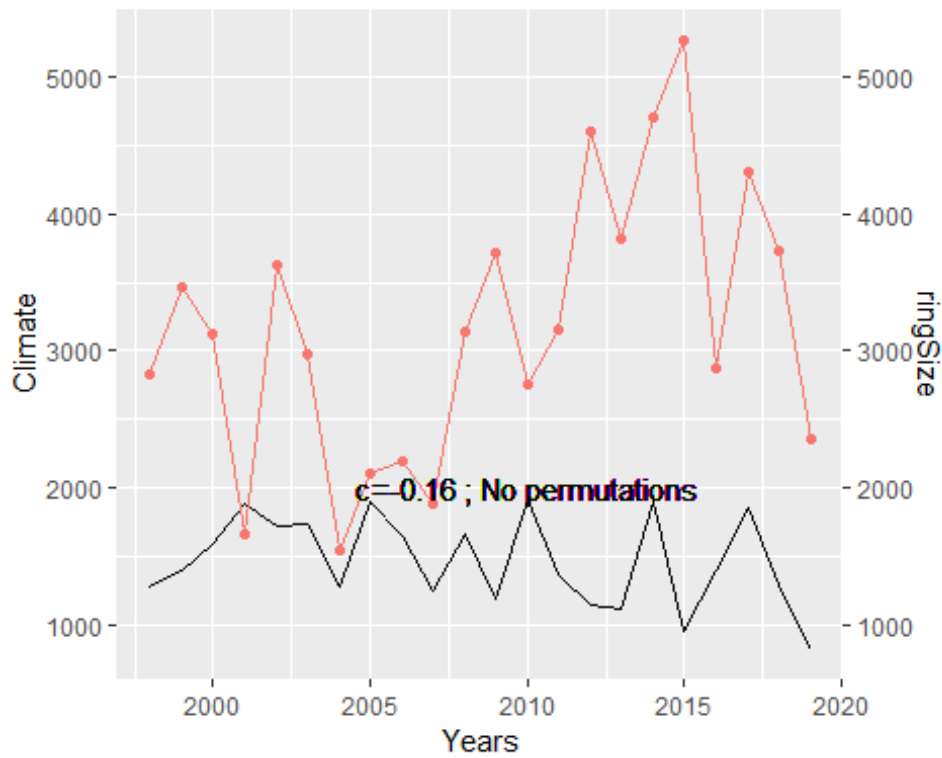
```
#Weather Data import
climate = treeRingData[c('Year','Rain_sum')]

#add the index in the last column to plot as x coordinate, We need this only for plotting
climate$idu <- as.numeric(row.names(climate))

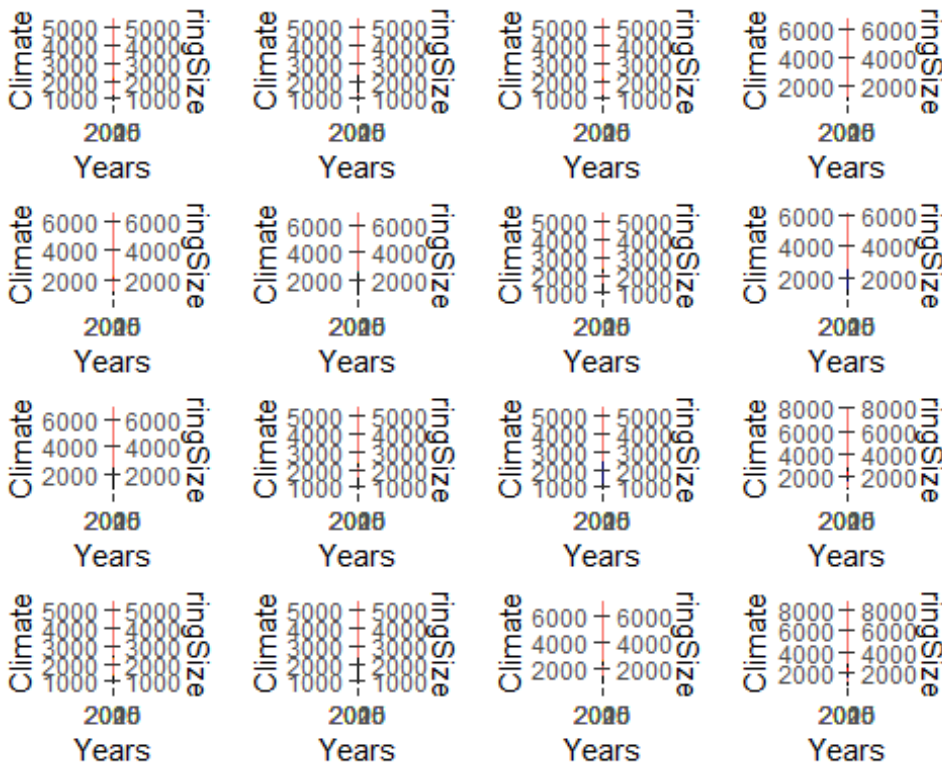
#Generate a plot for each climate location
plotClimate(climate,"climate")
```



```
#####
#####
#####
#####
#Example usage of the functions
#prepare the data properly before using these functions. Errors occur if the data does not have the correct number of columns/rows etc.
ringData=removeZeros(treeRingData[2])
climateCut=climateSameLengthAsRingData(climate,ringData)
onlyWeatherColumn=climateCut['Rain_sum']
#Using the functions
plotClimateAndRingCorrelation(climateCut,ringData,"No permutations", 2000,1)
```



```
plotGridOfPermutations(climateCut,ringData,0)
```



```
maximizeCorrelation2(onlyWeatherColumn,ringData,FALSE)
```

```
## [1] 0.07616053 2.00000000 16.00000000
```

```
maximizeCorrelation22(onlyWeatherColumn,ringData,FALSE)
```

```

## [1] 0.2515532 22.0000000 15.0000000 18.0000000

#maximizeCorrelation222(climateData,ringData,FALSE) #This takes longest and is therefore commented
maximizeCorrelation3(onlyWeatherColumn,ringData,FALSE)

## [1] 0.25047 3.00000 18.00000

maximizeCorrelation33(onlyWeatherColumn,ringData,FALSE)

## [1] 0.4351815 33.0000000 4.0000000 16.0000000

maximizeCorrelation23(onlyWeatherColumn,ringData,FALSE)

## [1] -0.4342233 23.0000000 10.0000000 17.0000000

#####
#####
#####
#####
#Loop over all treeRingDataSets and find max

treeRingDataReduced=treeRingData[,2:(length(treeRingData)-1)] # removes the year and rain data from the data frame
for(i in 1:ncol(treeRingDataReduced)){

  #get correct location weather
  ringData=removeZeros(treeRingDataReduced[c(i)])
  climateData=climateSameLengthAsRingData(climate,ringData)
  onlyWeatherColumn=climateData['Rain_sum']
  max=-1
  result=maximizeCorrelation2(onlyWeatherColumn,ringData,FALSE)
  if(result[1]>max){max=result[1];maxPermutation=result}
  result=maximizeCorrelation22(onlyWeatherColumn,ringData,FALSE)
  if(result[1]>max){max=result[1];maxPermutation=result}

  #The following permutations are commented.
  #They yield high correlation results but are questionable. Needs to be discussed
  ##result=maximizeCorrelation222(climateData,ringData,FALSE) #This takes longest and is therefore commented
  ##if(result[1]>max){max=result[1];maxPermutation=result}
  ##result=maximizeCorrelation3(climateData,ringData,FALSE)
  ##if(result[1]>max){max=result[1];maxPermutation=result}
  ##result=maximizeCorrelation33(climateData,ringData,FALSE)
  ##if(result[1]>max){max=result[1];maxPermutation=result}
  ##result=maximizeCorrelation23(climateData,ringData,FALSE)
  if(result[1]>max){max=result[1];maxPermutation=result}

  #print the maximal result

```

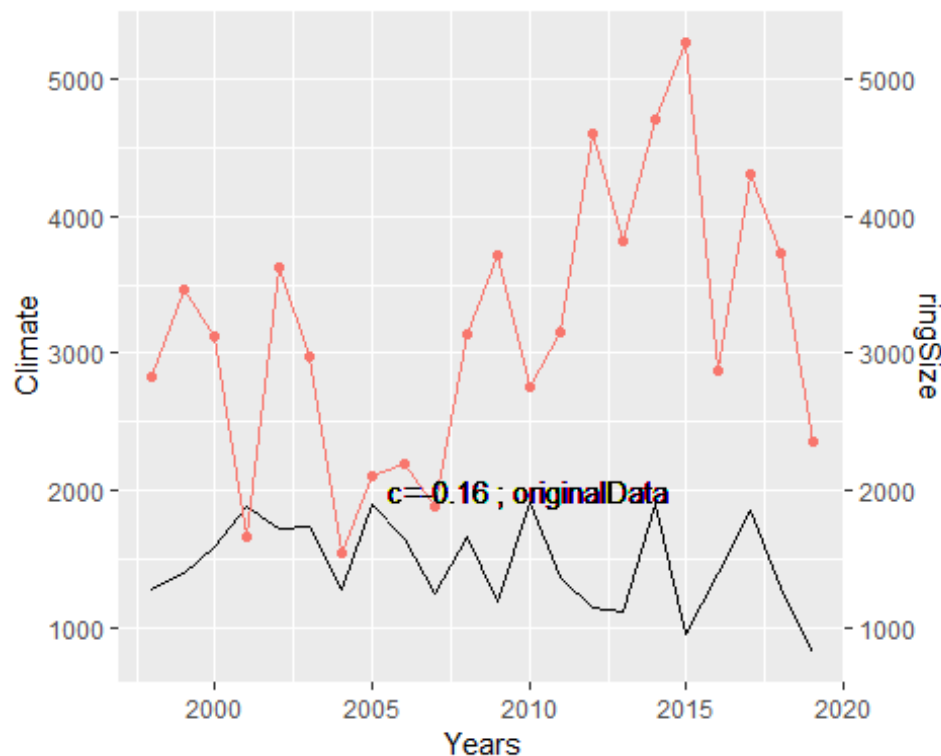
```

print(c(i,maxPermutation))
}

## [1] 1.0000000 0.2515532 22.0000000 15.0000000 18.0000000
## [1] 2.0000000 0.2515532 22.0000000 15.0000000 18.0000000

#use these lines to inspect individual permutations
indexRing=2
ringData=removeZeros(treeRingDataReduced[c(indexRing)])
climateData=climateSameLengthAsRingData(climate,ringData)
onlyWeatherColumn=climateCut['Rain_sum']
plotClimateAndRingCorrelation(climateData,ringData,"originalData",2000,1)

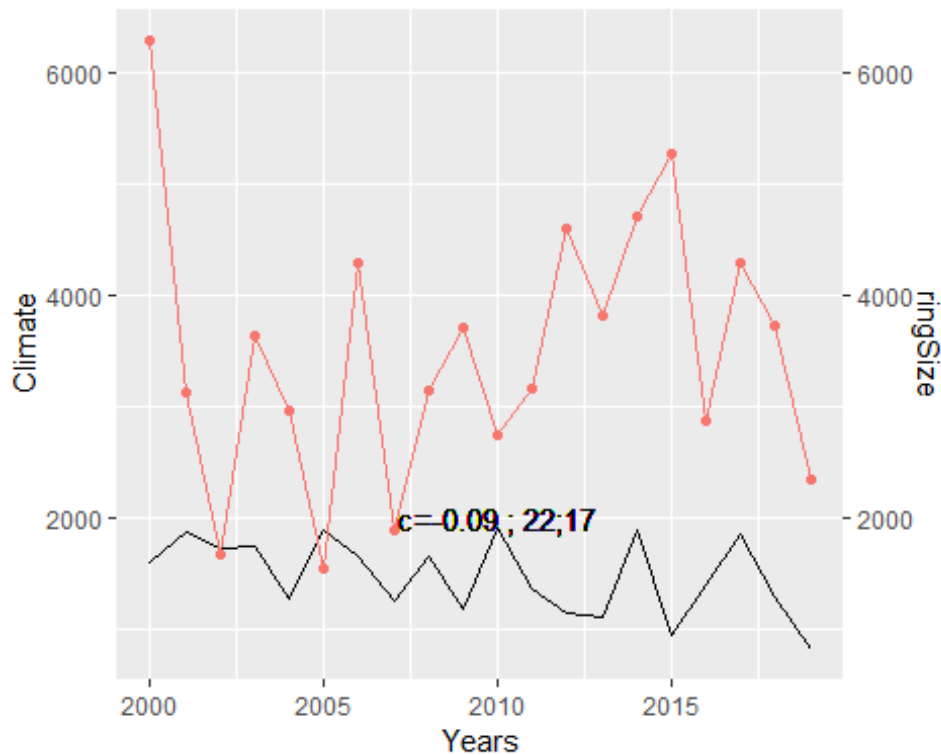
```



```

i=1
j=7
#permutedRingData=permuteData2(ringData,i)
permutedRingData=permuteData2(permuteData2(ringData,i),j) #use the correct permutation: 2,22,222,3,33,23
corr=getCorrelation(climateSameLengthAsRingData(onlyWeatherColumn,permutedRingData),permutedRingData)
#plotClimateAndRingCorrelation(climateData,permutedRingData,paste(c("2;",i),collapse=""),2000,1)
plotClimateAndRingCorrelation(climateData,permutedRingData,paste(c("22;",i,j),collapse=""),2000,1)

```



```
#maximizeCorrelation22(climateData,ringData,TRUE) #use the correct permutation: 2,22,222,3,33,2
3
```

```
#####
#####
#####
#####
```

```
#Calculate Correlation Matrix
```

```
#last row (31) in treeringdata didnt contains labels for locations. We dont want those here
```

```
treeRingData=treeRingData[c(-31),]
```

```
#Parallel loop over all samples to get correlation matrix between samples (Might be of interest)
```

```
samples=ncol(treeRingData)-1
```

```
correlationMatrix <- data.frame(matrix(0, nrow = samples, ncol = samples))
```

```
#setup parallel backend to use many processors
```

```
cores=detectCores()
```

```
cl <- makeCluster(cores[1]-1) #not to overload your computer
```

```
registerDoParallel(cl)
```

```
finalList <- foreach(i=1:samples, .combine=cbind) %dopar% {
```

```
  df = data.frame(matrix(0, nrow = samples, ncol = 1))
```

```
  for (j in 1:samples) {
```

```

    df[j,1]=getCorrelation(treeRingData[i],treeRingData[j])
  }
  df
}
l=finalList # parallel code returns a list of list
correlationMatrix = as.data.frame(matrix(unlist(l), nrow=length(unlist(l[1]))) # convert to dataframe
stopCluster(cl)

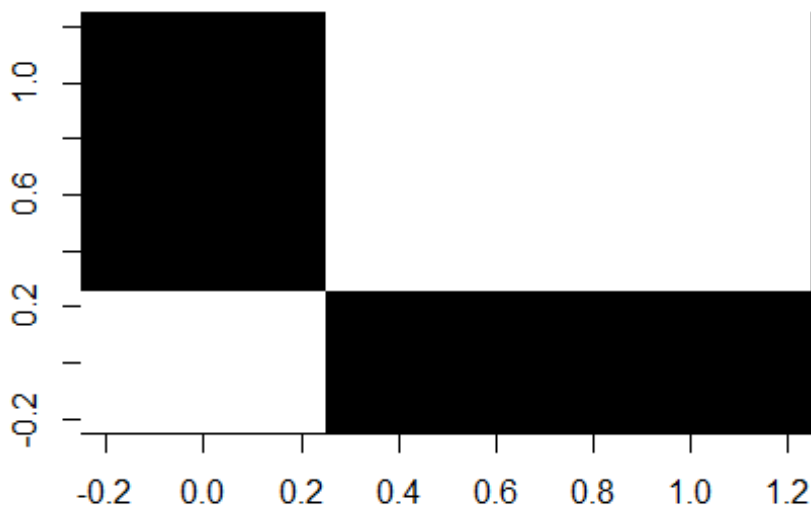
#same result can be achieved by this NOT parralized code
# correlationMatrix <- data.frame(matrix(0, nrow = samples, ncol = samples))
# for (i in 1:samples) {
#   print(i)
#   for (j in 1:samples) {
#     correlationMatrix[i,j]=getCorrelation(treeRingData[i],treeRingData[j])
#   }
# }

#print correlationmatrix and visualize
correlationMatrix

##      V1      V2      V3
## 1 1.000000 0.4362833 0.4362833
## 2 0.4362833 1.0000000 1.0000000
## 3 0.4362833 1.0000000 1.0000000

image(t(correlationMatrix),col=grey(seq(0, 1, length = 256)))

```



```
#####
#####
#####
#####
```

10.5 Maximized correlation outputs after permutations

These are the outputs of the R-Script after inserting all the ring width measurements and their corresponding precipitation. Correlations were calculated using TRMM data and Dr. Agathe Dié's data as well.

TRMM data outputs:

ID	Location	Corr TRMM	Correlation with precipitation (TRMM)	Permutation	Ring couples
AB1	Abie	0.42	weak	22	5,14
DI8	Sinfra	0.59	moderate	22	2,16
GA3	Bangolo	0.62	moderate	22	2,2
GA4	Bangolo	0.68	moderate	22	3,3
GA5	Daloa	0.38	weak	22	6,7
IS1	Gagnoa West	0.68	moderate	22	2,9
IS2	Gagnoa West	0.54	moderate	22	19,26
IS9	Daloa	0.43	weak	22	20,19
LOC1A1	Seguela	0.57	moderate	22	6,14
LOC1A3	Seguela	0.41	strong	22	10,10
LOC1AdA	Seguela	0.28	low	22	2,6
LOC1AdB	Seguela	0.16	low	22	3,7
LOC1AdC	Seguela	0.58	moderate	22	3,11
LOC1B1	Seguela	0.12	low	22	9,13
LOC1B2	Seguela	0.41	weak	22	1,1
LOC1B3	Seguela	0.37	weak	22	11,15
LOC1B4	Seguela	0.32	weak	22	2,6
LOC1B5	Seguela	0.33	weak	2	11
LOC2A1	Daloa	0.32	weak	22	13,13
LOC2A2	Daloa	0.52	moderate	22	5,14
LOC2A3	Daloa	0.59	moderate	22	9,11
LOC2A4	Daloa	0.35	weak	22	7,13
LOC2A5	Daloa	0.53	moderate	22	1,11

LOC2B1	Daloa	0.38	weak	22	11,14
LOC2B2	Daloa	0.47	weak	22	3,10
LOC2B3	Daloa	0.31	weak	22	18,23
LOC2B4	Daloa	0.57	moderate	22	3,19
LOC2B5	Daloa	0.32	weak	22	10,15
LOC2C2	Daloa	0.24	low	22	8,17
LOC2C3	Daloa	0.36	weak	22	20,20
LOC3A3	Gagnoa	0.7	strong	22	6,10
LOC3A4	Gagnoa	0.69	moderate	22	3,7
LOC3B1	Gagnoa	0.46	weak	22	1,12
LOC3B2	Gagnoa	0.29	low	22	6,13
LOC3B3	Gagnoa	0.39	weak	22	1,8
LOC3B4	Gagnoa	0.55	moderate	22	11,15
LOC3C1	Gagnoa	0.05	low	22	19,23
LOC3C2	Gagnoa	0.23	low	22	1,8
LOC3C3	Gagnoa	0.38	weak	22	20,20
LOC3C4A	Gagnoa	0.61	moderate	22	12,16
LOC3C4B	Gagnoa	0.48	weak	22	3,14
LOC3C5	Gagnoa	0.63	moderate	22	7,11
LOC3C6	Gagnoa	0.44	weak	22	19,23
LOC3C7	Gagnoa	0.24	low	22	3,10
LOC3C8	Gagnoa	0.6	moderate	22	4,4
LOC4A2	Abengourou North	0.2	low	22	11,15
LOC4A4	Abengourou North	0.17	low	22	4,11
LOC4A5	Abengourou North	0.21	low	22	1,1
LOC4A6A	Abengourou North	0.33	weak	22	11,18
LOC4A6B	Abengourou North	-0.07	low	2	12
LOC4AdA	Abengourou North	0.22	low	22	4,4
LOC4B1	Abengourou North	0.29	low	2	12
LOC4B2A	Abengourou North	0.3	weak	22	1,4
LOC4B2B	Abengourou North	0.33	weak	22	3,3
LOC4B3	Abengourou North	0.31	weak	22	11,19
LOC4B4	Abengourou North	0.42	weak	22	1,7
MA4	Duekoue	0.33	weak	22	3,10
MA5	Duekoue	0.19	low	2	19
SA2	San Pedro East	0.48	weak	22	2,6
SO1	Soubre East	0.33	weak	22	14,14

SO2	Soubre	0.2	low	2	7
SO3	Soubre East	0.28	low	22	12,16
SO4	Soubre	0.7	strong	22	3,7
SO5	Soubre	0.49	weak	22	3,10
SP2	San Pedro	0.5	moderate	22	1,4
SP3	San Pedro	0.59	moderate	2	12
SP4	San Pedro	0.36	weak	22	17,20

Dr. Agathe Dié's data outputs:

ID	Location	Corr AD	Correlation with precipitation (Dr. Agathe Dié)	Permutation	Ring couples
AB1	Abie	no data	no data	no data	no data
DI8	Sinfra	no data	no data	no data	no data
GA3	Bangolo	no data	no data	no data	no data
GA4	Bangolo	no data	no data	no data	no data
GA5	Daloa	0.43	weak	22	6,7
IS1	Gagnoa West	0.64	moderate	22	2,9
IS2	Gagnoa West	0.5	moderate	22	21,26
IS9	Daloa	0.39	weak	22	20,25
LOC1A1	Seguela	0.43	weak	22	3,14
LOC1A3	Seguela	0.45	weak	22	13,19
LOC1AdA	Seguela	0.3	weak	22	5,6
LOC1AdB	Seguela	0.02	low	2	13
LOC1AdC	Seguela	0.26	low	22	1,6
LOC1B1	Seguela	0.55	moderate	2	8
LOC1B2	Seguela	0.49	weak	22	8,9
LOC1B3	Seguela	0.46	weak	22	16,17
LOC1B4	Seguela	0.18	low	2	11
LOC1B5	Seguela	0.3	weak	22	5,11
LOC2A1	Daloa	0.16	low	22	13,13
LOC2A2	Daloa	0.67	moderate	22	3,14
LOC2A3	Daloa	0.51	moderate	22	1,4
LOC2A4	Daloa	0.41	weak	22	7,13
LOC2A5	Daloa	0.51	moderate	22	1,9

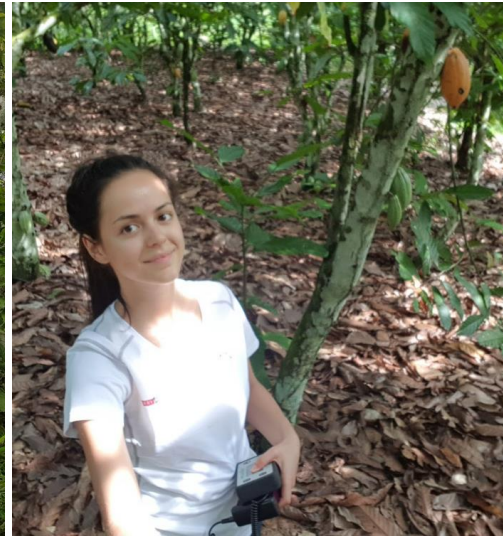
LOC2B1	Daloa	0.33	weak	22	14,15
LOC2B2	Daloa	0.4	weak	22	2,13
LOC2B3	Daloa	0.32	weak	22	3,23
LOC2B4	Daloa	0.56	moderate	22	12,19
LOC2B5	Daloa	0.32	weak	22	20,21
LOC2C2	Daloa	0.14	low	22	11,17
LOC2C3	Daloa	0.34	weak	22	19,20
LOC3A3	Gagnoa	0.74	strong	22	3,10
LOC3A4	Gagnoa	0.66	moderate	22	1,7
LOC3B1	Gagnoa	0.57	moderate	22	5,5
LOC3B2	Gagnoa	0.18	low	22	6,17
LOC3B3	Gagnoa	0.42	weak	22	1,12
LOC3B4	Gagnoa	0.44	weak	22	4,15
LOC3C1	Gagnoa	0.47	weak	22	12,23
LOC3C2	Gagnoa	0.13	low	22	1,12
LOC3C3	Gagnoa	0.67	moderate	22	20,20
LOC3C4A	Gagnoa	0.63	moderate	22	1,12
LOC3C4B	Gagnoa	0.28	low	22	10,14
LOC3C5	Gagnoa	0.59	moderate	22	1,11
LOC3C6	Gagnoa	0.3	weak	2	18
LOC3C7	Gagnoa	0.19	low	22	3,10
LOC3C8	Gagnoa	0.56	moderate	2	2
LOC4A2	Abengourou North	0.08	low	22	11,15
LOC4A4	Abengourou North	0.12	low	22	15,16
LOC4A5	Abengourou North	0.34	weak	22	1,2
LOC4A6A	Abengourou North	0.18	low	22	1,27
LOC4A6B	Abengourou North	0.12	low	22	12,16
LOC4AdA	Abengourou North	0.34	weak	22	2,7
LOC4B1	Abengourou North	0.23	low	22	4,4
LOC4B2A	Abengourou North	0.2	low	2	5
LOC4B2B	Abengourou North	0.46	weak	22	6,9
LOC4B3	Abengourou North	0.07	low	22	2,10
LOC4B4	Abengourou North	0.37	weak	22	2,3
MA4	Duekoue	no data	no data	no data	no data
MA5	Duekoue	no data	no data	no data	no data
SA2	San Pedro East	0.25	low	22	15,18
SO1	Soubre East	0.41	weak	22	11,14

SO2	Soubre	0.4	weak	22	6,6
SO3	Soubre East	0.42	weak	22	12,16
SO4	Soubre	0.71	strong	2	1
SO5	Soubre	0.49	weak	22	2,3
SP2	San Pedro	0.68	moderate	22	17,20
SP3	San Pedro	0.56	moderate	22	1,8
SP4	San Pedro	0.61	moderate	22	3,4

10.6 Sampling trips picture gallery

10.6.1 First sampling trip







10.6.2 Second sampling trip





Personal Declaration:

I hereby declare that the submitted thesis is the result of my own, independent work. All external sources are explicitly acknowledged in the thesis.

Alice Gargano

